
[All ETDs from UAB](#)

[UAB Theses & Dissertations](#)

2020

Co-Factors In Fgf Signaling

Christopher Yanucil

University of Alabama at Birmingham

Follow this and additional works at: <https://digitalcommons.library.uab.edu/etd-collection>

 Part of the [Medical Sciences Commons](#)

Recommended Citation

Yanucil, Christopher, "Co-Factors In Fgf Signaling" (2020). *All ETDs from UAB*. 718.
<https://digitalcommons.library.uab.edu/etd-collection/718>

This content has been accepted for inclusion by an authorized administrator of the UAB Digital Commons, and is provided as a free open access item. All inquiries regarding this item or the UAB Digital Commons should be directed to the [UAB Libraries Office of Scholarly Communication](#).

CO-FACTORS IN FGF SIGNALING

by

Christopher Yanucil

Stijn De Langhe
Christian Faul (MENTOR)
Stefanie Krick
Adam R. Wende
Bradley Yoder (CHAIR)

A DISSERTATION

Submitted to the graduate faculty of The University of Alabama at Birmingham,
in partial fulfillment of the requirements for the degree of
Doctor of Philosophy

BIRMINGHAM, ALABAMA

2020

Copyright by
Christopher Yanucil
2020

CO-FACTORS IN FGF SIGNALING

Christopher Yanucil

CELL, MOLECULAR, AND DEVELOPMENTAL BIOLOGY

ABSTRACT

The fibroblast growth factor (FGF) family consists of a group of proteins whose diverse biological functions are mediated by receptor tyrosine kinases, termed FGF receptors (FGFR) 1-4. While paracrine FGFs require heparin sulfate as a co-factor for FGFR binding and signaling, it has been assumed that endocrine FGFs, such as FGF23, do not bind heparin but instead require klotho, a family of transmembrane proteins, as a co-receptor on specific target cells. FGF23 acts as bone-derived hormone that targets tubular epithelial cells in the kidney via FGFR1 and α -klotho to reduce renal phosphate uptake. In chronic kidney disease (CKD), the kidney loses FGF23 responsiveness resulting in increased serum levels of phosphate and FGF23. Elevated FGF23 can activate FGFR4 in cells lacking α -klotho, such as cardiac myocytes, thereby contributing to cardiac injury, the leading cause of death in CKD. Here, we report that the soluble form of α -klotho (SKL), that is released from the kidney into the circulation, can bind FGF23 and specific FGFR isoforms thereby mediating FGF23 responsiveness in cells lacking klotho as well as inhibiting FGFR4-induced FGF23 effects in cardiac myocytes. This mechanism, combined with our finding that SKL can block the binding of certain paracrine FGFs to FGFRs and thereby their mitogenic effects, might underlie the pleiotropic, tissue-protective effects of SKL. To test these effects in pre-clinical and clinical studies, we have developed novel assays to detect and quantify levels of SKL as well as to produce recombinant SKL protein, which will help to identify animal models and patient populations with low SKL

levels and provide bioactive SKL for therapeutic administration. Surprisingly, we also found that heparin acts as a FGF23 co-receptor by mediating FGF23 binding mainly to FGFR4 and thereby increases FGF23 effects on cardiac myocytes. Our study suggests that frequent heparin injections routinely done during the hemodialysis process, contribute to cardiac injury and the high mortality in patients with end-stage kidney disease who have extremely high serum FGF23 levels. Our concern regarding the safety of a standard-of-care is supported by our studies in two animal models with elevated FGF23, where repetitive heparin injections significantly aggravate cardiac hypertrophy.

Keywords: Fibroblast growth factor, klotho, heparin, chronic kidney disease, phosphate, dialysis

Dedication

I would like to thank both of my parents, Timothy and Cindy Yanucil, for their never-ending support and patience, for reaching this point could not have occurred without it.

ACKNOWLEDGMENTS

I would like to thank my thesis mentor, Dr. Christian Faul for his guidance and dedication. Without his encouragement to think outside the box and blind faith in my abilities, none of this work would have been possible. I would also like to thank all the current and previous members of the laboratory for their input and support.

TABLE OF CONTENTS

	Page
ABSTRACT.....	iii
DEDICATION.....	v
ACKNOWLEDGMENTS.....	vi
LIST OF TABLES.....	x
LIST OF FIGURES.....	xi
CHAPTER	
1. INTRODUCTION TO FGF BIOLOGY AND FUNCTION.....	1
Characterization of FGFs.....	1
Characterization of FGFRs.....	7
Characterization of Klotho Co-Receptors.....	12
Endocrine FGFs.....	22
Endocrine FGFs in Disease and Therapeutics.....	30
Chronic Kidney Disease (CKD).....	35
CKD and Cardiovascular Disease (CVD).....	37
FGF23 and CKD.....	38
2. SKL MODIFIES FGF23 SIGNALING.....	40
Background.....	40
Methods.....	41
Plasmid Constructs.....	41
Antibodies, Recombinant Proteins.....	42
Expression and Purification of SKL.....	43
Flag Immunoprecipitations.....	44
Protein A/G Immunoprecipitations.....	45
SDS-PAGE and Western Blotting.....	46
Paracrine FGF Signaling in HEK 293T Cells.....	46
Plate-Based Assay to Detect SKL and to Study the Paracrine FGF-SKL Crosstalk.....	47
Results.....	48
Discussion.....	55

3. PRODUCTION AND DETECTION OF BIOACTIVE SKL	58
Background.....	58
Methods.....	60
SKL Half-Life.....	60
Plate-Based SKL Activity Assay Specificity Test.....	61
Isolation and Cultivation of NRVM	62
Immunocytochemistry and Morphometry of NRVMs	63
Results	63
Discussion.....	70
4. HEPARIN INCREASES THE AFFINITY OF FGF23 FOR FGFR4	75
Background.....	75
Methods.....	76
ARVM Isolation and Analysis of Calcium Transients	76
Isolated Mouse Heart Contractility.....	77
Results	78
Discussion.....	83
5. HEPARIN INJECTION INCREASE THE EFFECTS OF FGF23 IN MOUSE MODELS OF FGF23 ELEVATION	85
Background.....	85
Methods.....	86
FGF23 Serial Injections	86
Adenine Diet Mice	87
Morphology, Fluorescence Microscopy and Morphometry of Mouse and Rats Hearts.....	88
Echocardiography of Mouse Hearts.....	89
Serum Chemistry	89
Results	89
Discussion.....	95
6. CONCLUSIONS.....	96
Discussion of Current Results.....	96
SKL as a Co-Factor for FGF23 Signaling	96
Heparin as a Co-Factor for FGF23 Signaling.....	100
Therapeutic Implications	103
LIST OF REFERENCES	106
APPENDICES	

A IACUC Approval Form116

LIST OF TABLES

<i>Tables</i>		<i>Page</i>
1	FGF Specificity for FGFRs.....	8
2	Binding affinity for FGFRs for Klotho Family Members	11
3	FGF23 Ultrasound	91
4	Adenine Model Serum Chemistry	93

LIST OF FIGURES

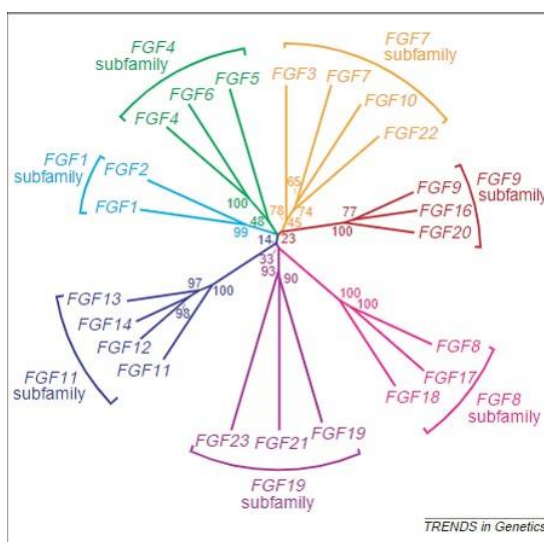
<i>Figure</i>		<i>Page</i>
1	The FGF Subfamilies	1
2	Domain Structure of FGF Family Members	2
3	Secretion Mechanism of FGF2	3
4	Heparin Binding Affinity in FGFs	5
5	FGFR Splice Variants	7
6	Aligned Heparin Binding Sites of FGFR1-4	10
7	Downstream Signaling of FGFR Activation.....	12
8	KL Tissue Expression by RT-PCR.....	13
9	Mechanisms of SKL Release	17
10	Effects of FGF19 on the Liver	24
11	Mechanism of FGF23 Production.....	26
12	Crystal Structure of FGF23-FGFR1-KL Complex	27
13	Effects of FGF23 Signaling	29
14	FGF23 Levels During CKD.....	36
15	FGF23 Signaling in Cardiac Myocytes.....	37
16	Hypothesis of SKL Modulation of FGF23 Signaling	40
17	FGF23 Binds SKL	48
18	SKL does not Bind FGF19 and FGF21	49

19	SKL Binds FGFR1 and FGFR4.....	50
20	SKL Interferes with Paracrine FGF Signaling.....	52
21	SKL Modulates FGF23 Signaling with Multiple FGFRs.....	53
22	SKL does not Modulate FGF19 or FGF21 Signaling.....	54
23	FGF23 Induced Hypertrophic Growth of Myocytes Requires FGFR4.....	64
24	SKL Blocks FGF23 Induced Hypertrophy	65
25	SKL and FGF23 Induce MAPK Signaling in NRVMs	66
26	Sensitivity of a Novel Assay Measuring SKL Activity	67
27	Purity of SKL Preparations.....	68
28	Comparing SKL Activity under Different Conditions.....	69
29	Half-Life Measurements of SKL	71
30	Heparin Plays a Role in FGF Signaling with FGFR4.....	78
31	Heparin Increases FGF23 Affinity for FGFR4.....	80
32	Heparin Increases the Effects of FGF23 on NRVMs	81
33	Heparin Increases the Effects of FGF23 Induced Calcium Handling	82
34	Heparin Increases the Effects of FGF23 on Cardiac Contraction.....	83
35	Heparin Increases the Effects of Recombinant FGF23 on Cardiac Hypertrophy	90
36	Representative Pictures of Cardiac Effects of FGF23 Injections	92
37	Heparin Increases the Effects of FGF23 in a Diet Induced Model of CKD	94

CHAPTER 1: INTRODUCTION TO FGF BIOLOGY AND FUNCTION

Characterization of FGFs

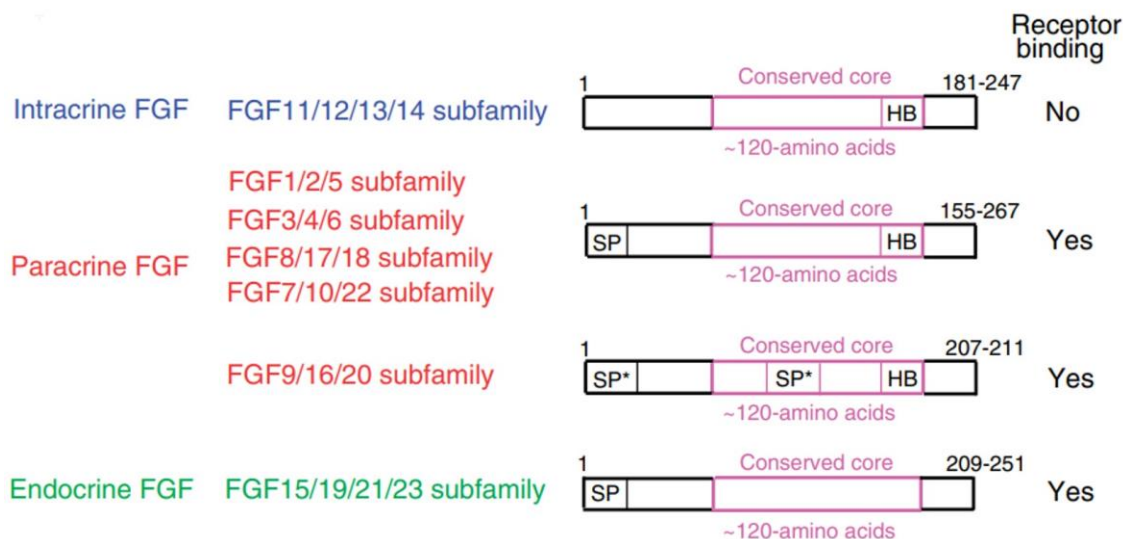
Fibroblast growth factors (FGFs) are a group of closely related proteins with diverse functions and roles. The first FGFs were purified from brain extracts of cows, with their noted abilities to stimulate cell proliferation in the NIH3T3 cell line.¹⁻³ These FGFs were aptly named FGF1 and FGF2, and since their discovery a total of 22 FGFs have



Note: From Itoh, N. and D.M. Ornitz, *Evolution of the Fgf and Fgfr gene families*. Trends Genet, 2004. **20**(11): p. 563-9. Copyright Elsevier 2004. Reprinted with permission

Figure 1. The FGF Subfamilies

been discovered.⁴ All FGFs are considered related based on a 120 amino acid (a.a.) core domain that has 30-60% sequence similarity.⁴ FGFs are further broken up into three groups based on their



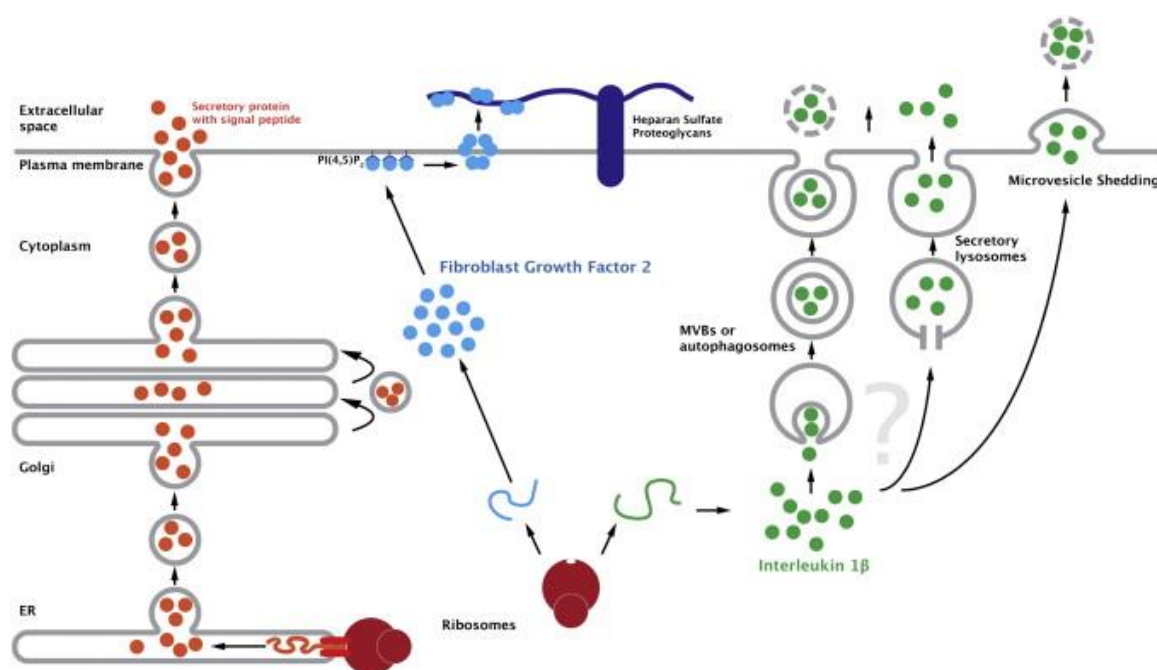
Note: From Itoh, N. and D.M. Ornitz, *Fibroblast growth factors: from molecular evolution to roles in development, metabolism and disease*. The Journal of Biochemistry, 2010. 149(2): p. 121-130 Copyright Oxford University Press 2010. Reprinted with permission

Figure 2. Domain Structure of FGF Family Members

mode of action and localization, i.e. intracrine, paracrine, and endocrine FGFs. FGFs can be further classified into seven subfamilies based on sequence homologies, as seen in Fig. 1, with many subfamily members having similar receptor binding profiles.^{4, 5} The FGF11 subfamily consists of four members that lack a secretion sequence and therefore cannot leave the intracellular space. These FGFs have been shown to interact with and block sodium channels, but further functions remain unclear.⁶

The differences in the three FGF subfamilies are detailed in Fig. 2. The largest family and most widely studied are the paracrine FGFs. These FGFs are able to be excreted by cells and participate in cellular signaling events with cognate extracellular FGF receptors (FGFRs). Paracrine FGFs play a major role in many biological processes, including development, division, metabolism, and regeneration. They are unique in their strong affinity for heparin sulfate.⁷⁻⁹ Heparin sulfate is a sulfated glycosaminoglycan that consists of repeating disaccharide units.^{10, 11} Sulfation can occur on the 2-O position or 6-

O position, and in different patterns, leading to a high degree of variability in size and shape of heparin units.¹² Heparin is covalently linked to serine residues in proteoglycans and basement membrane proteins, giving it a ubiquitous expression profile in the extracellular matrix and glycocalyx.¹⁰ The variability in heparin sulfation and size allows cells to uniquely control the binding and diffusion of paracrine FGFs.¹³ Their strong heparin binding affinity also limits the diffusion of these FGFs, regulating them to autocrine and paracrine signaling.^{14, 15} The binding of paracrine FGFs to heparin sulfate is controlled by



Note: From Steringer, J.P., H.M. Müller, and W. Nickel, *Unconventional secretion of fibroblast growth factor 2--a novel type of protein translocation across membranes?* J Mol Biol, 2015. 427(6 Pt A): p. 1202-10 Copyright Elsevier 2014. Reprinted with permission

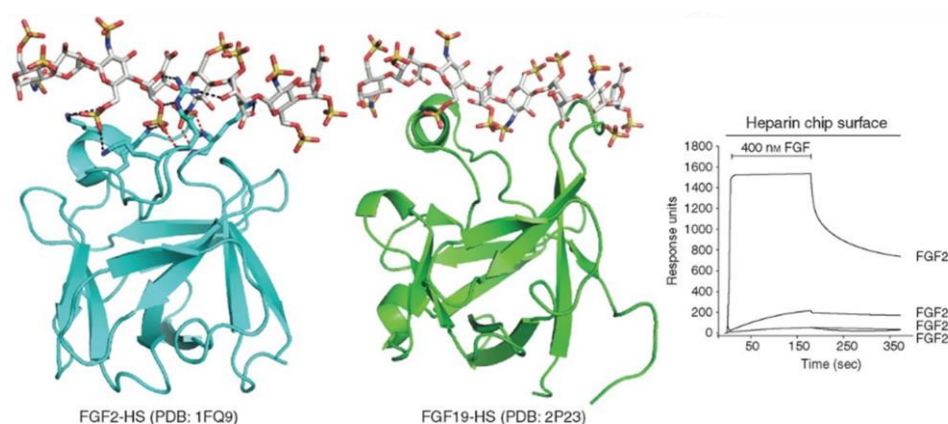
Figure 3. Secretion Mechanism of FGF2

the FGF's B1-B2 loop, as well as the B11-B12 sheet, exposing multiple basic residues that attract the negative charge of heparin.¹⁶ There is high variability between amino acids in this region, leading to differences in binding affinity for different species of heparin, but the overall shape is similar between paracrine FGFs.¹⁷ While heparin binding is a

common characteristic among paracrine FGFs, secretion can vary greatly between different proteins. Many have a cleavable N-terminal secretion sequence that is common in other proteins. However, the FGF9 subfamily lacks this secretion signal. Instead, they utilize a 7 a.a. non-cleavable sequence located in the center of the protein.¹⁸ While most FGFs and many other proteins utilize excretions pathways through the Golgi apparatus and secretory lysosomes, FGF1 and FGF2 lack a secretion sequence and utilize neither of these pathways. This is unique given that these are some of the most widely and strongest expressed FGFs. As seen in Fig. 3, FGF2 is recruited to the plasma membrane directly via binding to phosphoinositide. This leads to the formation of an ATP-dependent pore, that directly shuttles FGF2 to heparin sulfate on the outside of the plasma membrane.¹⁹

Endocrine FGFs, as seen in Fig. 2, contain a cleavable secretion sequence but are unique in their lack of a heparin binding site. This site lacks multiple key amino acids, which leads to a low affinity for heparin and provides these FGFs the ability to escape the glycocalyx and enter circulation.¹⁶ While these FGFs lack a heparin binding domain and have an extremely low affinity for heparin,^{5, 20} interestingly the original work of many groups shows that FGF19 and FGF23 signaling can be aided by heparin.^{21, 22} Asada and colleagues screened all known FGFs for their ability to bind heparin columns,¹⁴ as well as closely related molecules like chondroitins. Their screen identified many paracrine FGFs eluted from these columns with NaCl molarities between 1-1.5 M. Interestingly, FGF21 was the only FGF to not bind the column, while FGF19 and FGF23 eluted at a concentration of 0.5 M. This finding in comparison to paracrine FGFs led the authors to believe that these FGFs have low heparin binding activity, while in many other assays an elution at 0.5 molar NaCl could be considered strong binding. Further work by Yu and col-

leagues on FGF23²² showed that in combination with heparin, FGF23 was able to stimulate BaF3 cell proliferation when cells were transfected with different FGFR isoforms. The FGF23 dependent growth favored the addition of heparin chains that were highly sulfated, and heparin forms with higher molecular weights had a greater effect. Similar studies were conducted with FGF19 by Yang Li's group at Amgen,^{21, 23} showing that at high concentrations, FGF19 could induce mitogen-activated protein kinase (MAPK) activation when co-treated with heparin. Interestingly, while this signaling event does occur, it requires much higher concentrations of endocrine FGFs than what was seen with para-



Note: From Belov, A.A. and M. Mohammadi, *Molecular mechanisms of fibroblast growth factor signaling in physiology and pathology*. Cold Spring Harb Perspect Biol, 2013. 5(6) Copyright Cold Spring Harbor Press 2013. Reprinted with permission.

Figure 4. Heparin Binding Affinity in FGFs

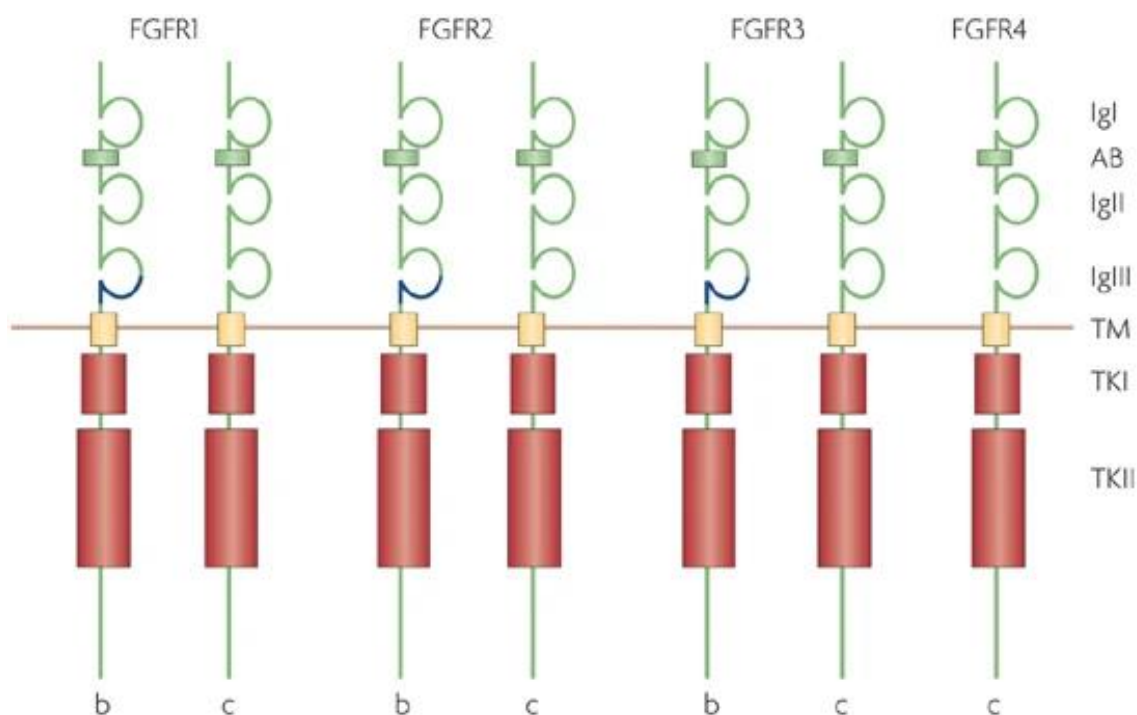
crine FGFs. When FGF crystal structures were analyzed for heparin binding, paracrine FGFs had binding sites with numerous basic residues to react with heparin, while endocrine FGFs lacked these residues, as seen in Fig. 4.¹⁶

Soon after, Makoto Kuro-o et al. published in *Nature* a mouse model wherein a novel gene was knocked out, leading to a severe aging-like phenotype.²⁴ This mouse was

created by serendipity, with a transgene being inserted into the promoter region of this novel gene. The encoded protein was subsequently named α -klotho (KL) after the Greek goddess who spins the threads of human life. The mouse suffered from bone deformities, vessel and organ calcification, and skin atrophy. Interestingly, FGF23 signaling is known to regulate phosphate metabolism, and its dysregulation can result in vascular calcification.²⁵ In 2006, Urakawa et al. showed that KL can act as a co-receptor for FGF23, replacing the role of heparin for paracrine FGFs.²⁶ The affinity of FGF23 binding to KL was much higher than the one previously described for the FGF23-heparin interaction and explained the signaling that occurred within physiological FGF23 concentrations. A second klotho family member was soon discovered, known as β -klotho (BKL). This family member functioned similarly to KL, but instead acting as a co-factor for FGF19 and FGF21. Unlike heparin, the klotho family members have very selective expression patterns, explaining the ability of endocrine FGFs to enter the circulation and to act on only distinct tissues and cell types. Endocrine FGFs are able to directly bind klotho co-receptors via their tail region. FGF19 and FGF21 bind to BKL, with FGF19 being the more potent binder, while FGF 23 binds to KL.²⁷

Characterization of FGFRs

FGFs exert their cellular influence through binding to their cognate FGF receptors, (FGFRs). They are single-pass transmembrane proteins with an extracellular region responsible for FGF binding and an intracellular tyrosine kinase domain responsible for downstream signaling.^{28, 29} Mammals have four FGFR genes, FGFR1-4. This work will mainly focus on the extracellular region, which is characterized by three immunoglobulin (Ig)-like loops known as IgI, IgII, and IgIII. As seen in Fig. 5, FGFRs 1-3 consist in two



Nature Reviews | Neuroscience

Note: From Mason, I., *Initiation to end point: the multiple roles of fibroblast growth factors in neural development*. Nat Rev Neuroscience, 2007. 8(8): p. 583-596 Copyright Springer Nature 2007. Reprinted with permission.

Figure 5. FGFR Splice Variants

splice variants, known as b and c, where variations occur in the IgIII loop. FGFR4 is the

only FGFR without a splice variant, exhibiting only a c isoform.^{30, 31} FGF ligands bind to the IgII and IgIII loop of the FGFR's, forming a dimer with 2 FGFRs and 2 FGFs.³² This

FGF subfamily	FGF	FGFR Binding
FGF1 subfamily	FGF1	All FGFRs
	FGF2	FGFR1c, 3c, >2c, 1b, 4
FGF4 subfamily	FGF4	FGFR1c, 2c, >3c, 4
	FGF5	
	FGF6	
FGF7 subfamily	FGF3	FGFR2b>1b
	FGF7	
	FGF10	
FGF8 subfamily	FGF22	FGFR3c>4>2c>1c>3b
	FGF8	
	FGF17	
FGF9 subfamily	FGF18	FGFR3c>2c>1c>3b>4
	FGF9	
	FGF16	
FGF19 subfamily	FGF20	FGFR1c, 2c, 3c, 4
	FGF19	
	FGF21	
FGF11 subfamily	FGF23	no activity
	FGF11	
	FGF12	
	FGF13	
	FGF14	

Table 1. FGF Specificity for FGFRs^{3, 32}

dimer formation is required for downstream signaling. Without dimer formation, auto-phosphorylation of the tyrosine kinase tail and downstream signaling cannot occur.³² As there are only 4 FGFRs and 22 FGFs, the three FGFR splice variants are extremely important. Since variation occurs in the D3 loop where FGF binding occurs, these splice variants determine the responsiveness of a cell type to specific FGFs, thereby providing an additional level of specificity to FGF stimulation.

Ornitz et al. undertook early work screening FGFRs for stimulation by FGFs.^{3, 33}

To accomplish this, they transfected BaF3 cells with FGFRs, and measured their cell

growth over time using radioactive thymidine incorporation. BaF3 cells are one of the few cell lines, which do not express FGFRs, so it was possible to isolate the effects to only the transfected receptor. Since FGFR3 and FGFR4 show low mitogenic activity due to their weak activation of MAPK signaling,³⁴ the cytoplasmic tails were replaced with FGFR1. While not a perfect assay due to the fact it only measures mitogenic based activity, it gave a starting point for screening the FGFR isoform specificity of the different FGFs. The results are listed below in Table 1. Interestingly, many FGFs were promiscuous, binding to multiple FGFRs with different activation levels, and most FGF family members tended to have similar FGFR binding affinity.

Given the promiscuity and overlap that FGF family members have for FGFRs, additional regulatory levels are needed to ensure specific FGF signaling. Co-factors can exert their control by directing the diffusion of FGFs to reach FGFRs, as well as by increasing the affinity of FGF-FGFR interactions. By cell type-specific expression, co-factors can directly control what FGFs are able to bind.³⁵⁻³⁷ Heparin isoform expression can be controlled by cells, which affects FGF binding to their receptors.³⁸ It has been found that different FGFs and FGFRs bind different heparin species with different kinetics, adding a regulatory layer to FGFR specificity.^{39, 40} Heparin binding to FGFRs plays a dual role, i.e. it is required to increase the affinity of FGFs for FGFRs, and also allows dimerization to occur.³⁸ Without dimerization, downstream signaling cannot occur, so heparin is a required co-factor for cellular FGF effects.⁴¹ The heparin binding sites are rather small within the IgII domain, and line up in the crystal structures on each FGFR in the dimer, showing that two heparin molecules are required, meaning a dimer consist of a

2:2:2 complex of FGF:FGFR:heparin molecules.⁴² Interestingly, even when KL binding occurs to increase FGF affinity, heparin still plays a role to induce dimer formation.⁴³

This heparin binding site on FGFRs offers a unique characteristic for researchers to take advantage of. Unlike FGFs, which have a broad heparin binding site over many amino acids, the FGFR binding site is a small conserved “canyon”.³² Given the promiscuity between FGFRs for FGFs and similarities in the binding pockets for FGFs, designing a specific drug can be rather difficult. Findings showing these heparin sites are unique between

```

FGFR1: 133 DSSSEEEKETDNTKPNRMPVAPYWTSPEKMEKLLHAVPAAKTVKFKCPSSGTP 184
FGFR2: 134 EDDTDGAEDFVSENSNNKRAPYWTNTEKMEKRLHAVPAANTVKFRCPAGGNP 185
FGFR3: 135 EDGEDEAEDTGVDTG----APYWTRPERMDKLLAVPAANTVRFRCPAAGNP 182
FGFR4: 128 EDPKSHRDPSNRHSYPQQ-APYWTHPQRMEKLLHAVPAGNTVKFRCPAAGNP 178

```

Figure 6. Aligned Heparin Binding Sites of FGFR1-4

receptors means this offers a specific target for blockade and modifications via drugs. As seen below in Fig. 6, the heparin binding sites are only conserved 60-75% between different FGFRs. During purification studies, we also observed different characteristics between FGFRs. The isoforms of heparin displayed on GE fast-flow heparin columns were only able to bind FGFR1 and FGFR3, while FGFR2 and FGFR4 did not bind and passed through our columns (data not shown). These unique characteristics imply that FGFRs can be targets to block signaling based on this region, allowing for drugs to differentiate between one select FGFR and preventing toxic off-target effects.

Along with binding FGFs and heparin, FGFRs are also able to bind klotho co-receptors. Unlike heparin, it has been shown that klotho family members only interact with the c splice variants of FGFRs.^{27, 44, 45} When overexpressed in HEK293T cells, it has been found that KL is able to be immunoprecipitated (IP) along with FGFRs in the absence of FGFs.^{26, 44} Further work has shown that both, KL and BKL, can bind FGFRs

alone in Biacore assays with high affinity, showing both KL and BKL have affinity for three different FGFRs.²⁷ As seen in Table 2, klotho family members have a surprisingly strong dissociation constant for FGFRs. KL seems to favor FGFR1, and BKL seems to favor FGFR4. Recently, the crystal structure of the ectodomains of KL and FGFR1, along

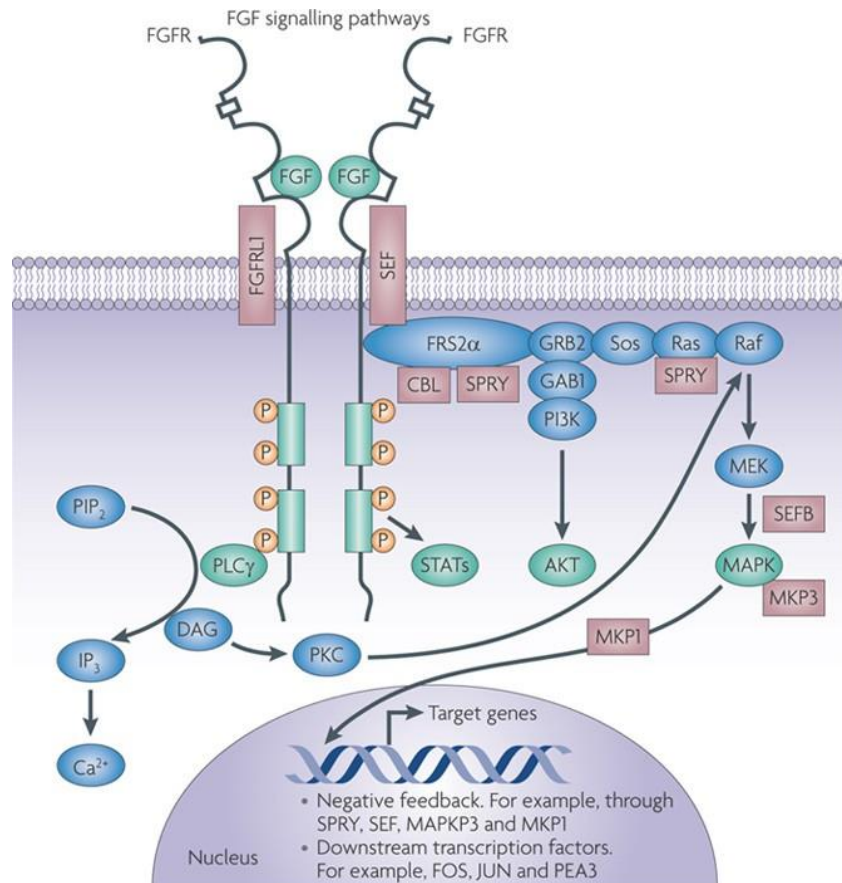
Klotho family member	FGFR			
	FGFR1	FGFR2	FGFR3	FGFR4
KL	72 nM	N/A	82 nM	123 nM
BKL	124 nM	170 nM	N/A	84 nM

Table 2. Binding affinity of FGFRs for Klotho family members²⁵

with FGF23 has been captured.⁴³ While FGFR1 binds FGF23 in a similar mechanism to other FGFs, KL binds FGFR1 in a motif below the FGF, consisting of areas located within IgII and IgIII of the receptor. While the crystal structure of BKL bound to a receptor has yet to be solved, sequence similarities predict that it might occupy the same site that KL binds to in FGFRs.

FGFRs are receptor tyrosine kinases, and their binding to FGFs elicits shape changes in their cytoplasmic tails that leads to phosphorylation and downstream signaling cascades.^{29, 46} Classical FGF23 signaling leads to phosphorylation of fibroblast growth factor receptor substrate 2 α (FRS2 α), which can lead to further activation of the MAPK and AKT signaling pathways.^{34, 47} This activation leads to the strong mitogenic response induced by FGFR1 and FGFR2.³⁴ FGFRs have also been shown to activate the 1-phosphatidylinositol 4,5-bisphosphate phosphodiesterase gamma (PLC γ) pathway⁴⁸ as well as signal transducer and activator of transcription (STAT)3,^{49 50} as seen in Fig. 7. While FGFR1 and FGFR2 are promiscuous with their activation, giving strong levels of STAT and PLC γ activation, FGFR3 and FGFR4 are found to activate these pathways to a

lesser extent, with FGFR4 showing only weak activation of PLC γ .³⁴



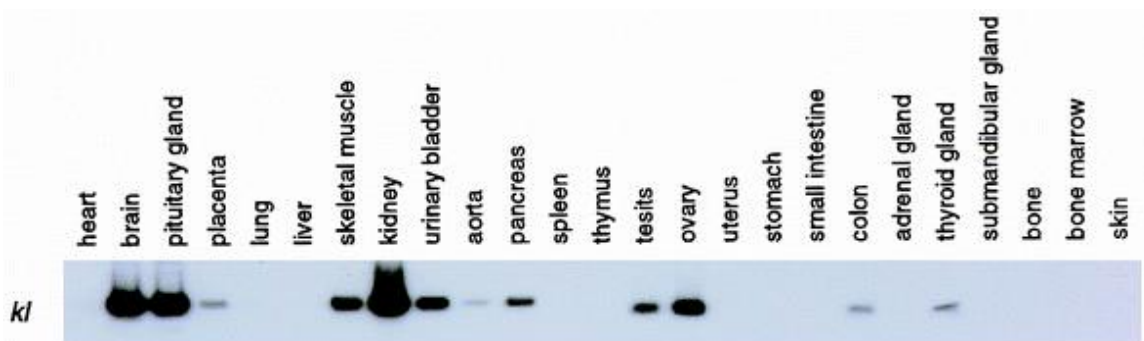
Note: From Turner, N. and R. Grose, *Fibroblast growth factor signalling: from development to cancer*. Nat Rev Cancer, 2010. 10(2): p. 116-29 Copyright Springer Nature 2010. Reprinted with permission.

Figure 7. Downstream Signaling of FGFR Activation

Characterization of Klotho Co-Receptors

As mentioned before, the first klotho family member, KL was discovered by Makoto Kuro-o et al. by serendipity in a knockout mouse. The severe aging phenotype brought up great excitement around this protein, hence its name after one of the three Greek fates. While the loss of KL results in accelerated aging, its general overexpression

increases lifespan 20-30% in mice.⁵¹ Kuro-o et al. demonstrated via RT-PCR that KL has a very specific expression pattern, as seen in Figure 8, with the strongest expression in the kidneys, brain, and pituitary gland.²⁴



Note: From Kuro-o, M., et al., *Mutation of the mouse klotho gene leads to a syndrome resembling ageing*. Nature, 1997. 390(6655): p. 45-51. Copyright Springer Nature 1997. Reprinted with permission.

Figure 8. KL Tissue Expression Pattern by RT-PCR

Most KL research has focused on these three highest expressing organs, with the kidney receiving the most attention. The KL protein is a 1,000 a.a. transmembrane protein, that is composed of a 980 a.a. extracellular domain, followed by a single pass 21 a.a. transmembrane domain and an 11 a.a. intracellular domain.⁵² Given the small size of the intracellular domain, research has mainly focused on the function of the large extracellular region of KL. It has two repeat regions that both span 440 a.a., termed KL1 and KL2. This extracellular region shows a similar homology to glycoside hydrolases, and it was hypothesized that KL has such an enzymatic function.⁵³ However, the recent crystal structure of KL solved by the lab of Moosa Mohammidi showed that this was not the case. They utilized assay kits to show that enzymatic activity was missing, and their crystal structure revealed that one of the key glutamate residues for this class of enzymes in the activation site was mutated in KL.⁴³ Further work by Pfizer recently verified this

while studying the glycosylation sites. They show that KL produced by HEK293 cells has minimal activity, while CHO cell-produced KL with a different glycosylation pattern has a small increase in activity that is still very low. When KL was mutated to replace the missing glycosidase activity residues to glutamate, they were able to markedly increase the activity of this KL mutant form.⁵⁴ Altogether these findings indicate that KL lacks inherent glycosidase activity, and must function mainly as a molecular scaffold for signaling.

As first elucidated by Urakawa et al., KL functions as a co-receptor for FGF23 signaling. When injecting mice and rats with recombinant FGF23, they specifically found that KL expressing organs showed phosphorylation of extracellular signal-regulated kinase (ERK)1/2 and increased expression early growth response 1 (EGR1) transcript, both hallmarks of FGF-based signaling. They were able to IP KL from kidney lysates using a FGF23-based sepharose column, and found KL-induced FGF23 signaling in cells, but not FGF2 signaling. Interestingly, KL expression seemed to slightly inhibit FGF2 based signaling.²⁶ When testing for complex formation in HEK cells, they observed that KL only interacted with FGF23 and FGFR1, elucidating that this was the receptor responsible for the downstream effects of this interaction. They conducted multiple iterations of these FGF23-KL-FGFR1 complex formations with the addition of heparin and received mixed results. In some experiments the addition of heparin increased signaling, while in others it had no effect. This left the field inconclusive on whether heparin could play a role in KL-dependent FGF23 signaling. Kuro-o et al. further looked at KL-binding effects in HEK293 cells. They observed in IP-based experiments that not only did KL bind to FGFR1, but also to FGFR3 and FGFR4. Furthermore, KL expression induced FGF23-

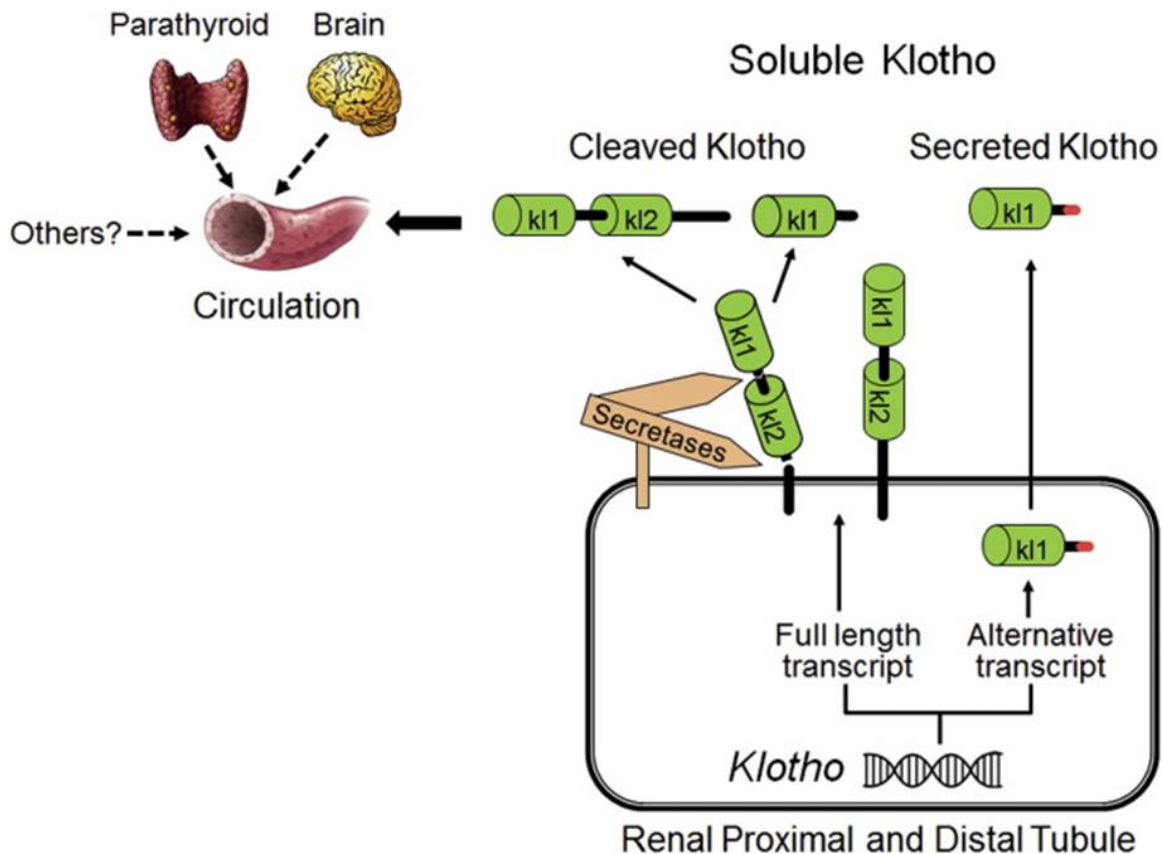
mediated ERK activation,⁴⁴ similar to Urakawa's work. However, given that HEK293 cells express all four FGFR isoforms,⁴³ the analysis of MAPK signaling cannot be used as a readout to elucidate which FGFRs play a role in FGF23-induced signaling. Also as previously stated, since FGFR3 and FGFR4 are much weaker activators of the MAPK pathway, this method of readout may not measure activation of these FGFRs. The lab of LD Quarles elucidated what FGFR isoforms activate KL in the kidney, by generating FGFR3 and FGFR4 knockout mice. They analyzed the physiological effects of FGF23 by crossing these mice with the HYP mouse, which is a genetic mouse model with elevated serum FGF23 levels. They found that FGFR3 or FGFR4 deletion did not affect phosphate excretion, stating in this case that FGFR1 is the principle receptor responsible the renal effects of FGF23. FGFR1 was not included in this knockout screen given that its deletion would cause too many effects outside of FGF23 functions. In this case, it may be that FGFR3 and FGFR4 have roles in the kidney outside of phosphate homeostasis.⁵⁵

The kidney is the organ with the highest expression levels of KL, and the absence of KL from the kidney seems to have the most deleterious effects, as seen with the massive calcification in the KL knockout mouse.²⁴ KL and FGF23 have been shown to be the master regulator of serum phosphate levels, with FGFR1 activation by this complex leading to the lowering of phosphate transporters NaPi-2a and NaPi-2b.⁵⁶ This in turn leads to a decrease in renal reabsorption of phosphate, and phosphaturia.⁵⁶ The disruption of phosphate homeostasis by a loss of KL means FGFR1 activation no longer occurs, phosphate transporter levels stay elevated, and the kidney reabsorbs phosphate. These pathological processes all contribute to the extreme elevations of phosphate in the KL knockout mouse, which in turn causes osteoporosis and bone deformities as well as tissue calci-

fication.²⁴ Razzaque et al. further proved this specific KL effect utilizing a combination of KL and FGF23 knockout models. They first noticed that the FGF23 null mouse had a similar phenotype as the KL knockout mouse, including premature aging, hyperphosphatemia, and calcification.⁵⁷ They further analyzed this link by utilizing the PHEX mouse, which has elevated serum FGF23 levels and suffers from hypophosphatemia. PHEX is a cell surface zinc metalloprotease that is mutated in many patients with FGF23-induced rickets, but its mechanism behind FGF23 regulation remains unclear.⁵⁸ They crossed this mouse with the KL knockout mouse, which under normal conditions develops hyperphosphatemia. If KL was unrelated to the FGF23-phosphate control system, this double mutant mouse would still suffer from hypophosphatemia due to elevated FGF23 levels. But since KL is the co-receptor for FGF23, elevated FGF23 levels in this model had no effect on the kidney.⁵⁹

Along with the kidney, KL is abundantly expressed in both the parathyroid gland and brain. In the parathyroid gland, FGF23 also signals through KL and FGFR1 to regulate parathyroid hormone (PTH) secretion, leading to secondary hyperthyroidism in diseases with FGF23 elevations.^{60, 61} KL is also highly expressed in the brain, and has become more of a recent focus as studies have shown it may be neuroprotective. Mucke et al. have published multiple papers focusing on these neuronal effects, and their work shows that KL expression may negatively correlate with aging and cognition decline. Their first paper found that patients with a rare KL allele, known as KL-VS, have improved cognition function, and overexpression of KL in mice results in improved memory performance.⁶² They analyzed KL expression during disease states, and overexpressed KL in the hAPP mouse model, which is a model for Alzheimer's based neuro-

degeneration. This overexpression increased lifespan and cognitive performance, generating great excitement and expectations in a disease with minimal treatments.⁶³ While the mechanism and FGF23's contribution to these effects has yet to be understood, the



Note: From Neyra, J.A. and M.C. Hu, *Potential application of klotho in human chronic kidney disease*. Bone, 2017. 100: p. 41-49. Copyright Elsevier 2017. Reprinted with permission.

Figure 9. Mechanisms of SKL Release

field has embraced this as a direction to move forward. A recent New York Times article was even published detailing these effects and proposing KL as a one-day option to improve brain function across the population.⁶⁴

A large focus of work around KL has also been its ability to be cleaved and act as a hormone. The secretion has been hypothesized to occur in two separate ways; one by

alternative splicing that leads to secretion of the KL1 domain,⁶⁵⁻⁶⁷ and a second by cleavage of the ectodomain from the cellular membrane of proximal tubule cells,⁶⁸⁻⁷⁰ as seen in Fig. 9.⁷¹ The literature around soluble klotho (SKL) has been very controversial, including its production, detection, and mechanism of action. Multiple reports have shown the detection of the alternatively spliced KL where the KL1 domain is produced. While this has been the case, there has not been convincing data for the protein being expressed. Hillebrand et al. looked further into this,⁷² and they were able to detect a splice variant corresponding with the KL1 domain of KL in the human kidneys, primary kidney cells, and the HK-2 kidney cancer cell line. When they further analyzed the fate of this RNA sequence, they found that it was highly unstable and quickly degraded. When they purified actively translating ribosomes, they found that the full-length membrane KL was the only sequence associated with them. They analyzed protein expression in cell lysates and media, demonstrating that the only KL produced was the size of a full-length protein. Therefore, the authors concluded that the KL1 domain was not translated into a protein. The second mechanism of KL secretion is direct cleavage of the full-length membrane KL. While multiple groups have shown this cleavage can occur, the group of Abraham identified the cleavage location in the KL sequence. They identified the sequence PGPET-LERF as the site, and that specific proteases, i.e. a disintegrin and metalloproteinase (ADAM)10 and ADAM17, are among the enzymes responsible for this cleavage.⁶⁹ They were able to detect cleavage of full-length KL expressed in the COS7 cancer cell line, and produced a mutant KL form with this sequence abolished, which resulted in a lack of detection of cleavage. While their mutant was not detected in media, it was still expressed and active on the cell surface via FGF23 co-receptor function, proving

that this KL form was still expressed by the cells and active. The activity of SKL was measured in conditioned media utilizing an assay measuring the blockade of cell proliferation. This cleavage site is only found in the human KL sequence, leaving open the question of cleavage in other species. The detection of KL is similarly difficult. Given the importance of the role KL plays in aging, much work has been done analyzing its expression levels in disease states. The most reliable work has been pursued on renal KL mRNA in models or patients suffering from kidney damage. Expression has been observed to decrease in multiple animal models, including ischemia reperfusion followed by nephrectomy,⁷³ 5/6 nephrectomy,⁷⁴ Db/Db model of diabetic neuropathy,⁷⁵ chronic kidney disease in humans.⁷⁶

The loss of SKL expression has been proven to be much more complicated. The field has struggled to produce assays to measure KL expression on protein level, as antibody production has proven to be challenging. One assay was developed by Orson Moe's group, consisting of the same antibody to IP SKL out of serum, followed by Western blotting to compare levels.⁷³ Utilizing this assay, they have found decreased KL levels in both animal models and human samples of serum and urine. Unfortunately, this method is not commercially available for use by other groups. Furthermore, commercial ELISAs have been developed to analyze KL reduction as a biomarker for aging and kidney injury. Two major assays have been developed to measure samples by ELISA, one from Cusabio⁷⁷ and another from Takasaki.⁷⁸ The NIGRAM consortium has looked into the detection of SKL levels in multiple publications, characterizing the SKL protein as unstable and difficult to detect in urine.⁷⁹ They followed up with a study comparing multiple commercially available assays, and struggled to find consistency between the

assays.⁸⁰ They found that the assays had a lot of variation between samples, and even comparing the standard controls between each assay led to vastly different readout values. Therefore, they conclude that additional work needs to be done to improve SKL detection before making statements about its effects on disease. Furthermore, another group utilized the previously mentioned IP assay and compared it with the commercially available ELISAs⁸¹ and demonstrated lower detection limits and stronger correlation between patient sample expression and results from their IP assay. Summarizing these findings, SKL detection and correlation as a biomarker of disease is difficult to decipher.

SKL activity has also been an area of recent interest and controversy. Kuro-o et al. showed that overexpression of the full-length form of KL extends the lifespan of mice via FGF23-dependent and -independent signaling. They found that KL had effects on both IGF1 signaling and insulin sensitivity. They found KL inhibited IGF1 signaling, blocking receptor phosphorylation and downstream signaling. When they inhibited IGF1 signaling in the KL knockout mouse, they were able to rescue some of the deleterious phenotypes and extending lifespan.⁵¹ Furthermore, SKL has been shown to have a multitude of effects interfering with other pathways, including WNT signaling,⁸² oxidative stress,⁸³ ion channel modification,⁸⁴ and nitric oxide synthesis via cyclic AMP activation.⁸⁵ Recent work has also shown that SKL has the ability to bind lipid rafts, downregulating lipid-dependent AKT signaling and decreasing endocytosis.⁸⁶ Mohammadi et al. questions many of these independent binding effects, stating that SKL effects are depended on FGF signaling in light of the recent crystal structure they published of SKL bound to FGFR1 and FGF23.⁴³ The overexpression of KL has a multitude of different effects, such as neuroprotection and anti-cancer, challenging the above statement given

the current data. One of the most interesting effects of SKL being anti-proliferative effects,^{87, 88} given that if SKL is acting as a scaffold for FGFR1 activation, this should lead to inducement of cancer rather than blockade.

BKL is the other member of the klotho family that has been shown to function as an endocrine FGF co-factor. Its function was discovered by Makoto Kuro-o's et al. in two seminal papers showing it interacts with FGF19 and FGF21, the two other endocrine FGF family members.^{45, 89} Just like KL, BKL expression occurs in very specific tissues, with the liver, adipose tissue, and pancreas showing strong expression.⁹⁰ BKL shares 41% sequence similarity to KL, and is also a single-pass transmembrane protein with a minimal sized cytoplasmic tail.⁹⁰ Similarly to KL and FGF23, BKL knockout mice show an overlapping phenotype to that of FGF19 knockout mice, with a suppression of bile acid synthesis.⁹¹ When BKL was IP'ed from HEK293 cell lysates, the elute contained FGFR1 and FGFR4 as the strongest signals, with a weak signal of FGFR2.⁸⁹ Moosa Mohammadi further detailed this analysis using surface plasmon resonance (SPR) experiments, and validated that BKL had a strong affinity for FGFR1 and FGFR4.⁹² He further analyzed the interaction of BKL and FGFs, and found a strong binding affinity of BKL for both FGF19 and FGF21, but not any for FGF23. By using FGF-based peptides as blockers, he further found that it was the C-terminal region of both FGFs that interacted with BKL. When comparing the two FGF isoforms, he found that FGF19 had a much more potent affinity for BKL. While examining downstream signaling, Kuro-o et al. analyzed ERK activation, similarly to FGF23-FGFR1-KL activation. Their group could demonstrate ERK was phosphorylated in hepatocytes treated with FGF19, and white adipose tissue treated with FGF21. When they used the 3T3-L1 adipocyte cell line, they

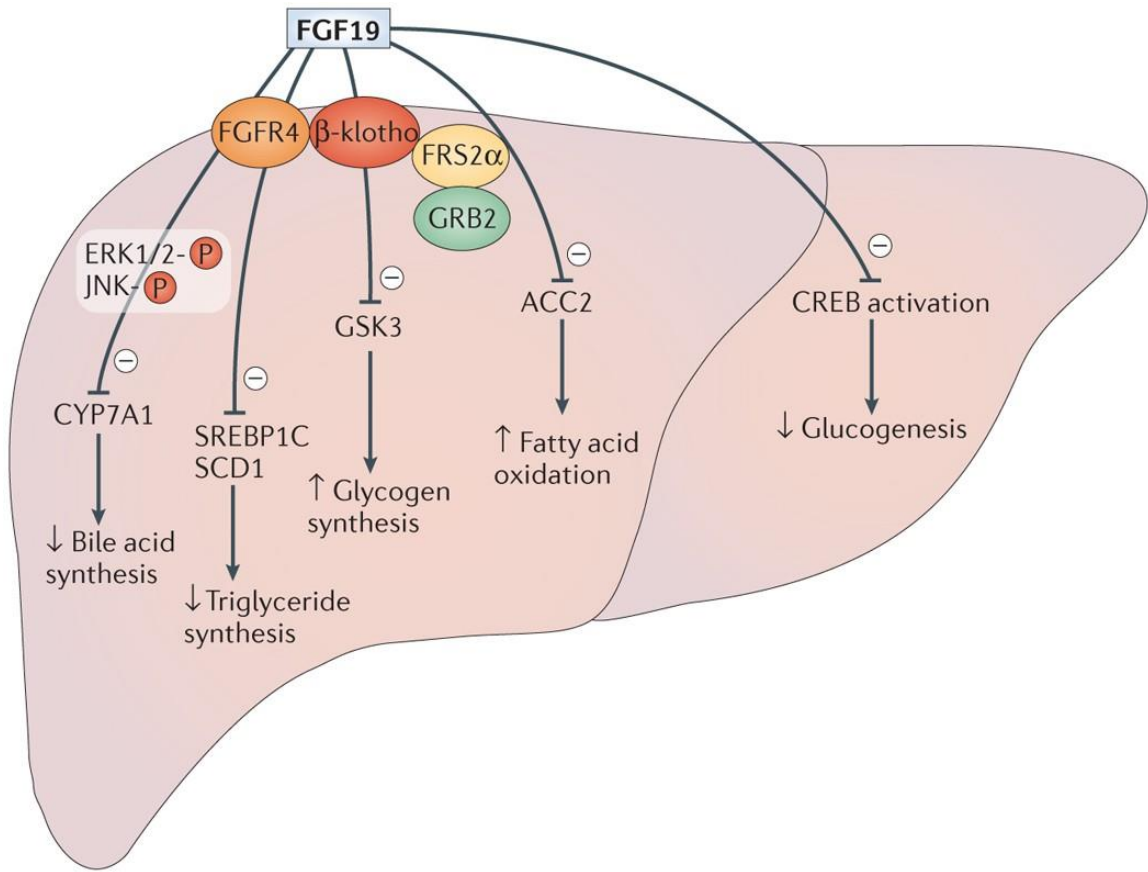
found responsiveness to both FGF19 and FGF21.⁴⁵ When analyzing receptor profiles of these cells, they found that hepatocytes heavily expressed FGFR4, adipose tissue FGFR1, and the adipocyte cell both FGFR isoforms. By this combination of BKL and FGFRs, these cells were able to regulate the way they respond to endocrine FGFs. Based on this work, klotho co-receptors add another layer to FGF signaling regulation, whereas tissues regulate FGF responses based not only on FGFR expression, but also by klotho expression. Unlike KL, there is much less controversy in regards to the function of BKL. A soluble form or cleavage site for BKL has yet to be described in the literature, and functional binding and signaling effects for BKL outside of FGF signaling have yet to be proposed.

Endocrine FGFs

FGF19 (mouse analog FGF15) is a secreted FGF that is 216 a.a. in length.⁹³ FGF19 was the first of the endocrine FGFs to be described,⁹³ and its low affinity for heparin compared to other paracrine FGFs was intriguing.¹⁶ This lower affinity allows FGF19 to be excreted and act as a hormone, targeting specific tissues throughout the body. FGF19 has been shown to signal in complexes with FGFRs and BKL exerting effects on tissues expressing these proteins.⁴⁵ FGF19 was found to be synthesized in the small intestine, via a signaling loop between the gut and liver. The liver naturally synthesizes bile acid for storage in the gall bladder and release into the small intestine. When there is ample bile acid, the Farnesoid X receptor (FXR) in the small intestine is activated, leading to increased expression of FGF19, which in turn signals in the liver via FGFR4 and BKL, leading to a suppression of CYP7a1 and turning off bile acid synthesis. When bile acid levels are low, the FXR receptor is not activated and FGF19 synthesis is shut off, which

in turn leads to bile acid synthesis in the liver.⁹⁴⁻⁹⁶ In addition to bile acid synthesis, FGF19 can exert other metabolic effects on the liver and hepatocytes, including lowering lipid content and inducing proliferation, as shown in Fig. 10.²⁰ FGF19 has also been shown to play a role in both lipid and glucose metabolism by signaling through adipose tissue.⁹⁷⁻⁹⁹ Given that FGF19 is promiscuous in its receptor affinities, it has been shown to act in this fashion through FGFR1 and BKL.⁹⁸ More recently, FGF19 has been shown to play a role in muscle mass regulation, promoting hypertrophy. Given the expression of both FGFR1 and FGFR4 along with BKL, this activation likely occurs through both receptors.¹⁰⁰

While most work on FGF19 activation has focused on BKL dependent effects, some literature has pointed to effects that are independent of BKL expression. Early work with FGF19 showed that it could bind the ectodomain of FGFR4 in the presence of heparin *in vitro*.⁹³ While the crystal structure reveals a highly mutated heparin binding site with low affinity,¹⁶ mutation analysis shows that beta-sheet loops 1-2 and 10-12 of FGF19 are still able to bind heparin.¹⁰¹ The C-terminal region of FGF19 has been shown to be required for BKL binding, and when a FGF19 variant missing this region is injected into mice, the adipocyte-dependent FGFR1-3 effects of FGF19 are abolished. Surprisingly, the FGFR4-dependent effects in the liver still occurred.¹⁰¹ While the affinity is lower for heparin, it leaves open the notion that BKL-independent effects may occur.



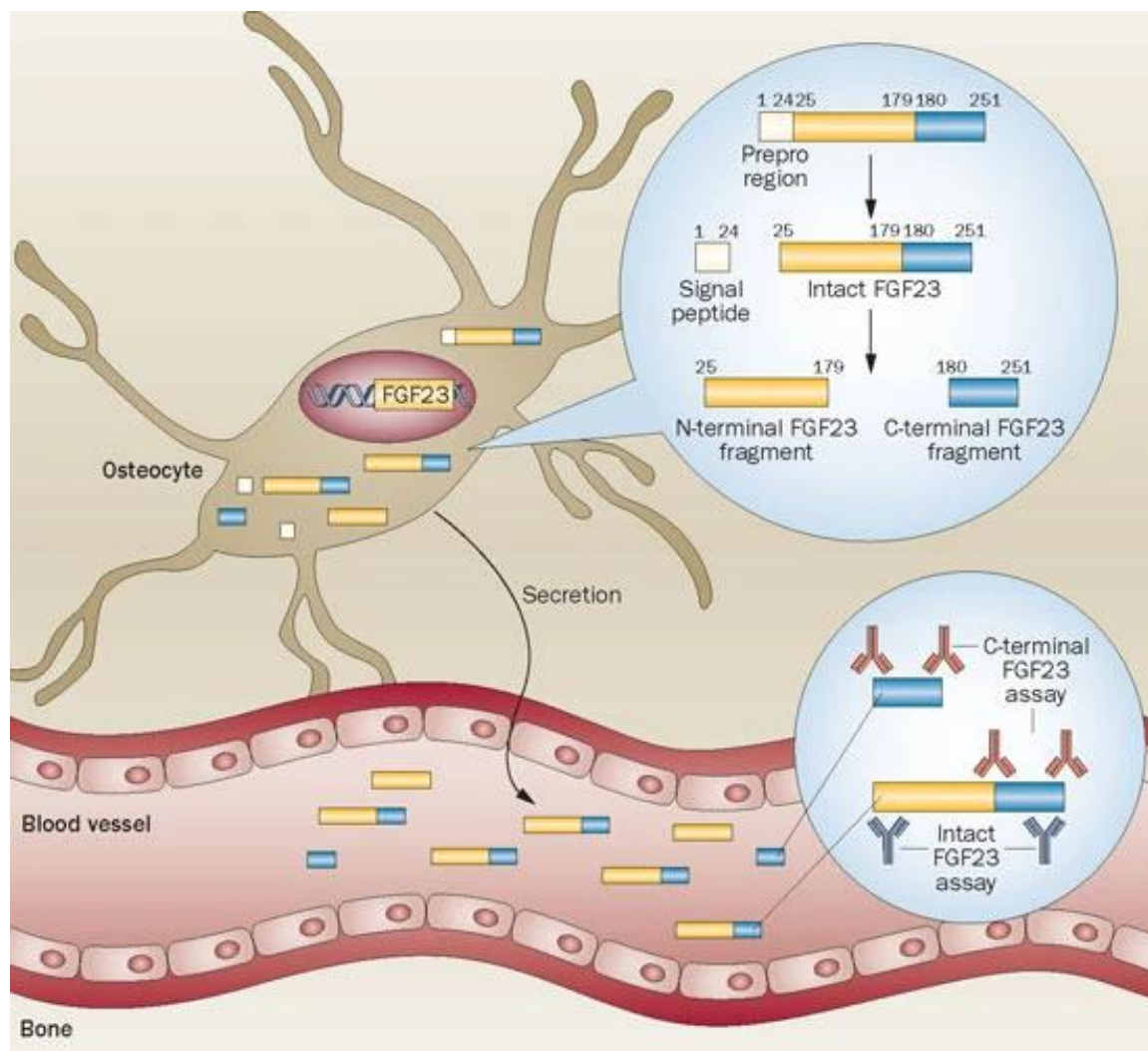
Nature Reviews | Drug Discovery

Note: Degirolamo, C., C. Sabbà, and A. Moschetta, *Therapeutic potential of the endocrine fibroblast growth factors FGF19, FGF21 and FGF23*. Nat Rev Drug Discov, 2016. 15(1): p. 51-69 Copyright Springer Nature 2016. Reprinted with permission.

Figure 10. Effects of FGF19 on the Liver

FGF21 has been shown to be a major regulator of energy metabolism and glucose levels.¹⁰² It is predominately expressed in the liver,¹⁰³ and its expression is controlled by peroxisome proliferator-activated receptors (PPAR) γ activation. FGF21 has been shown to be upregulated under conditions of metabolic stress, such as starvation or a high fat diet.¹⁰⁴ The excitement around FGF21 has been its focus in adipocyte signaling. It has been shown to bind to BKL and FGFR1, leading to an increased uptake of glucose.^{45, 102} Unlike insulin-dependent effects on glucose uptake, this was shown to be a slow effect, taking six hours for increases in uptake to occur and dependent on glucose transporter (GLUT) 1 expression.¹⁰² These FGF21 signaling events were shown to be BKL-dependent,¹⁰⁵ and activation of FGFR 1-3, with FGFR1 being the strongest binder of FGF21.⁴⁵ Given that FGF21 has been shown not to bind FGFR4, it is believed to be synthesized in the liver but unable to exert any effects even in the presence of BKL.⁹⁸ The long-term effects of this change in glucose metabolism in adipocytes has shown to have drastic changes. FGF21 treatment of animals induces a decrease in plasma glucose levels and a tight glycemic control.¹⁰² Overexpression of FGF21 in mice leads to weight loss in obese models, and a browning of adipocytes due to increases in uncoupling protein (UCP)1 and thermogenesis.^{106, 107} Interestingly, these effects lead to an extension of lifespan in mice, elucidating the hypothesis of FGF21 as an anti-aging hormone.¹⁰⁸ While these effects seem to be beneficial, FGF21 has also been shown to play roles in bone loss¹⁰⁹ and reproduction,¹¹⁰ leading to question its therapeutic potential. FGF21 has also been shown to have recent actions on the brain, with its signaling inducing a drinking response in mice and humans in response to alcohol consumption or dehydration.¹¹¹ Unlike

FGF19, no BKL-independent effects have been published for FGF21, with FGF21 having the weakest affinity of all FGFs for heparin.¹⁴

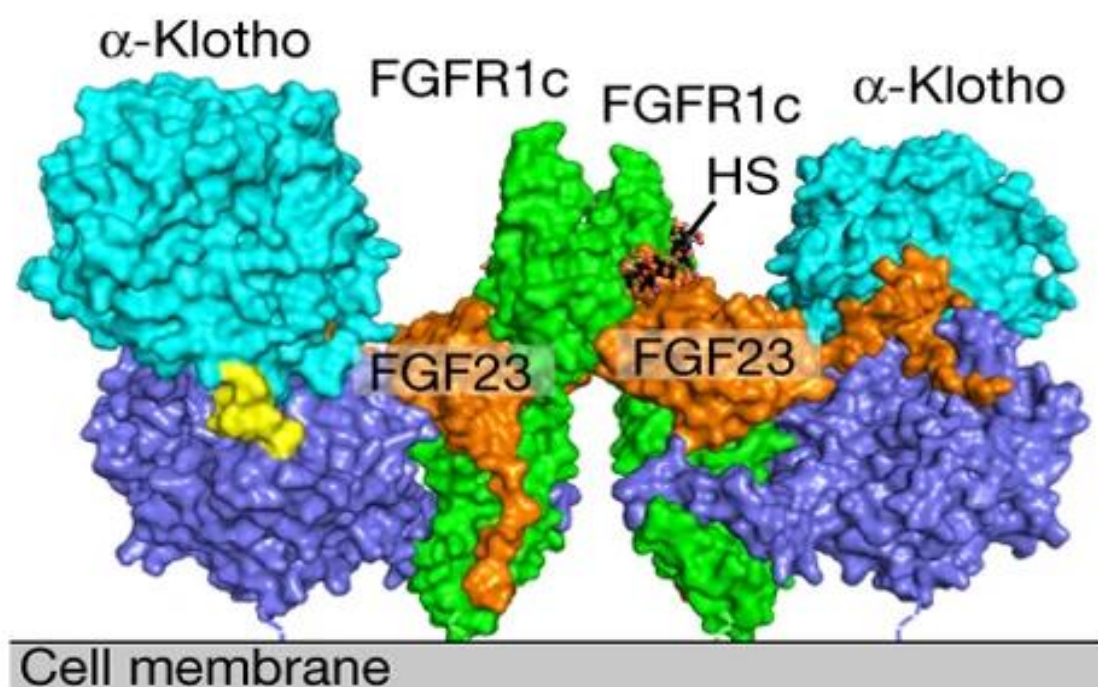


Note Komaba, H. and M. Fukagawa, *The role of FGF23 in CKD--with or without Klotho*. Nat Rev Nephrol, 2012. 8(8): p. 484-90. Copyright Springer Nature 2012. Reprinted with permission.

Figure 11. Mechanism of FGF23 Production

FGF23 is a 251 a.a. protein that has a 24 a.a. leader sequence that is cleaved during its secretion.¹¹² The mechanism behind FGF23 regulation and expression is not well understood, but it is believed phosphate levels play a role, with high serum phosphate concentrations inducing its expression.¹¹³ While a high phosphate diet or elevated serum

phosphate induces FGF23 elevations, there are conditions where FGF23 rises independent of phosphate.¹¹⁴ Treatment of mice or cultured osteoblasts with active vitamin D shows marked increases in FGF23 production.¹¹⁵ Interestingly, in tumor induced rickets, which is a rare tumor that secretes high levels of FGF23, FGFR1 is commonly over expressed or contains constitutively active mutations.¹¹⁶ The role that FGFR1 activation plays in FGF23 regulation outside of this tumor is poorly understood, but given this ef-



Note: Chen, G., et al., *alpha-Klotho is a non-enzymatic molecular scaffold for FGF23 hormone signaling*. Nature, 2018. 553(7689): p. 461-466 Copyright Springer Nature 2018. Reprinted with permission.

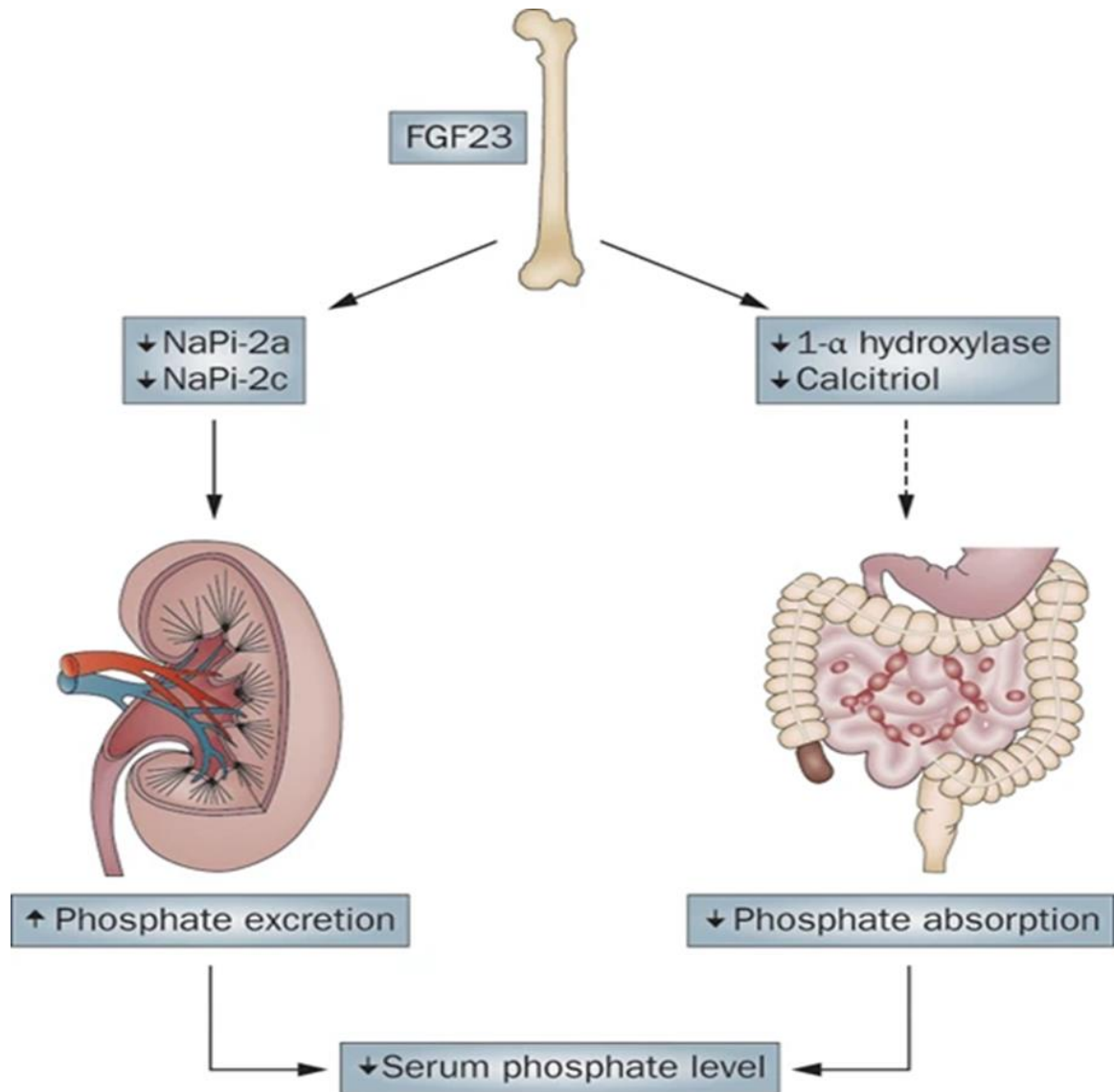
Figure 12. Crystal Structure of FGF23-FGFR1-KL Complex

fect there may likely be a physiological role FGFR1 plays that is not yet known.

Prior excretion, FGF23 has a second layer of regulation based on its proteolytic cleavage. FGF23 is mainly produced in osteocytes, and cells seem to constantly produce FGF23 protein and regulate its activity downstream of translation.¹¹⁷ After translation

FGF23 can enter two different posttranslational modification pathways. The amino acids R¹⁷⁶H¹⁷⁷T¹⁷⁸R¹⁷⁹S¹⁸⁰ are the target of this modification process, which are highly conserved across species expressing FGF23.¹¹⁸ One process is that FGF23 can be phosphorylated by family with sequence similarity (FAM20C), which protects FGF23 from other forms of modifications. This leaves FGF23 unprotected from cleavage via furin proteases. This results in two inactive fragments that are excreted, both C- and N-terminal fragments.¹¹⁹ The reason behind bone tissue making a cleaved version of FGF23 that is inactive is poorly understood, and it is possible that these fragments have some unknown function. Work has been done showing that injections of large amounts of C-terminal fragment can interfere with intact FGF23 signaling, and show therapeutic potential in certain instances.¹²⁰ When FGF23 is not phosphorylated, it is glycosylated by Polypeptide N-Acetylgalactosaminyltransferase (GALNT)3 on T¹⁷⁸.¹²¹ This leads to protection of its cleavage by furin proteases, and the excretion of a full-length FGF23 that is intact and active. A synopsis of this process can be seen in Fig. 11. Once secreted from bone into the bloodstream, the half-life of FGF23 is about 30-60 minutes.^{122, 123} Classical FGF23 signaling consists of binding to FGFR1 and KL, so tissues expressing these proteins are sensitive to FGF23's effects. FGF23 binding leads to downstream activation of the MAPK pathway and to transcriptional changes in proteins, the most recognized one being EGR-1.²⁶ A recent crystal structure has been solved modeling this complex. The N-terminal region of FGF23 binds to FGFR1, while the C-terminal tail of FGF23 binds to both the KL1 and KL2 domains of KL. KL also binds to FGFR1, creating a complex that leads to downstream activation. Interestingly, this complex also contains heparin, which is bound to both FGF23 and FGFR1. The crystal structure of this complex can be seen in

Fig. 12. The major expression site of KL and FGFR1 is the kidney,²⁴ where FGF23 can act to modulate the expression of phosphate transporters in the proximal tubule.²⁶ When expressed, the transporters sodium-phosphate cotransporter (Na-Pi)2a and Na-Pi2c cause the kidneys to reabsorb phosphate back into the bloodstream. Therefore, FGF23 signaling



Note: Razzaque, M.S., *The FGF23-Klotho axis: endocrine regulation of phosphate homeostasis*. Nat Rev Endocrinol, 2009. 5(11): p. 611-9 Copyright Springer Nature 2009. Reprinted with permission.

Figure 13. Effects of FGF23 Signaling

decreases their expression, causing phosphate to be excreted into the urine.¹²⁴ FGF23 can also signal in the parathyroid gland to suppress PTH secretion, which in turn leads to modifications in vitamin D levels and expression of phosphate transporters in the gut.¹²⁵⁻¹²⁷ This combination of events leads to a tight regulation serum phosphate as seen in Fig. 13, and any changes can lead to multiple disease states. FGF23 expression has also been shown to occur in the brain.¹¹² Given that KL is also expressed in select brain regions along with FGFR1, signaling very likely may occur but its function has yet to be understood.

Endocrine FGFs in Disease and Therapeutics

Given the roles of endocrine FGFs in metabolism and their ability to crosstalk between organs to maintain body homeostasis, their dysregulation can lead to devastating disease states, while influencing their action through therapeutic intervention can also show great promise. FGF19 has been implicated in multiple disease states, and given its mitogenic potential in the liver through FGFR4 signaling in hepatocytes, one of these is cancer. Under physiological conditions, FGF19 can induce hepatocyte proliferation for liver growth and repair when needed^{128, 129}, but its overexpression can lead to uncontrolled cell growth. The FGF19 transgenic mouse, where FGF19 is overexpressed in skeletal muscle, elucidates this role that FGF19 can play.¹³⁰ FGF19 was overexpressed at high levels with an average of 77 ng/mL compared with physiological levels of under 0.5 ng/mL¹³¹, and by two months of age these mice showed markers of cancer, and by ten months of age they developed hepatocellular carcinoma. While FGF19 is mainly expressed in the gut, cancer cells have the ability to ectopically express FGF19 which in an autocrine fashion signals through FGFR4.^{132, 133} The most common form of cancer studied that this auto-

crine activation by FGF19 occurs has been hepatocellular carcinoma, similar to the transgenic mouse.^{132, 134, 135} This has been shown to lead to a more aggressive cancer and a poorer patient prognosis, with this type of cancer more frequently gaining drug resistance.^{132, 134} Blocking FGF19 by antibody has been attempted as a therapeutic approach by Genentech, but the antibody proved to be too toxic. By inhibiting FGF19's native function of bile acid synthesis regulation, treated monkeys suffered from severe diarrhea and death via malnutrition.¹³⁶ There is currently a drug being investigated in a stage I clinical trial, BLU-554, that takes the opposite approach and blocks FGFR4. Early safety profile data does not show the same deleterious effects that FGF19 blockade showed. While liver cancer has gotten the bulk of the attention, it has been recently shown that the FGF19/FGFR4 axis can be activated in breast¹³³ and lung¹³⁷ cancer.

A second area of interest behind FGF19 work has been in chronic liver diseases. Nonalcoholic fatty liver disease (NAFLD) is estimated to affect up to 30% of the US population, and its progression can lead to Non-Alcoholic SteatoHepatitis (NASH), where there are limited treatment options aside from liver transplantation.¹³⁸ NAFLD is characterized by fat accumulation and deposition in the liver, which as it progresses, leads to fibrosis and scarring of the liver.^{139, 140} Hepatocytes are the main cell type undergoing injury during this process, where they undergo apoptosis, demonstrate ballooning, and overall liver inflammation.¹³⁹ The biggest risk factor for NAFLD is obesity, where many patients suffer from dysregulated glucose metabolism and fat storage due to diet and additional chronic comorbidities.¹⁴¹ Given FGF19's ability to signal in both hepatocytes and adipocytes, it has an attractive potential to modulate both the cells being directly affected and the indirect causes. The problem with FGF19 administration would be its

mitogenic potential, but work was done that shows FGF19's mitogenic potential was separate from its metabolism effects, and mutations were able to create variants that only induced one effect.¹⁰¹ NGM Bio was able to utilize this to create an FGF19 variant with three mutations known as NGM282, which signals in conjunction with both, FGFR4 and FGFR1, and with BKL. Interestingly, this variant was even able to block FGF19's cancer effects by outcompeting the wildtype protein for receptor binding.¹⁴² They show that wildtype FGF19 activated STAT3 when binding to FGFR4, while their mutant variant did not induce this effect. When investigating the effects of NGM282 on mouse models of diabetes and in humans, administration lowered blood glucose levels as well as body weight. Diabetes is a major causative agent of liver damage and NAFLD, and both mice and patients were protected from further liver damage, and actually showed improvements in liver function.¹⁴³ A further phase 2 trial was conducted, including patients with further advanced NASH, and similar to the diabetes based trial, patients showed improvements in liver fat content, body weight, and glucose metabolism.¹⁴⁴ Given the lack of treatment options in this patient population and strong effects seen, NGM282 is currently moving into pivotal phase III trials and showing the promise that modulating endocrine factors may have.

Given FGF21's ability to modify glucose metabolism and energy expenditure, and the high amount of the population suffering from metabolic diseases, its levels in disease settings and therapeutic potential has also been explored. FGF21 has garnered extra excitement due to its lack of mitogenic activity, with transgenic mice not suffering from cancer like FGF19 mice.¹²⁹ Work has looked at FGF21 levels in these metabolic diseases, and surprisingly its levels are found to be elevated in NAFLD, obesity, and type II diabe-

tes.^{145, 146} While it could seem counterintuitive to administer a protein where levels are already elevated, it has been hypothesized that FGF21 could be a protective elevation, and further levels could lead to further protection.²⁰ This idea has been shown in mice, where models of obesity do not respond to lower levels of FGF21, but under stronger administration, there are still beneficial effects.¹⁴⁷ This is further verified by FGF21 knockout, where mice were fed a ketogenic diet are much more sensitive to deleterious effects. These mice showed decreased glucose regulation, impairment in ketogenesis, and increased liver damage.^{148, 149}

FGF21 administration has shown many beneficial effects in models of disease. FGF21 has been shown to directly signal in beta-cells, preventing apoptosis and improved glucose metabolism. Given that beta-cell death occurs during diabetes and results in poor outcomes, this mechanism is exciting to help preserve pancreas function.¹⁵⁰ FGF21 signaling also results in increased energy expenditure in adipocytes. Mice over-expressing FGF21 show an increase in white fat conversion to brown fat, and an overall decrease in fat levels.^{106, 151} Given these effects on glucose lowering and fat levels, excitement has grown around therapeutic potentials. The first drug, LY2405319 was a mimetic version of FGF21 that resulted in an increased half-life of three hours.¹⁵² This drug showed great promise in models of diabetes in monkeys, showing marked improvements in body weight, blood insulin, and glucose levels.^{152, 153} Unfortunately, administration in humans did not have the marked effects that administration on monkeys had.¹⁵⁴ Even at high doses, only modest decreases in glucose were achieved, making this a poor drug for long-term administrations in a chronic disease. Multiple other mimetics have been attempted where half-life was increased, but studies have all stalled out.^{155, 156} Recent work

has looked to take the opposite approach to increase efficacy instead of prolonging half-life.¹⁵⁷ While a more potent molecule has yet to reach clinical trials, this may prove a more valuable strategy to improve the modest effects seen in early FGF21 iterations.

Unlike FGF19 and FGF21, FGF23 has shown less promise as a therapeutic agent and seems to have more deleterious effects in disease states. The function of FGF23 as a phosphate-regulating hormone elucidated in FGF23 related rickets diseases. In this disease, there are mutations in proteins that regulate FGF23 expression and processing, leading to serum elevations of FGF23 and decreases in serum phosphate levels.¹⁵⁸ The long-term manifestations of this disease include hearing loss, bone deformities, and muscle wasting.¹⁵⁸ FGF23-induced rickets can be caused by defects in multiple ways, one being mutations in the FGF23 protein, leading to cleavage resistance and elevations of active FGF23.¹⁵⁹ There can also be mutations in proteins related to FGF23 regulation, including (PHEX), dentin matrix acidic phosphoprotein (DMP1), and (FAM20C).¹⁶⁰⁻¹⁶² Recent work has shown a FGF23 blocking antibody developed by Kirin can prevent phosphate wasting in these patients and alleviate some of the symptoms associated with these effects.¹⁶³ Tumor induced rickets is another rare form of phosphate wasting, where slow growing mesenchymal-based tumors overexpress and excrete FGF23, leading to low serum phosphate levels.¹⁶⁴ Given the slow growth of these tumors, many can be removed surgically, giving a functional cure and restoring physiological FGF23 levels.¹⁶⁵ While these patients suffer from deleterious effects of FGF23 elevations, mitogenic potential and cancer is not one of the outcomes, similar to FGF21 elevations.

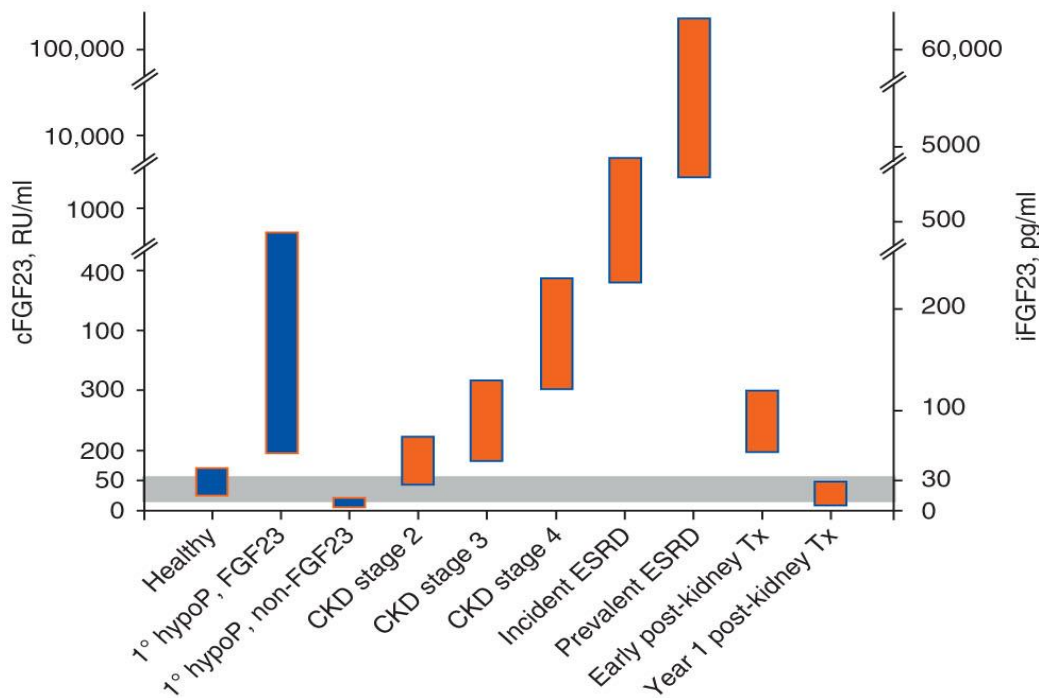
Chronic Kidney Disease (CKD)

CKD is defined as the progressive loss of kidney function over time. It is classified by two methods; abnormal albumin excretion or decreased kidney function measured by glomerular filtration rate (GFR).¹⁶⁶ GFR can be measured via creatinine levels by multiple methods; the less practical technique is the collection of urine over 24 hours along with a single serum measurement. The more common and practical technique is a single collection of serum creatinine, and using this value in an equation along with other patient parameters in either the Cockcroft-Gault or the Modification of Diet in Renal Disease Study estimating equations.¹⁶⁷ The National Kidney Foundation has divided CKD into five stages based on GFR levels to categorize the severity of disease:¹⁶⁸

- Stage 1: normal eGFR ≥ 90 mL/min per 1.73 m^2 and persistent albuminuria
- Stage 2: eGFR between 60 to 89 mL/min per 1.73 m^2
- Stage 3: eGFR between 30 to 59 mL/min per 1.73 m^2
- Stage 4: eGFR between 15 to 29 mL/min per 1.73 m^2
- Stage 5: eGFR of < 15 mL/min per 1.73 m^2 or end-stage renal disease (ESRD)

CKD is a massive problem in the US, with an estimated 13% of the population or 37 million Americans having some form of the disease.¹⁶⁹ The breakdown of CKD stages in the US population is: 1.8% for stage 1, 3.2% for stage 2, 7.7% for stage 3 and 0.35 % for stages 4 and 5. Stage 5 CKD is also known as ESRD, where patients have little to no kidney function.¹⁷⁰ These patients undergo dialysis, which is the temporary replacement of renal filtration or kidney transplant as the only options for treatment.¹⁷⁰ Along with a loss of kidney function, CKD patients suffer from other symptoms related to kidney failure

including: anemia, mineral metabolism, cardiovascular disease, inflammation, and dyslipidemia.¹⁶⁷ The costs of caring for these patients is an extreme burden on the healthcare system, with estimations on costs of just CKD stages 2-4 to Medicare being \$49 billion alone.¹⁷¹ Due to the shortage of usable donor kidneys, 70% of ESRD patients



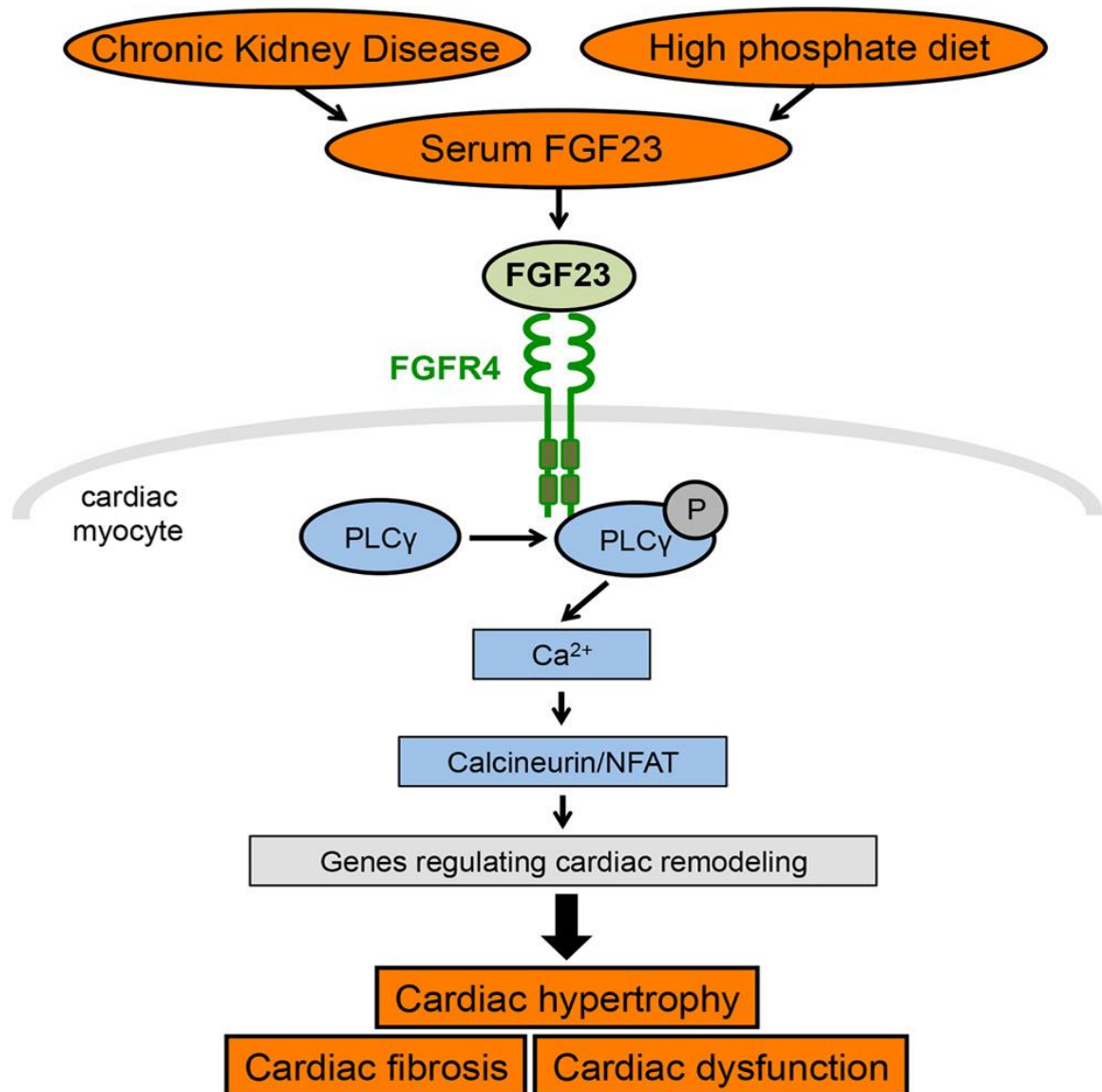
Note: Wolf, M., *Update on fibroblast growth factor 23 in chronic kidney disease*. *Kidney Int*, 2012. 82(7): p. 737-47 Copyright Elsevier 2012. Reprinted with permission.

Figure 14. FGF23 Levels During CKD

will have to undergo dialysis.¹⁷² Patients on dialysis have a 25% mortality rate after one year, and the dialysis five year survival rate is a grim 35% whereas kidney transplant patient's mortality rate is 3% after five years.¹⁷³

CKD and cardiovascular disease (CVD)

Patients with CKD have an increased mortality, with CVD being the most common form of death independent of CKD stage.¹⁷⁴ By ESRD 50% are due to CVD,¹⁷³ and the risk of suffering from CVD is 10-20 times in a CKD than the normal population.¹⁷⁵ Left Ventricle Hypertrophy (LVH) is a key finding in patients with CKD, which is a



Note: Grabner, A., et al., *Activation of Cardiac Fibroblast Growth Factor Receptor 4 Causes Left Ventricular Hypertrophy*. *Cell Metab*, 2015. 22(6): p. 1020-32. Copyright Elsevier 2015. Reprinted with permission.

Figure 15. FGF23 Signaling in Cardiac Myocytes

thickening of the left ventricle of the heart. LVH is evident in patients with stage 3 CKD with 16-31% of patients displaying this, and 90% of ESRD patients.¹⁷⁶ This pathology has been shown to contribute to diastolic dysfunction, congestive heart failure (CHF), and sudden cardiac death.¹⁷⁷ While early work contributed LVH in these patients to increases in blood pressure,¹⁷⁸ the lack of treatment success in blood pressure lowering therapy implies there is more at play than just this.^{179, 180}

FGF23 and CKD

Since the kidney is responsible for mineral metabolism, kidney failure results in disordered function of this. The main complication is hyperphosphatemia, where overexpression of phosphate transporters in the failing kidneys lead to an increased uptake in the tubules and lack of urinary excretion.¹⁸¹ Serum phosphate increases do not manifest in patients until Stage 4 of CKD, but by ESRD almost all patients show substantial increases in this.¹⁸² Given that FGF23 is one of the main hormones responsible for phosphate regulation, its levels become highly dysregulated in patients with CKD. Patients show marked elevations of FGF23 in early stages of CKD, even before increases in serum phosphate are detected.¹⁸³⁻¹⁸⁵ As is shown in Fig. 14, elevations of FGF23 can reach 1000-fold above normal in individuals with ESRD. Dialysis has minimal effects on these levels, with the only fix being a kidney transplant.

The increases in FGF23 levels have been shown to correlate with mortality and specifically CVD.^{184, 186, 187} Furthermore, FGF23 levels are specifically shown to associate with increases in LVH.^{188, 189} Our group, as well as others have shown that FGF23 is not just a biomarker of CVD, but it can directly act on the heart in these situations and induce cardiac hypertrophy.^{183, 190-192} This was previously not hypothesized as the heart does not

express KL, the necessary co-factor for FGF23 signaling. Our group demonstrated that under conditions of these extreme FGF23 elevations, FGF23 is able to signal through FGFR4 expressed on cardiac myocytes and induce an increase in cell area.^{192, 193} Since FGFR4 is a poor activator of the MAPK pathway, this was previously not detected in EGR1-based screens of cardiac tissue,²⁶ and instead activates the pro-hypertrophic PLC γ /calcineurin/NFAT pathway, shown in Fig. 15.

CHAPTER 2: SKL MODIFIES FGF23 SIGNALING

Background

The ectodomain of KL can be proteolytically cleaved in the kidney, creating a soluble fragment, known as SKL, that can traverse the body.^{69, 194, 195} SKL has been shown to have pleiotropic, tissue protective effects, and is believed to act as a hormone to perform these functions. These actions have been hypothesized to be through multiple mechanisms, including lipid raft binding,⁸⁶ glucuronidase activity,⁶⁷ and insulin-like growth factor (IGF) signaling modification.⁵¹ The recent crystal structure of SKL binding FGFR1 and FGF23 has called this into question, pointing towards SKL's effects being FGF23-dependent. If SKL does act as a FGF23-dependent co-receptor,⁴³ the question is

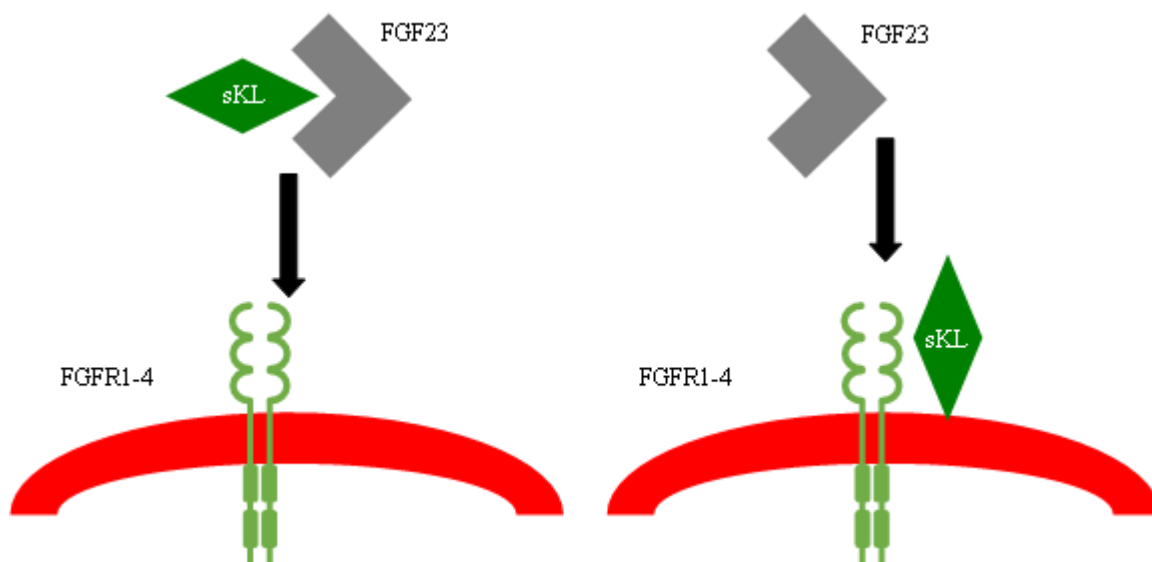


Figure 16. Hypothesis of SKL Modulation of FGF23 Signaling

raised still for its order of operations. A crystal structure is a snapshot in time and does not answer the question how this complex is formed. As seen in Fig. 16, SKL could still function via two different methods to modulate signaling. SKL could be secreted and bind to FGF23 in serum, thereby modulating FGF23's affinity for FGFRs. Alternatively, SKL could circulate and bind to FGFRs, creating a high affinity binding pocket for FGF23.

Since animal models of CKD have been shown do have decreased SKL levels, and SKL has been shown to be protective, the loss in SKL has been proposed as a mechanism of CKD damage.¹⁹⁶ Increasing and modifying FGF23 signaling could be a mechanism behind this, as FGF23 has been shown to induce cardiovascular injury, as well as SKL could restore FGF23's ability to induce phosphate excretion. While this could be a mechanism during CKD, this does not explain SKL's other tissue protective effects. MAPK activation as well as FGFRs have been shown to play important roles in cancer,¹⁹⁷ so if SKL is truly an inducer of FGF23 signaling and MAPK activation, this anti-cancer effect would not seem plausible. Given all of this, it is important to analyze SKL's mechanisms of action to understand its therapeutic potential.

Methods

Plasmid Constructs

Mouse soluble and full-length KL and BKL cDNAs were kindly provided by Dr. Makoto Kuro-o (University of Texas Southwestern Medical Center, Dallas, TX) (ref), and human soluble and full-length klotho cDNA constructs were from Amgen (San Francisco, CA). Inserts were subcloned into vectors with appropriate epitope-tags, i.e. C-

terminal Strep/6xHis (OG1240, Oxford Genetics) or C-terminal FLAG/His (OG1232, Oxford Genetics). Subcloning was performed with appropriate restriction enzymes (NEB) according to the manufacturer's protocols, and constructs were verified by Sanger sequencing. The EGFP-N1 vector used for GFP overexpression was obtained from Clontech.

Antibodies, Recombinant Proteins

The following recombinant proteins were purchased from R&D Systems: human FGF2 (233-FB/CF); human FGF5 (237-F5/CF); human FGF7 (251-KG/CF); human FGF8b (423-F8/CF); human FGF19 (969FG025/CF); human FGF21 (2539FG025/CF); human FGF23 (2604FG025/CF); mouse FGF23 (2629FG025/CF); human FGFR1c (658FR050); human FGFR2c (712FR050); human FGFR3c (766FR050); and human FGFR4 (685FR050). Our own made SKL is mouse (aa-35-982) and human (34-981). Mouse SKL from R&D Systems (1819KL050) is aa 35-982; human KL1 from Peptotech is aa 34-549. Heparin solution is from Pfizer Injectables (NDC0069005902). Primary antibodies used are anti-FGF19 (AF969, R&D Systems); anti-FGF21 (AF2539, R&D Systems); anti-FGF23 (AF2604, R&D Systems); anti-FLAG (F1804, Sigma-Aldrich); anti-human Fc (W4031, Promega); total ERK (4695S, Cell Signaling); phospho-ERK (9101S, Cell Signaling); GAPDH (CB1001, Millipore); and sarcomeric α -actinin (EA-53; Sigma-Aldrich). Secondary antibodies are horse radish peroxidase (HRP)-conjugated anti-goat (V8051, Promega); anti-mouse (W4021, Promega); and anti-rabbit (W4011, Promega) for Western blotting; HRP-coupled anti-human (109035098, Jackson Immunolabs); and anti-FLAG (A8592, Sigma-Aldrich) for the plate-based binding assay; and Cy3-conjugated goat-anti mouse (115165166, Jackson Immunolabs) for immunocytochemis-

try. To block FGF23 effects *in vitro*, we used an anti-FGF23 antibody provided by Amgen (San Francisco, CA).

Expression and Purification of SKL

Expi-HEK293 cells (A14527, Thermo Fisher) were adapted to attached growth in DMEM (10013CV, Corning) supplemented with 10% FBS (26140079, Gibco) and 1x Pen/Strep (15140122, Gibco). Cells were transfected with appropriate klotho cDNA vectors using Fugene 6 (E2691, Promega) in OptiMEM (31985062, Gibco). After 2 days, clones were selected by using 1 $\mu\text{g}/\text{mL}$ puromycin (A1113803, Gibco). The clone with the highest expression was selected and re-adapted to suspension growth in Expi293 expression media (A1435101, Thermo Fisher) supplemented with 1 $\mu\text{g}/\text{mL}$ puromycin and 1x Pen/Strep. Cells were grown in 250 mL shaker flasks with 100 mL media on a MaxQ CO₂ plus shaker (88881101, Thermo Fisher) at 14 g, 37°C and 5% CO₂. For protein production, cells were allowed to reach maximum density and collected via centrifugation at 400 g and re-seeded at densities of 1:100. Cells from 500 mL of media were pooled and lysed in 150 mL of a RIPA-based buffer (50 mM sodium phosphate pH 7.5, 200 mM NaCl, 1% Triton X-100, 0.25% deoxycholic acid) with addition of protease inhibitors (11873580001, Roche) for 30 minutes. The mixture was then centrifuged at 20,000 g for 1 hour to remove cell debris, and the supernatant was sterile filtered for purification. Lysate was applied to a 5 mL Talon column (28953767, GE Healthcare) on an Akta Start system (GE Healthcare), in a running buffer containing 50 mM sodium phosphate and 300 mM NaCl. Elution was performed in running buffer supplemented with 200 mM imidazole.

For Strep-tagged SKL, fractions positive for SKL protein were diluted 1:2 in Buffer W (100 mM Tris pH 8.0, 150 mM NaCl), captured on a 1 mL Streptactin XT column (24025001, IBA Lifesciences) and eluted with 100 mM biotin (BP2321, Fisher) in Buffer W. Positive fractions were collected, diluted 1:10 in 25 mM Tris pH 8.0 running buffer and applied to a 1 mL HiTrap Q HP column (29051325, GE Healthcare). The sample was eluted with running buffer in 500 mM NaCl, and SKL was aliquoted and flash frozen. Protein concentration was determined on Coomassie gels in comparison to a BSA gradient.

For FLAG-tagged SKL, talon column-positive fractions were diluted 1:10 in a 10 mM Tris pH 7.0 running buffer and applied to a 5 mL heparin column (17040701, GE Healthcare). The sample was eluted on a linear gradient of 0.0-1.0 M NaCl. Positive fractions for SKL were identified via our plate-based detection assay (detailed below) and pooled. Sample was diluted 1:10 and applied to a 1 mL HiTrap Q HP column (29051325, GE Healthcare) after talon column purification and further eluted with a 0.0-0.5 M NaCl gradient. Again, positive SKL fractions were identified by our klotho detection assay and flash frozen. Protein concentration was determined via Coomassie gel analysis in comparison to a BSA gradient.

FLAG-Immunoprecipitations

FLAG-beads (A2220, Sigma-Aldrich) were used at 50 μ L of 50% stock slurry per sample. Beads were washed 5x with activity buffer (50 mM Tris pH 7.4, 200 mM NaCl, 0.01% Tween 20). Bead spin downs were all performed for 2 minutes at 5,000 g. 50 μ L of a 50% slurry of beads per sample were resuspended in 1 mL of activity buffer in a 1.5

mL snap cap tube. 1 μ g of SKL or C-terminal FLAG-tagged BAP (P7457, Sigma-Aldrich) were incubated with the beads for 1 hour on a bead rotator. Beads were then pelleted at 5,000 g for 2 minutes, and washed 5x with activity buffer. Beads were resuspended in 1 mL of activity buffer and samples with 500 ng of FGF. Beads were incubated for 1 hour on a tube rotator and beads were pelleted and washed as before. 100 μ L of 1x Laemmli sample buffer (1610737, Bio-Rad) with 1.42 M 2-mercaptoethanol was added boiled for 5 minutes and analyzed by SDS-PAGE and Western blotting, as described below.

Protein A/G Immunoprecipitations

Protein A beads (6501, Biovision) and protein G beads (6511, Biovision) were used at 25 μ L of a 50% stock slurry per sample, in a total of bead volume of 50 μ L. Beads were washed 5x in activity buffer (50 mM Tris pH 7.4, 200 mM NaCl, 0.01% Tween 20). Bead spin downs were all performed for 2 minutes at 5,000 g. Beads were resuspended in 1 mL of activity buffer in a 1.5 mL snap cap tube. 1 μ g of Fc-tagged FGFR1-4 were incubated with the beads for 1 hour on a bead rotator. Control samples were incubated with 2 μ g of anti-FGF antibody instead of Fc-FGFR. Beads were then pelleted at 5,000 g for 2 minutes, and washed 5x with activity buffer. Beads were resuspended and incubated with different combinations of 500 ng of FGF, 1 μ g of SKL, 1.6 USP heparin, or PBS. Beads were incubated for 1 hour on a tube rotator and beads were pelleted and washed as before. 100 μ L of 1x Laemmli sample buffer (1610737, Bio-Rad) with 1.42 M 2-mercaptoethanol added and boiled for 5 minutes. Samples were analyzed by SDS-Page and Western blotting as described above.

SDS-PAGE and Western Blotting

20 μ L of sample was loaded onto a mini protean 4-20% gradient TGX gel for experiments with less than 9 samples (4568094, Bio-Rad) or a criterion 4-20% gradient TGX gel (5678094, Bio-Rad) for experiments with more than 9 samples. Gels were run in 1x Tris/Glycine/SDS buffer (1610732, Bio-Rad) at 150 V and stopped when sample dye reached the end of the gel. Gels were removed and electro transferred via a semi-dry cassette (1703940, Bio-Rad) in 1x Tris/Glycine Buffer (1610734, Bio-Rad) with 20% methanol. Gels were transferred onto PVDF membranes (IPVH00010, Merck Millipore) at 20 V for 1 hour. Membranes were then blocked in 5% dried milk with 0.5% Tween 20 diluted in Tris buffered saline (TBS) pH 7.5 for 1 hour and probed with antibodies against specific antigens at 1:1,000 in TBS with 5% dried milk and 0.5% Tween. Blots were washed 3x for 5 minutes in TBS and probed with HRP-coupled secondary antibodies against specific species at 1:10,000 in TBS with 5% dried milk and 0.5% Tween. Membranes were imaged on an SRX-101A X-ray film developer.

Paracrine FGF Signaling in HEK293T Cells

HEK293 cells were seeded in 6-well plates in DMEM (26140079, Gibco) supplemented with 1x Pen/Strep (15140122, Gibco) and 10% FBS (26140079, Gibco) and grown for 48 hours. Upon reaching 80% confluence, cells were serum-starved overnight in DMEM and 1x Pen/Strep without FBS. Media was changed and cells were treated with SKL at 2 μ g/mL or vehicle for 15 minutes. Cells were then treated with various FGFs at 1.1 nM for 10 minutes. Cells were lysed in 200 μ L of a RIPA-based buffer (50 mM sodium phosphate pH 7.5, 200 mM NaCl, 1% Triton X-100, 0.25% deoxycholic acid) with

addition of protease inhibitor (11836153001, Roche) and phosphatase inhibitors (P5726, P0044, Sigma-Aldrich) for 30 minutes. The mixture was then centrifuged at 20,000 g for 60 minutes to remove all cell debris. 100 μ L of 1x Laemmli sample buffer (1610737, Bio-Rad) with 1.42 M 2-mercaptoethanol added and boiled for 5 minutes. 20 μ L of samples was loaded onto 12% SDS-PAGE gels and analyzed by Western blotting.

Plate-Based Assay to Detect SKL and to Study the Paracrine FGF-SKL Crosstalk

FGFs or FGFR ectodomains were coated on 96-well plates (Maxisorp; 439454, Thermo Fisher), and proteins were added to wells in 100 μ L ELISA coating buffer (E107, Bethyl) with a lid placed overtop and incubated at 4°C overnight. Plates were washed 5x with 350 μ L assay buffer (50 mM Tris pH 7.4, 200 mM NaCl, 0.01% Tween 20) on a 50TS microplate washer (BioTek). Plates were blocked for 1 hour in 200 μ L assay buffer with 0.5% BSA. Plates were washed as before and proteins were incubated on plates in 100 μ L assay buffer with 0.5% BSA. Proteins or heparin were incubated in orders described in respective figure legends. Assays utilizing FLAG-tag based detection were treated with anti-FLAG coupled to HRP at 1:20,000, and assays utilizing Fc detection were treated with anti-human Fc coupled to HRP at 1:10,000. Plates were washed as above and 100 μ L TMB substrate (E102, Bethyl) was added for 15-20 minutes until positive wells developed a dark blue color. Reactions were stopped with an ELISA stop solution (E115, Bethyl) and analyzed on a Synergy H1 plate reader (BioTek) at 450 nm wavelength. All samples were run in triplicate with individual readouts displayed on graphs. As a control to remove background absorbance values, wells were coated with an equal amount of BSA to match the amount of protein coated in experimental wells and treated the same as experimental wells. To study the effects of SKL on the binding be-

tween paracrine FGFs and FGFRs, plates were run as above except coated with paracrine FGFs. FGFR1-Fc was pre-incubated with SKL or vehicle for 60 minutes, and then the combination was added to wells and the assay was run as before.

Results

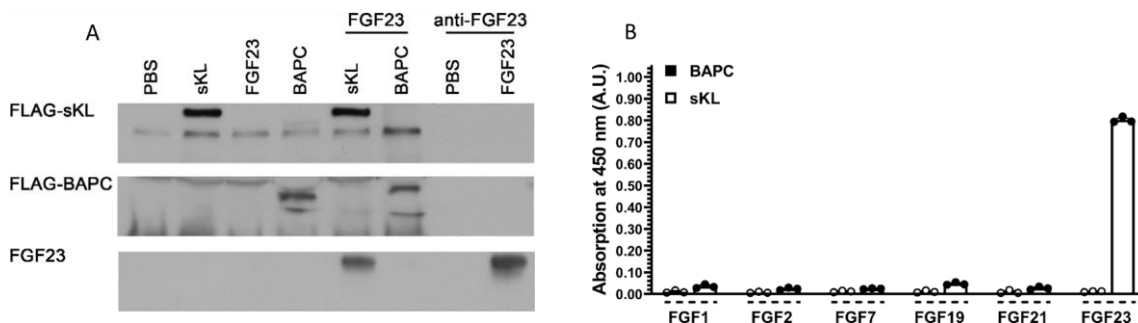


Figure 17. FGF23 Binds SKL

(a) FLAG-tagged SKL or BAPC (used as negative control) was immobilized on anti-FLAG beads, and then incubated with recombinant FGF23 protein or solvent (PBS). Protein A/G beads with immobilized anti-FGF23 antibody and incubated with FGF23 served as a positive control for FGF23 precipitation. FLAG-SKL, but not FLAG-BAPC, binds FGF23. (b) 96-well plates were coated with 10 ng of recombinant FGF1, FGF2, FGF7, FGF19, FGF21, or FGF23, washed and incubated with 40 ng of FLAG-tagged SKL or BAPC. After subsequent washes, and incubation with HRP-coupled anti-FLAG and HRP substrate, absorbance at 450 nm was measured (presented as arbitrary units; A.U.). Of all tested FGF isoforms, only FGF23 bound FLAG-SKL. All graphical values are expressed as mean \pm SEM; for plate-based assays $n = 3$ replicate wells

First, we wanted to determine if FGF23 could bind SKL. We explored this in Fig. 17 via two methods. First, purified FLAG-tagged SKL was bound to anti-FLAG beads, and binding partners were explored by immunoprecipitation and analyzed by Western blotting. When FGF23 was added to beads that contained SKL, FGF23 was immunoprecipitated with SKL. When a FLAG-tagged control protein, bacterial alkaline phosphatase (BAPC), was added instead, FGF23 was unable to bind and to be pulled down. An anti-FGF23 antibody was bound to protein A+G beads as a positive control, which was able

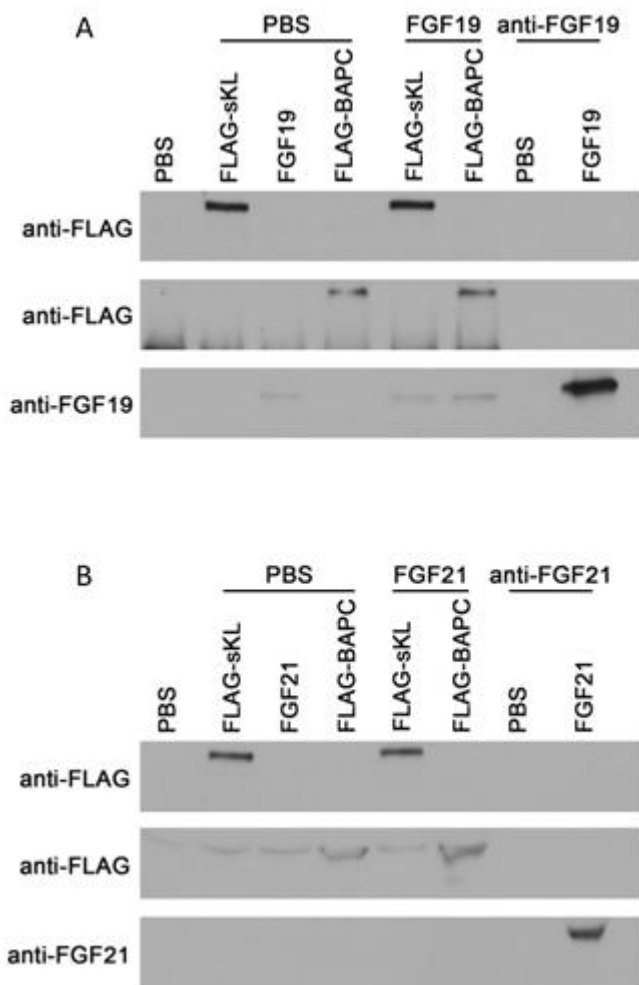


Figure 18. SKL does not Bind FGF19 and FGF21 (a, b) FLAG-tagged SKL or BAPC (used as negative control) was immobilized on anti-FLAG beads, and then incubated with recombinant (a) FGF19 or (b) FGF21 protein or solvent (PBS). Protein A/G beads with immobilized anti-FGF19 or anti-FGF21 antibody and incubated with FGF19 or FGF21 served as a positive control for FGF19 and FGF21 precipitations, respectively. FLAG-SKL does not binds FGF19 or FGF21.

to pull down FGF23 with a similar affinity to SKL. To further verify that this effect is due to true binding and not a non-specific event, we bound different FGFs to a 96-well plate.

Wells were then incubated with either FLAG-tagged SKL or BAPC, and binding detected via an anti-FLAG antibody tagged with horseradish peroxidase (HRP). FGF23 bound SKL to the plate, while failing to bind BAPC, confirming the strong

binding affinity to FGF23 and SKL. The other control FGF proteins did not bind SKL except FGF19. While FGF19's affinity for SKL was much lower than FGF23, there was a slight

amount of binding which was surprising. To further explore if SKL can modulate any other FGF signaling, we repeated the above immunoprecipitation with FGF19 and FGF21. As can be seen in Fig. 18a and Fig. 18b, neither FGF19 nor FGF21 were able to

bind SKL like FGF23 did, while the control anti-FGF19 and anti-FGF21 antibodies were used to pull down these FGFs. These data support that SKL exclusively binds FGF23.

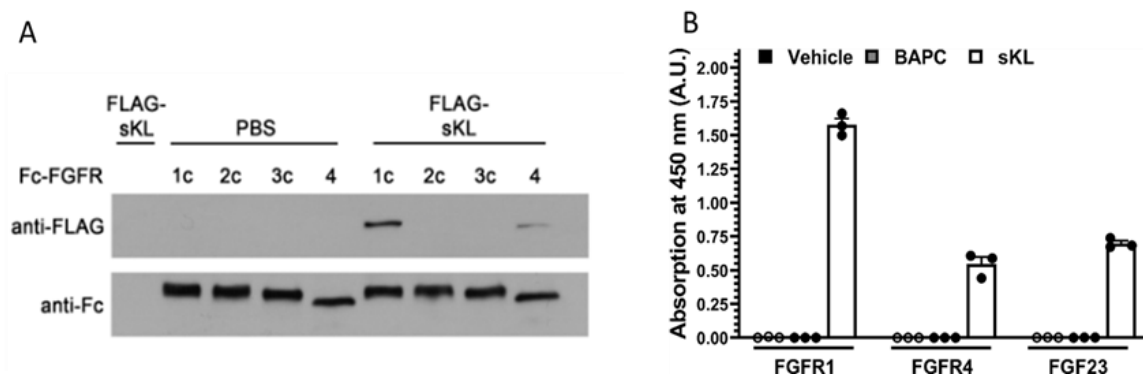


Figure 19. SKL Binds FGFR1 and FGFR4

(a) Fc-tagged FGFR isoforms 1c, 2c, 3c, or 4 were bound to protein A/G beads and treated with either FLAG-tagged SKL or PBS. FLAG-SKL bound to FGFR4, and to a weaker extent to FGFR4. (b) 96-well plates were coated with 40 ng of FGFR1c or FGFR4, or with 20 ng of FGF23, washed and incubated with 80 ng of FLAG-tagged SKL or BAPC, or PBS. Wells were washed again, treated with HRP-coupled anti-FLAG and HRP substrate, and analyzed for absorbance at 450 nm. FLAG-SKL bound FGFR1c and to a lower extent FGFR4 and FGF23. All graphical values are expressed as mean \pm SEM; for plate-based assays n = 3 replicate wells

Next, we examined whether SKL could only bind FGF23, or if it could bind FGFRs as well. Therefore, we conducted immunoprecipitation studies, by binding the ectodomains of the four different FGFRs that are tagged with antibody IgG fragments to protein A+G beads. We then incubated the bound beads with SKL, as seen in Fig. 19a. Surprisingly, we found that FLAG-tagged SKL bound to both FGFR1 and FGFR4, with the higher affinity for FGFR1. Previous studies have focused on KL binding and signaling in respect to FGFR1, so the detected FGFR4 binding is quite surprising. Due to the nature of immunoprecipitations and the different beads required for immobilization of FGF23 and FGFRs, comparing their binding affinities to SKL would not be possible in this way. To accomplish this, we bound either FGFR1, FGFR4, or FGF23 to wells in a 96-well plate at a molar ratio. We then added FLAG-tagged SKL as per the FGF plate

experiment, and found that SKL preferred binding to FGFR1, almost 3-fold higher when compared to either FGFR4 or FGF23.

Given the strong binding to FGFR1, we became interested if SKL is able to interfere with FGF signaling aside from FGF23, with an interest if SKL binding could occupy the binding site in FGFR1 that paracrine FGFs utilize for signaling. In Fig. 20, we explored this utilizing our plate-based assay as well as cell-based signaling. First in Fig. 20a, we coated wells in a 96-well plate with either FGF2 or FGF7. FGF2 is a known binder to FGFR1, while FGF7 is known to not interact with the c splice variant of any FGFR isoform. Since paracrine FGFs utilize heparin as a necessary co-factor for binding, we also introduced heparin as a pre-binding step to the FGFs. We found that FGF2 bound FGFR1 while FGF7 did not, and heparin increased this binding greatly. Since the FGFR1 ectodomain protein is IgG-tagged, we utilized an anti-Fc HRP tagged antibody to detect the presence of FGFR1. We also included wells where we first pre-incubated FGFR1 with SKL and then added this to wells, and binding was greatly blocked between FGF2 and FGFR1. Heparin did not seem to have an effect, with blockade occurring either way. We repeated this experiment in Fig. 20b with two other paracrine FGFs. Just like FGF2, SKL interfered with FGFR1 binding to both, FGF5 and FGF8b. To elucidate if these effects can also occur on a cellular level, we pre-treated HEK293T cells with SKL. HEK cells express all four FGFR isoforms, and are able to respond to paracrine FGF signaling. The pre-treatment allowed SKL to bind to FGFR1, and we then treated cells with paracrine FGFs or FGF23. As can be seen in Fig. 20c, the paracrine FGFs were able to elicit FGFR activation as indicated by increased ERK phosphorylation. Given no KL was present, FGF23 was not able to illicit this response. When pretreated with SKL, just like in

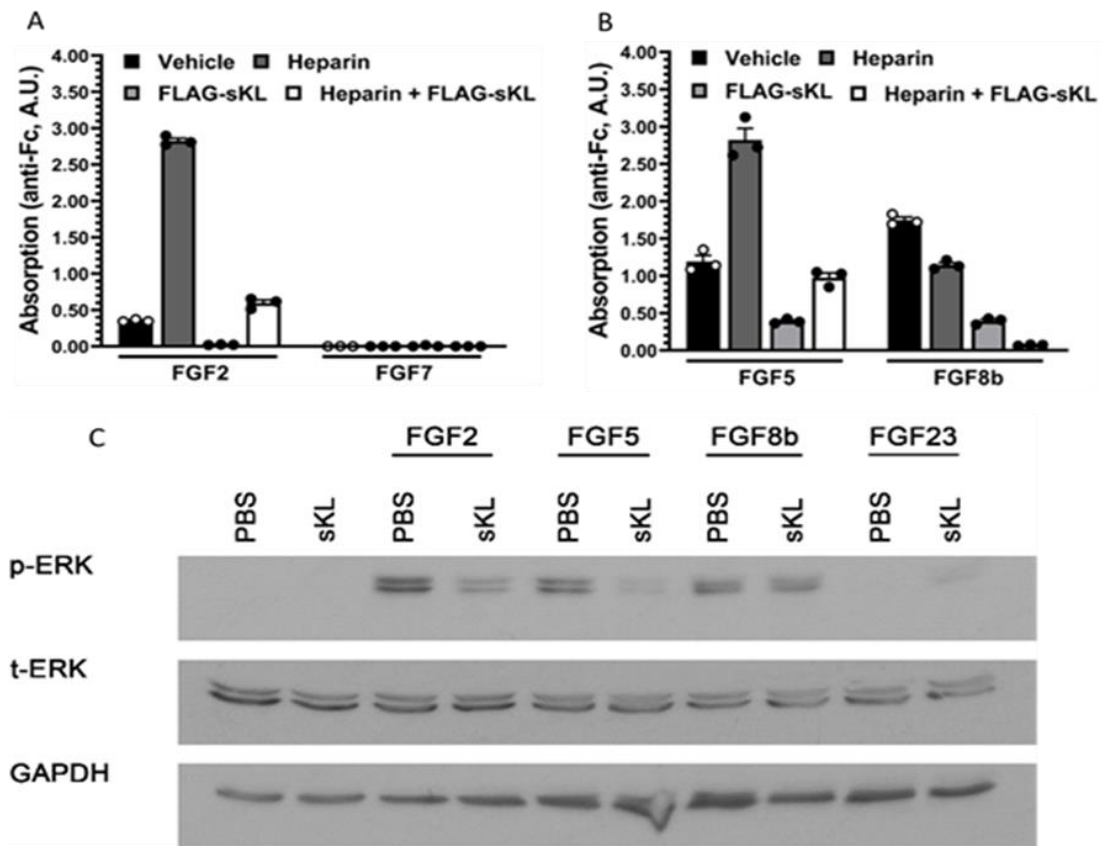


Figure 20. SKL Interferes with Paracrine FGF Signaling

(a, b) 96-well plates were coated with (a) 12.5 ng of FGF2 or FGF7, or (b) 100 ng of FGF5 or FGF8b and incubated with 0.4 USP heparin or PBS (vehicle). Wells were washed, incubated with 25 ng (for FGF2 and FGF7) or 200 ng (for FGF5 and FGF8b) of Fc-tagged FGFR1c, washed again, treated with HRP-coupled anti-Fc, and HRP substrate, followed by the analysis of absorbance at 450 nm. In reactions receiving SKL, Fc-FGFR1c was pre-incubated with 50 ng (for FGF2 and FGF7) or 400 ng (for FGF5 and FGF8b) of FLAG-tagged SKL prior to the addition to wells. Heparin increased the binding of FGF2 and FGF5 to FGFR1c, but this effect did not occur in the presence of SKL. (c) Serum-starved HEK293T cells were treated with FLAG-tagged SKL or PBS for 15 minutes, followed by stimulation with FGF2, FGF5, FGF8b, or FGF23 for 10 minutes. Total protein extracts were analyzed by Western blotting. Treatment with FGF2, FGF5 and FGF8b increased levels of phosphorylated ERK (pERK) in comparison to total levels of ERK (tERK), which did not occur if cells were pre-treated with SKL. In contrast, FGF23 treatment increased pERK levels in the presence of SKL. GAPDH served as loading control. All graphical values are expressed as mean \pm SEM; for plate-based assays $n = 3$ replicate wells

the plate-based assay, FGFR1 activation was blocked by paracrine FGFs. While much

weaker activation than the paracrine FGFs, the presence of SKL now allowed FGF23 to activate FGFR1. Given this data, SKL is able to modulate FGFR1 signaling not just by

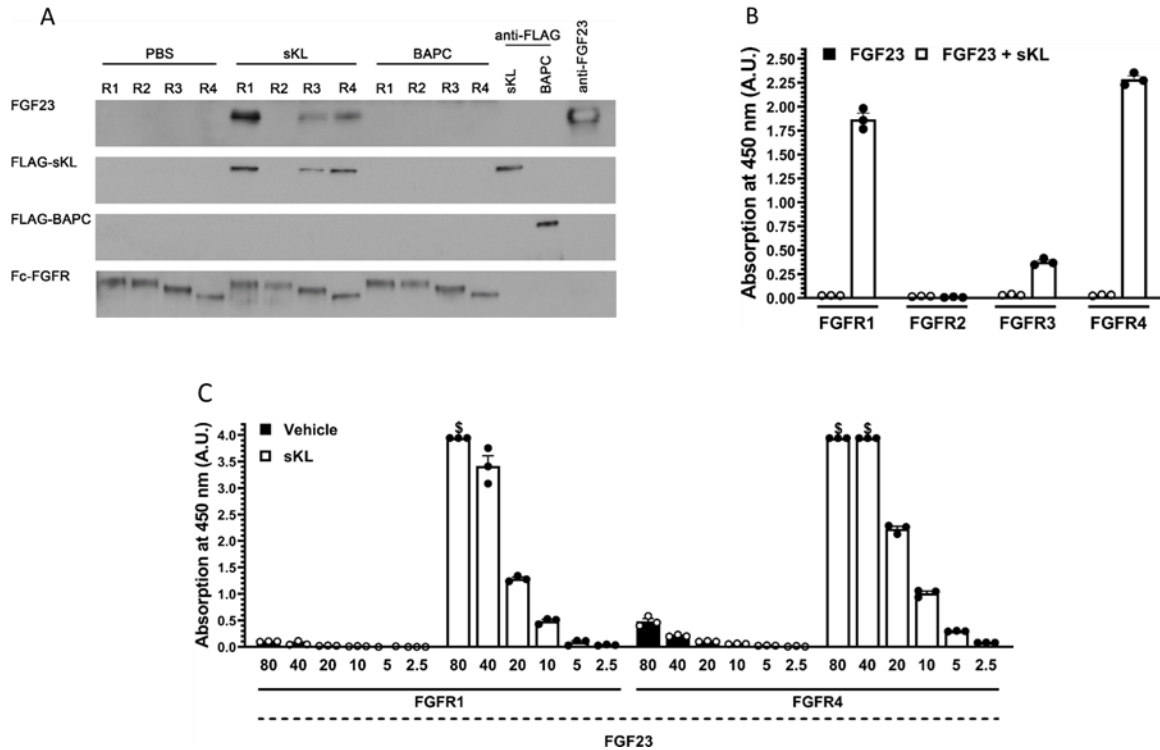


Figure 21. SKL Modulates FGF23 Signaling with Multiple FGFRs

(a) 1 μ g of Fc-tagged FGFR isoforms 1c, 2c, 3c, or 4 were bound to protein A/G beads and treated with either 2 μ g of FLAG-tagged SKL or BAPC, or PBS, all in combination with 500 ng of FGF23. Anti-FLAG beads incubated with either FLAG-SKL or FLAG-BAPC, and anti-FGF23 antibody immobilized on protein A/G beads and treated with FGF23 served as positive controls for FLAG- and FGF23-precipitations, respectively. Co-treatments with FGF23 and SKL lead to complex formation with FGFR1c, and to a lesser extent with FGFR3c and FGFR4. (b) 96-well plates were coated with 4.5 ng of FGF23, washed and then sequentially incubated with 18 ng of FLAG-tagged SKL or PBS, 50 ng of Fc-tagged FGFR 1c, 2c, 3c, or 4, HRP-coupled anti-Fc, and HRP substrate, followed by absorbance measurement. The complex of FGF23 and SKL bound FGFR1 and FGFR4 the strongest, with weaker binding to FGFR3. (c) 96-well plates were coated with 2-fold dilutions of FGF23, ranging from 80-2.5 ng. Wells were washed, and sequentially incubated with 320-10 ng of FLAG-tagged SKL or PBS, followed by 160-5 ng of Fc-FGFR1c or Fc-FGFR4, HRP-coupled anti-Fc, and HRP substrate. Binding of the SKL/FGFR1c and SKL/FGFR4 complexes occurred in relation to the amount of coated FGF23. In the absence of SKL, FGF23 bound FGFR4 with weak affinity, but not FGFR1c. All graphical values are expressed as mean \pm SEM; for plate-based assays n = 3 replicate wells; \$ indicates that the absorbance at 450 nm surpassed plate reader limit.

increasing FGF23 binding, but by blocking all other FGF signaling outside of this.

Given this, we then further explored the role of SKL on FGF23 signaling with all

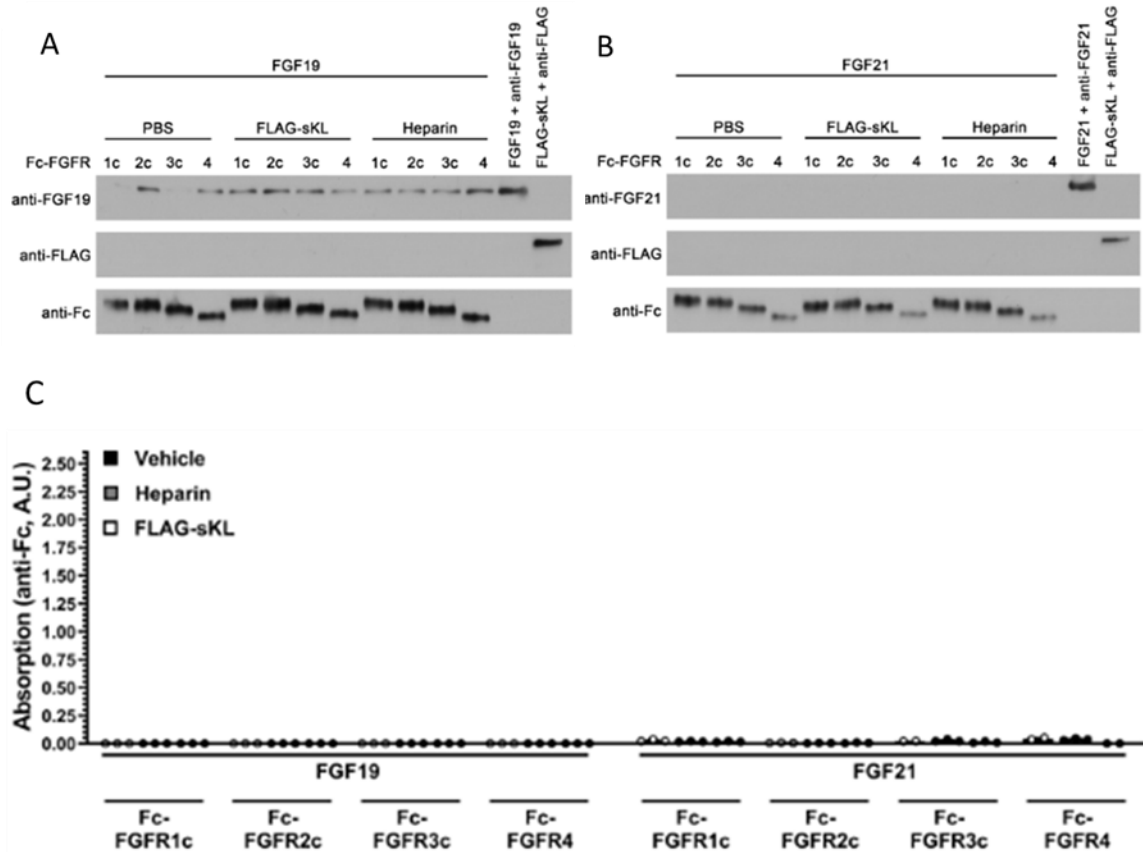


Figure 22. SKL does not Modulate FGF19 or FGF21 Signaling

(a) FGF19 or (b) FGF21. Anti-FLAG beads incubated with FLAG-SKL, and anti-FGF19 or anti-FGF21 antibody immobilized on protein A/G beads and treated with FGF19 or FGF21 served as positive controls for FLAG- as well as FGF19- and FGF21-precipitations, respectively. Co-treatments with SKL and FGF19 or FGF21 did not lead to complex formation with any of the FGFR isoforms. (c) 96-well plates were coated with 4.5 ng of FGF19 or FGF21, washed and then sequentially incubated with 18 ng of FLAG-tagged SKL, 0.4 USP of heparin or vehicle (PBS), 50 ng of Fc-tagged FGFR 1c, 2c, 3c, or 4, HRP-coupled anti-Fc, and HRP substrate, followed by absorbance measurement. The complex of FGF19 and SKL or of FGF21 and SKL did not bind any of the FGFR isoforms. All graphical values are expressed as mean \pm SEM; for plate based-assays n = 3 replicate wells.

FGFRs in Fig. 21. To accomplish this, we first bound FGFRs to protein A+G beads, and then added either FLAG-tagged SKL or BAPC in combination with FGF23. When no co-

factor was present, we did not detect any FGF23 binding to any of the four FGFRs. The addition of SKL to the reaction had marked effects on FGF23 binding. As expected, SKL increased the affinity of FGF23 for FGFR1. Surprisingly, it also increased the affinity to a lesser degree of both FGFR3 and FGFR4 to FGF23. FLAG-tagged BAPC had no effect on FGF23 binding. We then further verified this utilizing our plate-based approach in Fig. 22b-c. We coated plates with FGF23, and in a stepwise fashion, added saline or SKL, FGFRs, and then anti-Fc HRP to detect receptor binding. As demonstrated in the immunoprecipitation-based assay, SKL increased the affinity of FGF23 to FGFR1, FGFR3, and FGFR4. To further prove this effect was specific, we then coated plates with 2-fold dilutions of FGF23, and again treated stepwise with molar ratios of FGFR1 and FGFR4. As expected, we found that signals decreased in a concentration dependent manner. We also found that at higher concentrations, FGF23 was able to bind to FGFR4 in the absence of SKL, confirming earlier published work that FGF23 favors FGFR4 at elevated levels seen during CKD. To further analyze these effects on other FGFs, we repeated these assays with FGF19 and FGF21. As shown in Fig. 22a-c, SKL had no effects on FGF19 or FGF21 binding with any FGFR.

Discussion

In summary, our results characterize the novel role of SKL demonstrating its modulation of FGF signaling. We validated findings that SKL can directly bind FGF23. This means that the FGF23-SKL complex can likely exist in serum, may circulate and interact with FGFRs. We found that this high affinity interaction is unique for FGF23, and little binding occurred for other FGFs in our screen. We did see low affinity binding of FGF19 for SKL in our highly sensitive plate-based assay. This leaves the possibility

that at high concentrations, SKL may be able to interact with and affect FGF19 signaling. Previous publications have proposed that SKL may be able to affect FGF19,²³ so given this result we cannot rule this out. But on the other hand, our later receptor-based assays showed no changes in FGF19 affinity for FGFRs in the presence of SKL. What we found very interesting was that SKL also had a strong affinity for FGFRs in the absence of FGF23. Given the recent crystal structure showing the RBA site on SKL binds to the FGFR while FGF23 is in complex, it is this site on SKL that is likely responsible for this interaction even without FGF23.⁴³ When comparing the affinity for FGF23 vs FGFRs, we found that FGFR1 had a three times higher affinity for SKL compared to FGFR4 or FGF23. We found this very surprising since SKL has been hypothesized to be able to circulate and act as a hormone. Given that FGFR1 is so ubiquitously expressed in various cell types and organs, it would seem likely that SKL would quickly bind to the nearest FGFR and never escape the immediate cells, similar to paracrine FGFs with heparin. Or it could be that SKL levels are restricted to certain stimuli, and upon this expression is increased enough to overcome this binding. Given the struggles in detecting SKL, as well as the fact that BKL has not been shown to exist as a soluble factor, this could call into question the existence of high levels of SKL in serum. Furthermore, this receptor binding may explain some of SKL's other tissue protective effects. Paracrine FGFs are responsible for a multitude of effects and have been implicated in cancer.²⁹ This blockade of FGFR1 binding to paracrine FGFs may explain many of the FGF23 independent effects. This further makes sense when analyzing phosphate regulation in the kidney. Since FGFR1 is able to be activated by multiple paracrine FGFs, this would mean that other FGFs expressed in the kidney could in theory signal via FGFR1 to regulate phosphate

levels. By KL acting as a blocker, this allows only FGF23 to signal via FGFR1, and creates a very specific receptor for only FGF23.

While SKL has both an affinity for FGF23 and FGFRs, the order of events seems to play a role on its promiscuity. While FGF23 is not present, SKL binds to FGFR1 and to a lesser degree FGFR4. If SKL binds to FGF23 first or is introduced at the same time as FGF23 to the FGFR, a complex is formed for FGFR1, FGFR3, and FGFR4. The complex formation is also very strong for FGFR4, in our plate-based assay it was measured at similar levels to FGFR1. This piece of data necessitates the change in theory that SKL and KL in general may not signal through just FGFR1, but also through two other FGFRs. Since FGFR3 and FGFR4 are poor activators of ERK, this may be why this piece of data has escaped the literature for so long. While FGFR1 may be the only FGFR responsible for phosphate control, this opens the door to SKL having other functions in the kidney via FGFR3 and FGFR4 that have yet to be explored, as well as other KL containing organs such as the brain and parathyroid gland. If SKL is an excreted factor or if SKL is ever administered in a therapeutic role, this also means that FGFR3 and FGFR4 activation could occur across a multitude of cell types, similar to FGFR1 activation. Overall, this data elucidates that SKL is a bona fide scaffold for FGF signaling that can influence the binding of FGFs to FGFRs.

CHAPTER 3: PRODUCTION AND DETECTION OF BIOACTIVE SKL

Background

SKL has garnered recent interest due to its therapeutic potential.^{198, 199} Based on its multitude of tissue protective effects, early work has shown that KL has the potential to be a treatment option for cancer, neurodegeneration, and CKD. Unfortunately, struggles in the field have led to SKL never reaching its true potential yet. A few commercial preparations of SKL are available on a research level, and a few other groups and companies are working on developing a SKL-based product. But due to the multitude of functions, with no clear mechanism of action, and difficulties expressing and purifying SKL, measuring the activity of the protein has not yet been possible. This has made it difficult to utilize this protein for treatments, as there is no way to measure the quality or activity of purified preparations of SKL. Furthermore, given the struggles to detect SKL, data identifying patient populations low in SKL levels is unreliable.^{80, 81}

While these struggles persist, ways to bypass these barriers have been developed to test the protective properties of SKL. While the quality is unknown, many groups have utilized two commercial preparations for testing, one from Peprtech that only contains the KL1 domain of SKL, and a second from R&D Systems that is the full-length SKL. To get around using these proteins, other groups have looked to induce native KL expression in mice. One model is an overexpression model of KL.⁵¹ This model is intriguing as it is

not overexpressing SKL, but the membrane-associated version of KL using a promotor that induces expression in all tissue types. This mouse has been shown not only to have an extended lifespan in general, but to be protected from chronic diseases like CVD and CKD. A secondary method of treatment has been developed at first by Eli Lilly, where only the SKL protein is elevated in serum by utilizing an AAV-based overexpression system.²⁰⁰ SKL is specifically overexpressed and secreted by the liver, and the levels are extremely high, above anything that could be seen physiologically. Interestingly, in this mouse, FGF23 levels are also highly elevated. Given that FGF23 elevations have been shown to be detrimental during CKD, this calls into question if this could hamper SKL's beneficial effects. In light of these elevations, mice undergoing this treatment in kidney injury models are still protected from some of the detrimental effects. These mice show decreased cardiac hypertrophy, serum phosphate levels, and even a protection of kidney function and fibrosis.^{200, 201}

While protective to the heart, the question is how SKL performs these functions. Does SKL interact with the kidney and provide protective functions to the heart by indirect improvements in kidney filtration and serum phosphate levels? Or is it due to SKL directly interacting with cardiac myocytes, either through a hypothesized SKL receptor or by modifying FGF23 signaling? Given our data described in Chapter 2, it remains plausible that SKL could modify FGF23 signaling due to its high affinity binding. Our early working hypothesis was that in the absence of SKL in conditions like CKD, FGF23 would signal through FGFR4 in cardiac myocytes and promote cell growth and cardiac hypertrophy. When SKL is reintroduced, it would bind to FGF23 and promote binding to FGFR1, providing cardiac protection and a decrease in hypertrophy. To our surprise,

SKL also greatly increased the binding affinity of FGF23 to FGFR4. This raises the question whether SKL would still have direct protective effects in cardiac myocytes.

Methods

SKL Half-Life

Strep-tagged mouse SKL was purified as noted above. Each group consisted of 3 male Sprague Dawley rats, 9 weeks of age weighing around 300 g. For injections and bleedings, rats were anesthetized with 2.5% isoflurane. For injections, a shielded IV catheter (BD Insyte™ Autoguard™ 0.7 x 19mm, cat. no 381412) was inserted into the lateral tail vein and flushed with 100 µl isotonic saline (0.9%). 1 mL of purified SKL protein dissolved in isotonic saline (100µg/kg) or isotonic saline was then injected, and the catheter was flushed again with 100 µL isotonic saline. For bleedings, a shielded IV catheter (BD Insyte™ Autoguard™ 0.7 x 19mm, cat. no 381412) was inserted into the lateral tail vein. Blood samples (300 µl) were taken after 15, 30 and 60 minutes as well as 3, 6, 12, and 48 hours, and blood was collected into multivette serum gel tubes (15.16.74, Sarstedt) and centrifuged at 10,000 g for 5 minutes to purify serum. Serum was then aliquoted and stored at -80°C before analysis. For the SKL activity assay, wells were coated with 500 ng of mouse FGF23 in 100 µL of coating buffer (E107, Bethyl) at 4°C overnight. Plates were washed 5x at 350 µL of assay buffer (50 mM Tris pH 7.4, 200 mM NaCl, 0.01% Tween 20) on a 50TS microplate washer (BioTek). Plates were blocked for 1 hour in 200 µL assay buffer with 0.5% BSA. Plates were washed and incubated with 30 µL per well and 70 µL assay buffer with 0.5% BSA. Standards were run at noted concentrations, using our purified Strep-tagged mouse SKL protein with 30 µL control serum

and 70 μ L assay buffer with 0.5% BSA added to ensure consistency. All samples and standards were run in triplicates. After 1 hour, plates were washed, and 150 ng of FGFR1c-FC were incubated on plates in 100 μ L volume of assay buffer with 0.5% BSA. After 1 hour, plates were washed and incubated with anti-human Fc-HRP at 1:10,000. Plates were washed as above and 100 μ L TMB substrate (E102, Bethyl) was added for 15-20 minutes until positive wells developed a dark blue color. Reactions were stopped with an ELISA stop solution (E115, Bethyl) and analyzed on a Synergy H1 plate reader (Bio-Tek) at 450 nm wavelength. Amounts of SKL were calculated by taking the slope of the standard curve and calculating where the sample points fit in.

Plate-Based SKL Activity Assay Specificity Test

HEK293 cells were plated in 10 cm dishes supplemented with 10% FBS (26140079, Gibco) and 1x Pen/Strep (15140122, Gibco). Cells were transfected with appropriate klotho or GFP cDNA constructs. After 2 days, clones were selected by using 1 μ g/mL puromycin (A1113803, Gibco). Cells were then split and plated on 10 cm dishes in DMEM supplemented with FBS and puromycin. After 48 hours, cells were lysed in 1 mL of a RIPA-based buffer (50 mM sodium phosphate pH 7.5, 200 mM NaCl, 1% TritonX-100, 0.25% deoxycholic acid) with addition of protease inhibitors (11873580001, Roche) for 30 minutes. The mixture was then centrifuged at 20,000 g for 1 hour to remove all cell debris. Activity assay was run as above in the SKL half-life study. Instead of serum, 20 μ L of indicated cell lysate was used and combined with 80 μ L of activity assay buffer. All other conditions were as listed above, and data displayed as absorbance after 15-20 minutes.

Isolation and Cultivation of NRVM

Neonatal rat ventricular myocytes (NRVMs) were isolated using a kit following the manufacturer's protocol (LK003300, Worthington Biochemical Corporation), as done before.^{183, 190, 193} Briefly, hearts from 1- to 3-day old Sprague Dawley rats were harvested and minced in calcium- and magnesium-free HBSS, and the tissue was digested with 50 µg/mL trypsin at 4°C for 20 to 24 hours. Soybean trypsin inhibitor in HBSS was added, and the tissue was further digested with collagenase (in Leibovitz L-15 medium) under slow rotation (0.14 g) at 37°C for 45 minutes. Cells were broken up by triturating the suspension 20x with a standard 10-mL plastic serological pipette. Cells were then filtered through a cell strainer (70 µm, BD Falcon). Cells were incubated at room temperature for 20 minutes and spun at 100 g for 5 minutes. The cell pellet was resuspended in plating medium (DMEM Base (10013CV, Corning); 17% M199 (12350039, Gibco); 15% FBS (26140079, Gibco); 1x Pen/Strep (15140122, Gibco)). For cell tracings, NRVMs were grown in 24 well-plates on glass coverslips (CLS1760012, Chemglass). Slips were pre-coated with laminin (23017015, Invitrogen) at 10 µg/mL for 1 hour at 37°C dissolved in PBS) Laminin was aspirated and cells and media added. Cells were counted by hemocytometer and plated at 4×10^5 cells per well. Myocytes were grown for 72 hours in the presence of plating media, media was removed and maintenance media (DMEM Base (10013CV, Corning)); 20% M199 (12350039, Gibco); 1% insulin-transferrin-sodium selenite solution (I18841VL, Sigma-Aldrich); 1x Pen/Strep (15140122, Gibco); and 100 µM 5-bromo-2'-deoxyuridine (B9285, Sigma-Aldrich)) was added. After 48 hours, maintenance media was replaced, and after another 48 hours cells were ready for treatment, giv-

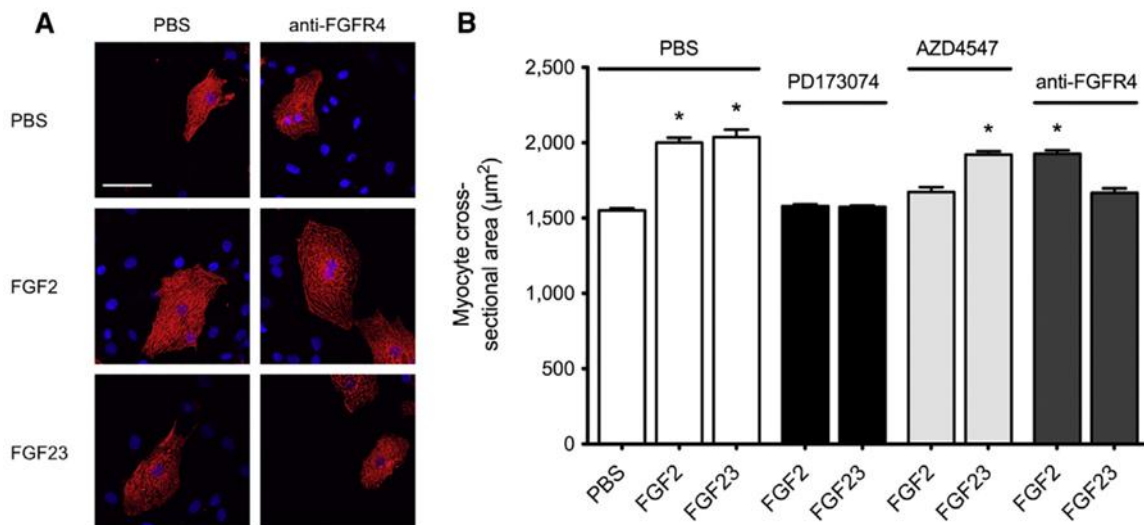
ing a total of 72 hours of plating media and 96 hours of maintenance media before treatment. Cells were then treated for 48 hours.

Immunocytochemistry and Morphometry of NRVMs

Media was aspirated and cultured NRVMs were fixed in 2% paraformaldehyde (P-6148, Sigma-Aldrich) and 4% sucrose dissolved in PBS for 5 minutes followed permeabilization with 1% Triton X-100 dissolved in PBS for 10 minutes. Cover slips were washed 3x in PBS and blocked for 1 hour in blocking solution (2% FBS (26140079, Gibco), 2% BSA (BSA50, Rockland), and 0.2% coldwater fish skin gelatin (900033, Aurion) dissolved in PBS). Blocking solution was aspirated and 100 μ L of 1:1,000 α -actinin primary antibody was added for 1 hour. The primary antibody was aspirated, and coverslips were washed 3x with blocking solution, and then 100 μ L of Cy3-conjugated goat-anti mouse secondary antibody diluted at 1:300 was added. After 1 hour, coverslips were washed 3x with blocking solution, dabbed dry, and mounted in ProLong Antifade Mountant with DAPI (P36962, Invitrogen) for visualization of nuclei. Immunofluorescence images were taken on a Leica Dmi8 fluorescence microscope with a 60x oil objective. Myocyte cross-sectional area was measured based on α -actinin-positive staining using ImageJ software (NIH). Each slide was from a different isolation to ensure reproducibility.

Results

Given the data from Chapter 2 and SKL's pleiotropic effects, we wanted to elucidate if its protective effects on cardio myocytes occurred directly by the blockade of FGF23 signaling or secondarily by improving kidney function. To accomplish this, we



Note: Grabner, A., et al., *Activation of Cardiac Fibroblast Growth Factor Receptor 4 Causes Left Ventricular Hypertrophy*. *Cell Metab*, 2015. 22(6): p. 1020-32. Copyright Elsevier 2015. Reprinted with permission.

Figure 23. FGF23 Induced Hypertrophic Growth of Myocytes Requires FGFR4

(a) Immunofluorescence confocal images of isolated NRVM that were co-treated with FGF2 or FGF23 and anti-FGFR4 for 48 hr. Myocytes are labeled with anti- α -actinin (red), and DAPI (blue) identifies nuclei (original magnification, 363 \times ; scale bar, 50 μ m). NRVM treated with FGF23 or FGF2 appear larger than PBS-treated control cells. Anti-FGFR4 blocks the effect of FGF23, but not FGF2. (b) Compared with PBS-treated control cells, 48 hr of treatment with FGF23 or FGF2 significantly increases cross-sectional area of isolated NRVM (mean \pm SEM). Co-treatment with the pan-FGFR inhibitor, PD173074, prevents any increase in area regardless of the FGF. Inhibition of FGFR1–3 by AZD4547 prevents FGF2-induced, but not FGF23-induced, hypertrophy. An FGFR4-specific blocking antibody (anti-FGFR4) prevents FGF23-induced, but not FGF2-induced, hypertrophy (150 cells per condition; n = 3 independent isolations of NRVM; *p < 0.0001 compared with vehicle)

utilized primary isolated neonatal myocytes as a model. We have previously utilized this as a model for in vitro cardiac hypertrophy induced by FGF23, as seen in Fig. 23.^{183, 193}

Neonatal myocytes are the preferred method for hypertrophic studies due to their abilities to survive for extended periods of time, but act similarly to cardiac myocytes in vivo due to their non-proliferative nature and ability to increase in size in response to stimuli. To measure this response, cells are stained for a specific cardiac cell marker, α -actinin, and

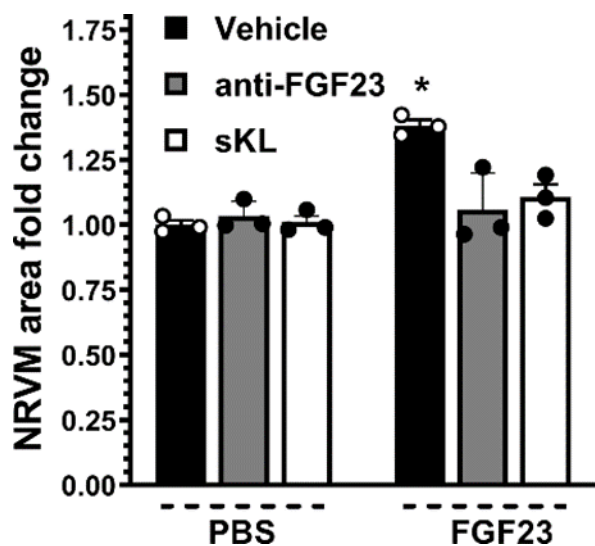


Figure 24. SKL Blocks FGF23 Induced Hypertrophy

(a) NRVMs were co-treated with FGF23 (25 ng/mL) or vehicle (PBS), and with FLAG-tagged SKL (100 ng/mL), an anti-FGF23 blocking antibody (1 ug/mL) or vehicle. FGF23 treatments caused an increase in cell area, while SKL and anti-FGF23 blocked this effect. $n = 3$ independent isolations, 50 cells per slide, 150 total cells per condition; * $p \leq 0.05$ vs. all other groups

their area is measured by confocal microscopy. As seen in Fig. 23, cells treated with either FGF2 or FGF23 responded by increasing in size. The pan-FGFR blocker PD173074 was able to block the response to both FGFs. To assess which FGFRs are responsible, we utilized the compound AZD4547 which is a FGFR1-3

blocker and found that this blocked FGF2 induced growth, but not FGF23 growth.

When co-treatment occurred with an FGFR4 blocking antibody, FGF23 induced cell growth was blocked while FGF2 growth was not. In light of this, FGF23 is able to induce hypertrophic

growth in this model, specifically through

FGFR4.

We now repeated this experiment, but replaced the FGFR blockers with SKL. As shown in Fig. 24, FGF23 was able to induce an increase in cell area as before; treatment with either SKL or an anti-FGF23 antibody alone had no effect on cell size. When FGF23 treatment occurred after pre-treatment with either of these compounds, its effects on cell area were blocked. This shows that SKL is able to directly modify FGF23 signaling in cardiac myocytes, and prevent the effects seen in CKD. On top of this data, SKL has

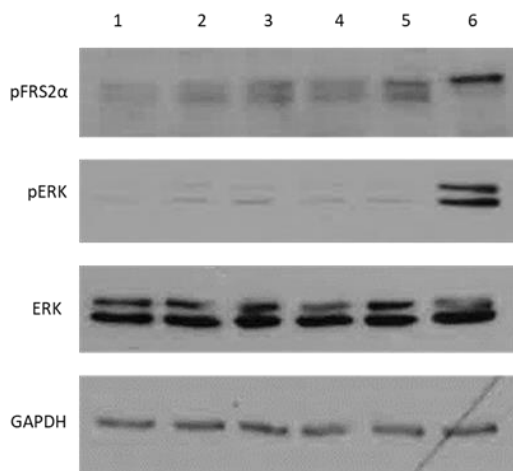


Figure 25. SKL and FGF23 Induce MAPK Signaling in NRVMs
NRVMs were treated with the following combinations of FGF23 and SKL based on lane: 1. Saline, 2. FGF23, 3. SKL, 4. SKL+FGF23, 5. Pretreatment with SKL followed by FGF23 treatment, 6. Pre-incubation of FGF23+SKL in media before cell addition. Total protein extracts were analyzed by Western blotting. When SKL and FGF23 were pre-incubated and then added to cells, ERK was phosphorylated. FGF23 was used at 25 ng/mL, SKL was used at 100 ng/mL. Pre-incubations were done for 60 mins, and cell treatments were for 30 mins.

been recently shown by other groups to prevent FGF23-dependent calcium signaling in adult rat cardio myocytes (ARVM),²⁰² as well as prevent hypertrophic growth in mice injected repeatedly with FGF23.²⁰³ We then further looked into the signaling effects that SKL was mediating in myocytes in Fig. 25.

We treated cells with different combinations of a molar ratio of FGF23 and SKL to assess if this order of events had any effect on signaling. FGF23 or SKL had no effects on MAPK signaling, and oddly also the simultaneous addition of SKL and FGF23 did not have any effect either. We then pretreated cells with SKL for one hour before adding FGF23 which did not activate MAPK sig-

naling. When we pre-incubated FGF23 in combination with SKL for one hour, and then added this to cells we saw a positive increase in MAPK signaling.

In light of this data on SKLs effects on FGF23 signaling, and our plate-based assay that can measure binding, we developed an assay that can measure the activity of purified SKL. We previously found that SKL induced FGF23 binding to FGFR1 and FGFR4 with high affinity, but since FGFR4 bound FGF23 in the absence of SKL while FGFR1 did not, we utilized FGFR1 binding to FGF23 to measure the presence of SKL. A

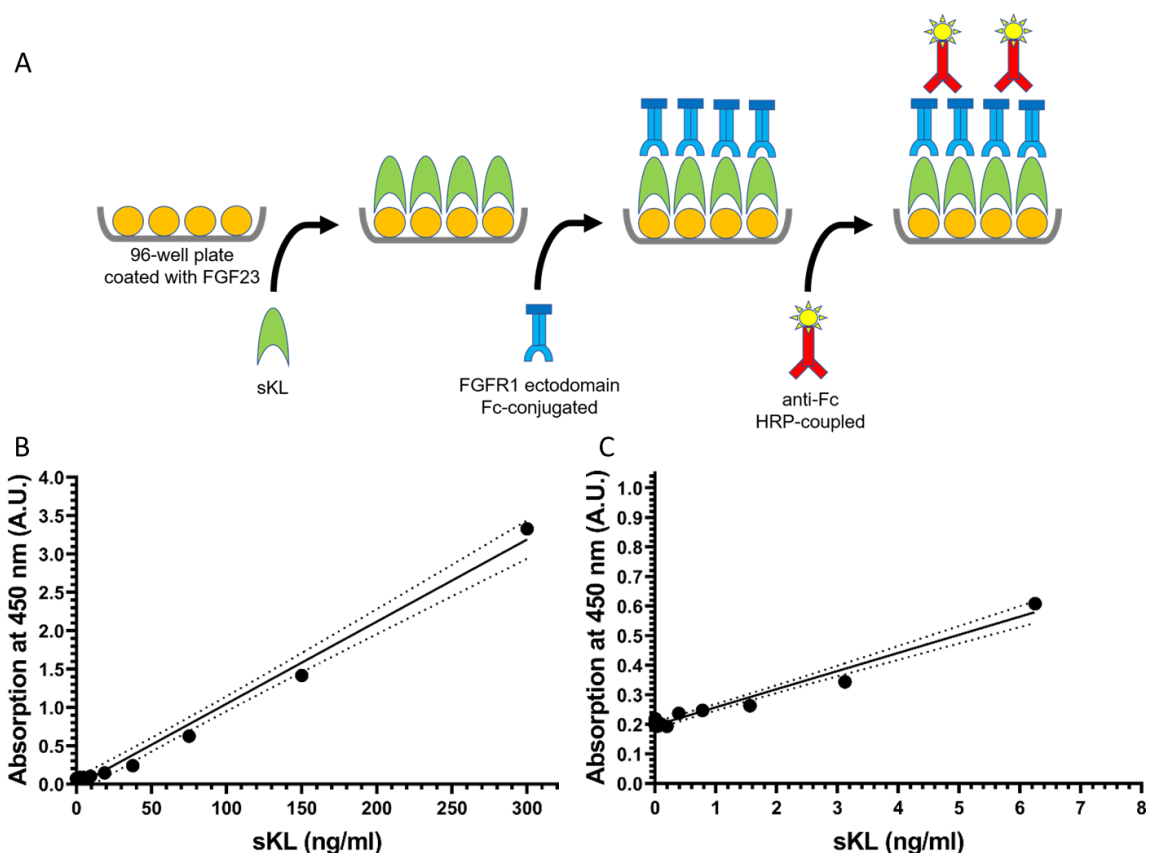


Figure 26. Sensitivity of a Novel Assay Measuring SKL Activity
 (a) Schematic of our SKL activity assay (b, c) Standard curves (linear regression) for the measurements of FLAG-tagged SKL using our plate-based assay, with FGF23 coated on 96-well plates and incubations with HRP-coupled Fc-FGFR1c for detection. SKL was applied in (a) assay buffer or (b) in rat serum as diluent. For SKL in buffer, the assay gives a linear range allowing for the calculation of SKL concentrations in samples with a limit of detection (LOD) of around 300 pg/mL. For SKL in serum, the assay is about 10x less sensitive, with an LOD of around 10 ng/mL. Absorbances measured are depicted in arbitrary units (A.U.) as individual dots, standard curves as straight lines.

schematic of our assay design is shown in Fig. 26a. Plates are coated with FGF23, and in stepwise addition with washes between each step: SKL, FGFR1 ectodomain, and anti-Fc coupled HRP are added to wells. FGF23 and FGFR1 act similarly to antibodies in a sandwich ELISA, only binding when SKL is present.

We first tested the robustness of the assay in a neutral buffered system as well as in spiked rat serum in Fig. 26b-c. We found our assay could detect SKL activity in a neu-

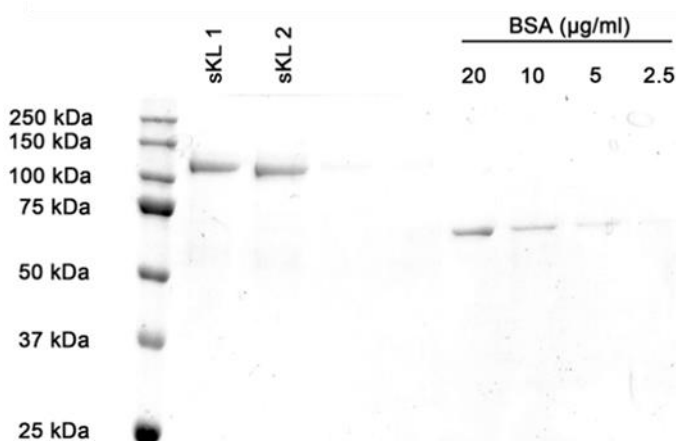


Figure 27. Purity of SKL Preparations
 Analysis of 2 preparations of recombinant SKL protein from HEK293 cell lysates using a 3-step affinity purification process using a His-tag cobalt column, followed by a Strep-tag column, and eventually a Q column. 30 μ L of sample was analyzed by SDS-PAGE and visualized on Coomassie gels. A gradient of BSA standards was used as reference. One band was detected with the expected molecular weight for SKL of 100-150 kDa.

tral buffer down to concentrations of 300 pg/mL, and in rat serum around 10 ng/mL, about a 10-fold decrease in sensitivity. While these levels would not detect physiological concentrations of SKL in serum, this provides a useful tool to study SKL further. Given the questionable quality of commercial SKL, which we personally struggled with, we looked to devise a method to purify our own SKL. We overexpressed SKL in liquid adapted HEK293T cells

and utilized a dual tag approach to allow a very selective purification process to obtain pure SKL from mammalian cell lysates while still maintaining optimal activity. We performed lysis in an ethylenediaminetetraacetic acid (EDTA)-free lysis system to avoid stripping SKL's recently discovered zinc ion, followed by a three step purification process of polyhistidine (HIS) tag purification, Strep-Tactin purification, and finally clean up

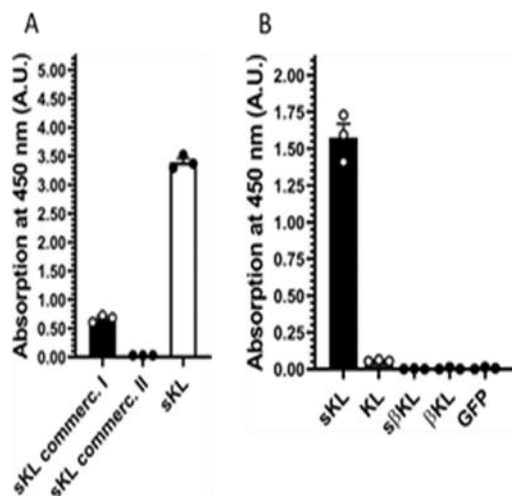


Figure 28. Comparing SKL Activity under Different Conditions

(a) Two commonly used commercial preparations of SKL (Com.SK) and KL1 were analyzed in our SKL detection assay in comparison to our own FLAG-tagged SKL. Our SKL protein showed about 7x higher binding activity compared to Com.SK, and we detected no binding of KL1. (b) Using our FGF23/Fc-FGFR1c-based detection assay, we analyzed binding affinities of different variants and isoforms of klotho, i.e. SKL and full-length klotho (KL), as well as soluble β -klotho (s β KL) and full-length β -klotho (β KL). HEK293T cells were stably transfected with FLAG-klotho constructs or a GFP vector used as negative control, and total cell lysates were analyzed. A strong signal was observed for SKL, and much weaker binding for KL. GFP, s β KL and β KL showed no measurable binding activity.

via ion affinity Q column purification. As seen in Fig. 27, our product is very pure by demonstrating a single band at the expected 120 kDa molecular weight of SKL. We utilized our klotho-based assay to measure the activity of our product during different purifications (data now shown) and optimized our buffer system to obtain the product with the highest activity.

We then compared the SKL we purified versus the two commonly available SKL preparations in Fig. 28a. The first we analyzed was from R&D systems. Compared to our SKL preparation, we saw 7 times less activity. We also compared our SKL to one from Peprotech, which is only the KL1 domain of SKL. For this sample, we detected no measurable activity. We then further analyzed the robustness of our assay in HEK293T cell lysates in Fig. 28b. We transfected cells with full-length and soluble versions of KL and BKL to see if any other forms or family members could

cause false readings in our assay. The activity assay detected a strong signal for HEK cell lysates that contained SKL, and we detected a very faint signal for lysates containing KL.

Samples containing a form of BKL or GFP showed no activity in our assay, confirming it is specific for SKL. Given the proven robustness of our assay and the quality of our SKL preparation, we then measured the half-life of SKL in serum. Rats were injected with 100µg/kg SKL, and serially bled at different time points to measure the activity of SKL in their serum over time in Fig. 29. We found a surprisingly short half-life of under 15 minutes, and by six hours we were unable to detect any activity of SKL in serum as seen in Fig. 29a. Given that SKL injections have been shown to increase phosphate excretion, and animal models of extreme elevations of SKL have increased levels of FGF23, we measured these parameters as well in Fig. 29b-c.^{43, 200, 201} Contrary to other reports, our single tail vein injection of SKL did not induce any changes in serum phosphate levels across all time points. When looking at FGF23 levels, we saw a small but significant change in FGF23 levels across multiple time points in rats injected with SKL.

Discussion

Given that the MAPK pathway is pro-hypertrophic²⁰⁴ and our data shows that SKL activates this pathway in the presence of FGF23, cardiac protection via this mechanism could be surprising. We showed for the first time that SKL does in fact attenuate FGF23-mediated myocyte growth. Multiple groups have shown that FGF23 binds FGFR4 at high concentrations, in the absence of any KL co-receptor.^{190, 203, 205} This in turn can cause a change in calcium handling,²⁰² contraction,¹⁹⁰ and cell growth,¹⁹³ inducing hypertrophy and cardiac dysfunction seen in disease settings with increased FGF23 levels. While SKL can modify FGF23 to bind FGFR1, it also induces FGF23 to bind FGFR4 at an even higher affinity than in its absence, which in theory could lead to a more potent FGFR4 activation. When we treated NRVMs with FGF23 and SKL, we did

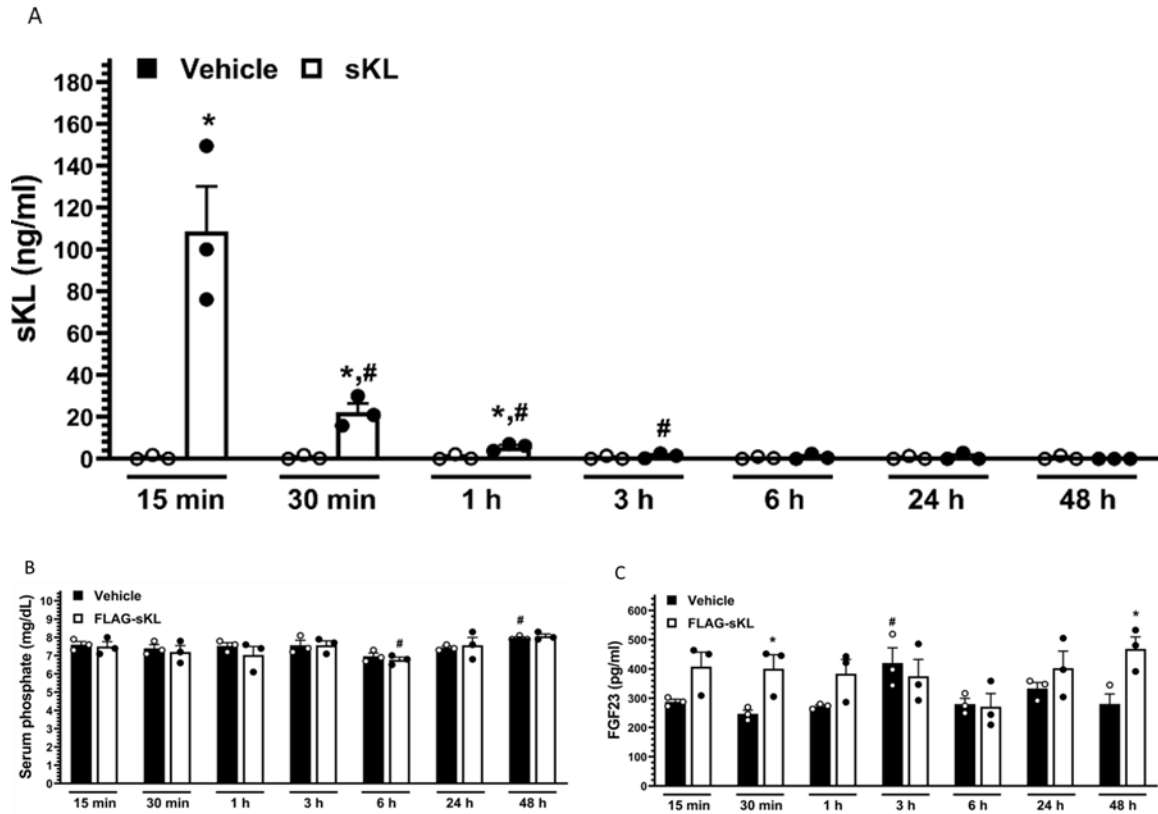


Figure 29. Half-Life Measurements of SKL

(a) Rats were injected via the tail vein with FLAG-SKL (100 μ g/kg) or vehicle (PBS), and serial bleeds were taken at different time points and analyzed by our FGF23/Fc-FGFR1c-based detection assay. At the 15-minute time point, high levels of SKL were detected in SKL-injected rats compared with vehicle-injected controls. SKL exhibited a half-life of less than 15 minutes and starting at 3 hours post injection we could not detect SKL anymore. (b) Phosphate levels were not significantly altered in any of the serum samples. (c) Intact FGF23 levels were significantly elevated in some serum samples derived from rats which received SKL, including the 48-hour time point. Comparison between groups was performed in form of two-tailed t-tests (a, b). A significance level of $p \leq 0.05$ was accepted as statistically significant. (a, b) $n = 3$; * $p \leq 0.05$ vs. vehicle treated at same time point, # $p \leq 0.05$ vs. same treatment in preceding time point. All Values are expressed as mean \pm SEM.

indeed see an inhibition of FGF23 induced cell area increase. This could be in fact due to multiple different mechanisms. The first could be that SKL has the highest affinity (3-fold) for FGFR1, as shown in our previous data. Given that cardiac myocytes are known to express high amounts of FGFR1, along with nearby cardiac fibroblasts, SKL may preferentially bind FGFR1 over FGF23 or FGFR4. This in turn would lead to a high af-

finity binding site for FGF23 and competitively inhibit FGF23 binding for FGFR4. Previous work has shown that FGFR4 is a poor activator of ERK, and our data shows that FGFR4 activates PLC γ in myocytes when stimulated by FGF23.³⁴ FGFR1 is a strong activator of the MAPK pathway, and this switch in signaling from PLC γ to ERK may be protective. A secondary option could be a shape change that is elicited by SKL and FGF23 to FGFR4. NGM Bio designed an FGF19 mimetic known as NGM282, and this mimetic had three point mutations making it more stable and potent. NGM found that the wildtype FGF19 was not only an inducer of the MAPK pathway, but also activated STAT3 in cells that contained BKL and FGFR4.¹⁴² When they treated the same cells with their mimetic, FGFR4 was still activated, but this activation led only to MAPK activation without STAT3 activation. This implies that the shape of the substrate in the binding pocket in the ectodomain of the FGFR could in fact play a role in the intracellular activation by the receptor tyrosine kinase domain. If this is the case, SKL may modify the shape of FGFR4, preventing PLC γ activation. We show that in the presence of SKL, the MAPK pathway is activated. But our data does not show which receptor is activated, and more work would need to be done to uncover this exact mechanism.

The pre-incubation of FGF23 and SKL being the only condition that caused an increase in MAPK activation is quite surprising. When cells were treated simultaneously with FGF23 and SKL or pretreated with SKL before FGF23 addition, we did not see any MAPK activation. In Chapter 2, we saw weak activation of HEK293 cells when pretreated with SKL, so to not see this in myocytes is surprising. But in our HEK293 cells we used a very high concentration of SKL compared to FGF23 to ensure binding to as much FGFR1 as possible. In the case of the NRVMs, we used a molar ratio of SKL to

FGF23, which could mean that SKL may in fact quickly bind FGFR1 and be diffused over numerous cells. The amount of FGFR1 containing SKL may be too diffuse for FGF23 to bind to and mount a MAPK response via receptor activation, in turn leading to an undetectable signal. A larger amount of SKL, as in the HEK293 cells before, may have been able to induce this response. Another reason for this could be the data from our receptor affinity readout. When alone, SKL has a high affinity for only FGFR1, but when pre-bound to FGF23, this complex is promiscuous for FGFR1, FGFR3, and FGFR4. The co-incubation before cell addition allows this complex to form, and it may be this multi-receptor activation that leads to the strong MAPK signaling we observed.

Utilizing the strong and selective binding between FGFR1 and FGF23, we were able to design a novel assay to measure SKL levels, and more importantly, SKL activity. Our assay was both robust in a neutral buffer, and in serum. We also were able to detect SKL in HEK293 cell lysates and found that BKL did not interfere with our assay. We also found that full-length membrane KL did not induce any activity in our assay, which we hypothesize might be based on the aggregation of KL. Since this form has a hydrophobic membrane-spanning region, this may cause aggregation during cell lysis, leading to a loss in activity to promote FGF23 binding.

This assay aided us in designing a novel method to purify SKL. Given the ability to measure the activity of our product in a high-throughput and quantitative way, we were able to modify our techniques and buffer system to give us the best possible KL based on this activity. When compared to commercial products available, our SKL promoted FGFR1 binding with a much higher affinity. When analyzing the other products, we were able to deduce why this is the case. The SKL product from R&D Systems is stored in a

buffer containing EDTA. EDTA is used as a preservative and protease inhibitor, due the fact it has a strong affinity for divalent cations. Given that many proteases contain a metal ion, EDTA is able to inactivate them and preserve proteins in solution from degradation. The recent crystal structure of SKL shows that SKL contains a zinc ion, and when mutation analysis was performed to remove this ion, these mutant SKLs became unable to promote FGF23-FGFR1 signaling.⁴³ Therefore, by storing their SKL in EDTA, the zinc ion is removed and this SKL preparation has limited functional activity compared to SKL that contains this ion. The second preparation we looked at from Peptotech only contains the KL1 domain of SKL. The recent crystal structure showed that both KL domains are required for FGF23 and FGFR1 binding. Given this, it is of no surprise that this protein showed no activity in our assay. Overall, it is extremely important to have a SKL activity assay to measure protein quality and have a good preparation of SKL to test its effects in models of disease. If data is continued to be generated using these poor quality SKL products, the true therapeutic potential of SKL may never be unraveled.

This activity assay also gave us the ability to measure SKL activity in serum. While our current limit of detection (LOD) was too high to measure if physiological levels of SKL exist, it did give us the potential to measure the half-life of SKL. We found an extremely short half-life, which is under 15 minutes. This would currently mean SKL would be poorly suited as a therapeutic agent, as a much longer half-life would need to be achieved to realistically treat patients. While this may seem disheartening, other wildtype FGFs show a similar short half-life.^{206, 207} Mimetics of these proteins are being developed that offer a much longer half-life, so the same will need to be done for SKL.^{208, 209}

CHAPTER 4: HEPARIN INCREASES THE AFFINITY OF FGF23 FOR FGFR4

Background

Classical signaling by the hormone FGF23 is through binding to FGFR1c and the cognate co-receptor KL, leading to activation of the MAPK pathway.²⁶ This has been used to screen target tissues and cell types for FGF23 susceptibility, and it is believed that cells lacking KL or MAPK activation in response to FGF23 stimulation are unable to respond to FGF23. While this is the case, early work on FGF23 signaling that precluded KL discovery focused on cellular responses to FGF23 in cells that lacked KL.²² FGF23 signaling was analyzed in BaF3 cells, a cell line lacking all FGFRs, allowing them to be transfected with only a single FGFR isoform to analyze responses. The authors had to use supraphysiological concentrations and demonstrated that FGF23 was able to increase cell proliferation in the presence of heparin, with FGFR1-3c splice variants and FGFR4. They found that out of all four receptors, FGFR4 had the most potent effect on FGF23 dependent cell division. The authors then focused on FGF23's relationship with FGFR1, since this was the receptor believed to play a role in phosphate regulation. They introduced highly sulfated heparin glycosaminoglycans (GAGs), and found that the higher degree of sulfation and the longer the chain, the higher the potency of FGF23 to induce cell growth. This was one of the first instances where FGF23 was shown to act independent of KL.

Our recent work on FGF23 in CKD matches up with this early work. We found that FGF23 is highly elevated above physiological levels, and under these conditions it is able to signal through FGFR4. Unlike their findings of all four FGFR receptors, we found that this effect was FGFR4-specific. Our work did not elucidate if there was a co-factor that played a role in this FGFR4 dependent effect, so we looked to explore this further.

Methods

ARVM Isolation and Analysis of Calcium Transients

As done before,²¹⁰ adult male Wistar rats (150-200 g) were sacrificed and hearts were quickly removed and cannulated via the ascending aorta on a Langendorff system where they were retrograde perfused and digested by type II collagenase. Hearts were perfused with calcium-free Tyrode's solution supplemented with EGTA 0.2 mmol/L for 3 minutes. For the digestion, hearts were perfused with Tyrode's solution containing 0.1 mmol/L CaCl₂, 1 mg/mL type II collagenase (Worthington) and 1 mg/mL BSA for 3-4 minutes at room temperature. Cells were resuspended in Tyrode's solution containing 1 mmol/L CaCl₂. Tyrode's solution contains 130 mM NaCl, 5.4 mM KCl, 0.4 mM NaH₂PO₄, 0.5 mM MgCl₂, 25 mM HEPES, 22 mM glucose. ARVM were load with fluorescence Ca²⁺ dye Fluo-3 AM for cytosolic Ca²⁺ measurements. Loaded-ARVM were acutely perfused during 2 minutes with vehicle, FGF23 (10 ng/mL) or a combination of FGF23 and heparin (0.7 USP/mL). Cytosolic Ca²⁺ transients were recorded under 1 Hz of field stimulation using two parallel platinum electrodes. Images were obtained with confocal microscopy (Meta Zeiss LSM 510, objective w.i. 40x, n.a. 1.2) by scanning the cell with an Argon laser every 1.54 milliseconds. Fluo-3AM was excited at 488 nm and emis-

sions were collected at >505 nm. Cell contraction was stimulated as the difference of cell length between rest and contraction (during electrical stimulation), expressed as a percentage of shortening of cell length. Image analysis was performed by homemade routines using IDL (Research System Inc.) and ImageJ (NIH) software.

Isolated Mouse Heart Contractility

Isolated heart contractility was performed as previously described.^{205, 211, 212} Briefly, 2-3-months old male CD-1 mice were anesthetized using 3% isoflurane, and hearts were carefully removed and placed into oxygenated Ringer's solution composed of 140 mM NaCl, 2.0 mM KCl, 2.5 mM CaCl₂, 1.0 mM MgSO₄, 1.5 mM K₂HPO₄, 10 mM HEPES, 10 mM glucose, pH 7.4. Atria were then removed, and the intact ventricular muscle was attached to small metallic clips hung vertically from a force transducer (ADInstruments,) between bipolar platinum-stimulating electrodes and suspended in 25-mL glass tissue chambers (ADInstruments). Heart muscles were superfused with Ringer's solution continuously bubbled with 100% O₂ at room temperature. Hearts were stretched to the length of maximum force development and paced at 1 Hz (5-millisecond pulse duration, 30-60 V; Grass Technologies stimulator SD9). After a stable baseline was obtained, hearts were treated with either vehicle or with FGF23 (9 ng/mL) and heparin (0.06 USP/mL) while contractile force output was monitored for 30 minutes. The contractile data were recorded and analyzed on LabChart 8 software (ADInstruments). Waveform changes were analyzed for peak contraction force (mN) and maximal slope of force development and presented as fold change from baseline values.

Results

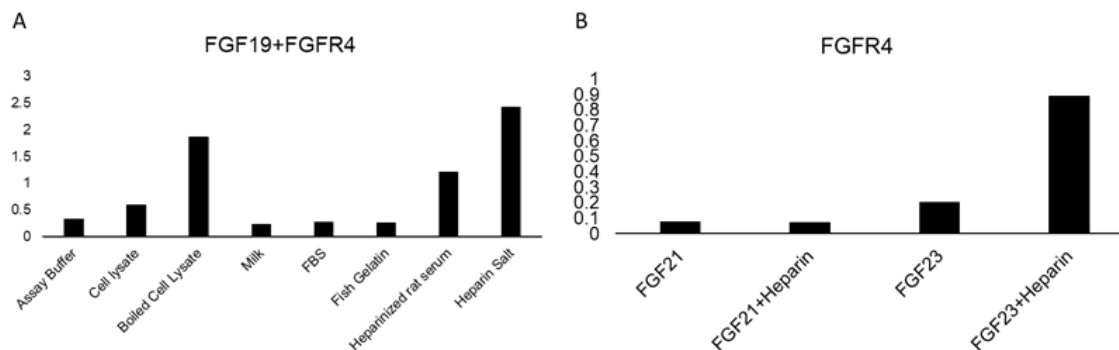


Figure 30. Heparin Plays a Role in FGF Signaling with FGFR4

(a) 96-well plates were coated with 250 ng of FGF19. Plates were incubated with either 5% cell lysate or blocker, or 0.4 USP heparin. Wells were washed, incubated with 500 ng of Fc-tagged FGFR4, washed again, treated with HRP-coupled anti-Fc, and HRP substrate, followed by the analysis of absorbance at 450 nm (b) 96-well plates were coated with 250 ng of FGF21 or FGF23. Plates were incubated with either 0.4 USP heparin or PBS. Wells were washed, incubated with 500 ng of Fc-tagged FGFR4, washed again, treated with HRP-coupled anti-Fc, and HRP substrate, followed by the analysis of absorbance at 450 nm

While exploring our FGF plate-based activity assay, we found that in the absence of SKL, FGFR4 was able to bind FGF23. This effect is much weaker than the effect seen in the presence of SKL, but it plausibly could happen during states of FGF23 elevation. While testing our assay under different buffer conditions, we noticed the addition of a cellular lysate seemed to increase the binding of FGF23 to FGFR4 (data not shown). We became curious what in this cell lysate could be increasing this binding; keeping in mind that heparin has previously been shown to play a role in FGF23 signaling. We tested this in Fig. 30 on all endocrine FGFs. As seen in Fig. 30a, we looked to find what aspect of the cell lysate could be increasing the binding affinity for FGFR4. We utilized FGF19, as this has been previously published to have BKL independent effects.¹⁰¹ We saw that when a cell lysate was added to wells, binding was slightly increased. We then utilized a

cell lysate that had been boiled, which in theory should denature all proteins that could be responsible for increasing binding, but heparin being a GAGs would still be active. This had a positive effect, as the affinity for FGFR4 by FGF19 increased even more. Other control blockers that would not contain heparin had no effect on binding, while heparin salt or a rat serum containing spiked heparin greatly increased FGFR4 binding. To analyze if this played any role with the other two endocrine FGFs or just FGF19, we re-ran the same assay with heparin salt except with either FGF21 and FGF23, and we found that FGF23 had a similar increase in binding affinity to FGFR4 in Fig. 30b. This was our first piece of evidence showing that heparin may in fact be the co-receptor responsible for FGF23 binding to FGFR4, challenging the idea that endocrine FGFs do not utilize heparin as a binding partner.

To further analyze the effects heparin could have as a co-receptor, we immobilized ectodomains of each FGFR isoform coupled to an Fc domain on protein A/G beads, followed by the co-incubation with heparin or SKL and FGF23 in Fig. 31a. We found that the combination of SKL and FGF23 caused a co-precipitation of a complex as before with FGFR1, FGFR3, and FGFR4. When SKL was replaced with heparin, we found a weak precipitation of FGF23 with FGFR1-3. FGFR4 showed a much stronger precipitation. While the amount of FGF23 precipitated was lower than when SKL was present, it still showed that FGFR4 was the preferred FGFR isoform when heparin was present. We repeated this experiment in Fig. 22a-b, and unlike FGF23, we did not see similar effects with FGF19 or FGF21. We then utilized our plate-based assay in Fig. 31 b-c. In Fig. 31b, we looked to see how heparin would have effects on all four FGFRs. Without heparin, we found FGF23 had a slight affinity for FGFR4, while no other FGFR had any measurable

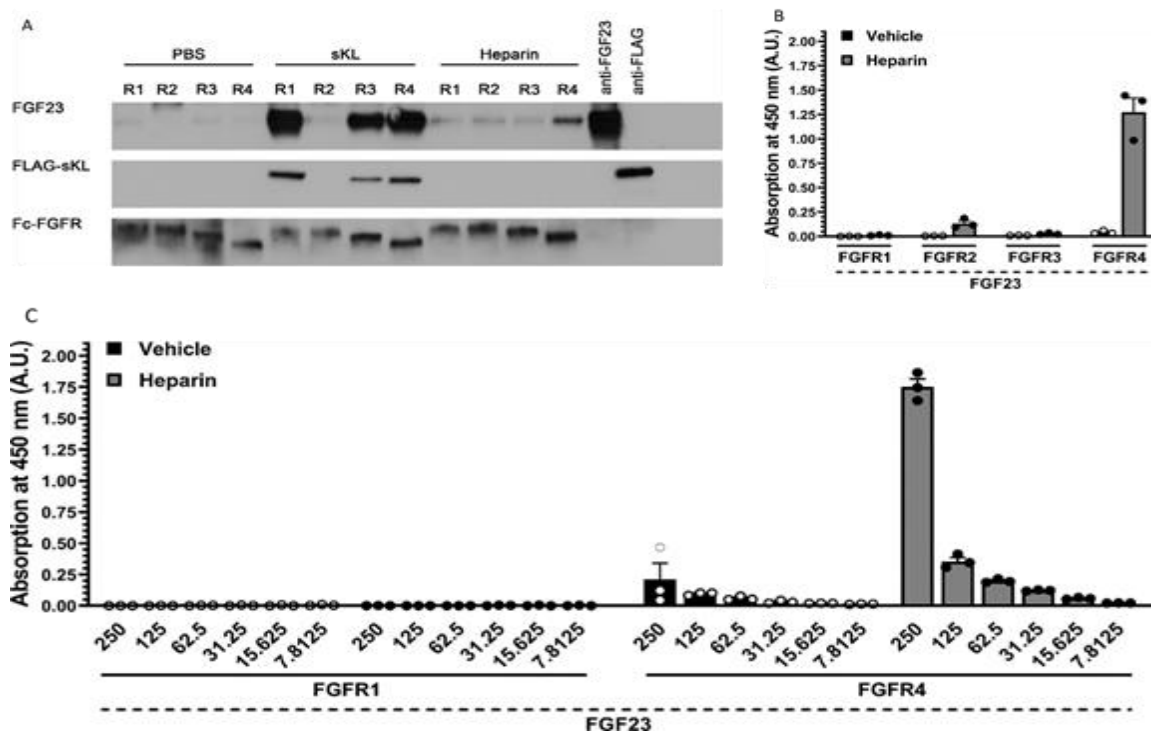


Figure 31. Heparin Increases FGF23 Affinity for FGFR4

(a) Fc-tagged FGFR isoforms 1c, 2c, 3c, or 4 were bound to protein A/G beads and treated with FGF23 in combination with either FLAG-tagged SKL, heparin or PBS. Anti-FLAG beads incubated with FLAG-SKL and anti-FGF23 antibody immobilized on protein A/G beads and treated with FGF23 served as positive controls for FLAG- and FGF23-precipitations, respectively. Co-treatments with FGF23 and SKL lead to complex formation with FGFR1c, and to a lesser extent with FGFR3c and FGFR4. Co-treatment with heparin increased binding of FGF23 to FGFR4 and to a much lesser degree to the other FGFR isoforms. (b) 96-well plates were coated with 250 ng of FGF23, washed and then sequentially incubated with 0.4 USP of heparin or vehicle (PBS), 500 ng of Fc-tagged FGFR 1c, 2c, 3c, or 4, HRP-coupled anti-Fc, and HRP substrate, followed by absorbance measurement. In the presence of heparin, FGF23 bound FGFR4 the strongest, with weaker binding to FGFR2c, and no measurable binding to FGFR1c and FGFR3c. (c) 96-well plates were coated with 2-fold dilutions of FGF23, ranging from 250 ng - 7.8125 ng. Wells were washed, and sequentially incubated with 0.4 USP of heparin or vehicle (PBS), followed by 500-15.625 ng of Fc-FGFR1c or Fc-FGFR4, HRP-coupled anti-Fc, and HRP substrate. In the presence of heparin, FGF23 did not bind to FGFR1c, and binding of the heparin/FGFR4 complexes occurred in relation to the amount of coated FGF23. In the absence of heparin, FGF23 bound FGFR4 with weak affinity, but not FGFR1c. (b, c) $n = 3$

binding. When heparin was introduced, we saw a slight increase in FGFR2 binding to FGF23, but a large increase in FGFR4 binding. FGFR1 and FGFR3 still showed no binding even with heparin addition. In Fig. 22c, we repeated this with FGF19 and FGF21, and

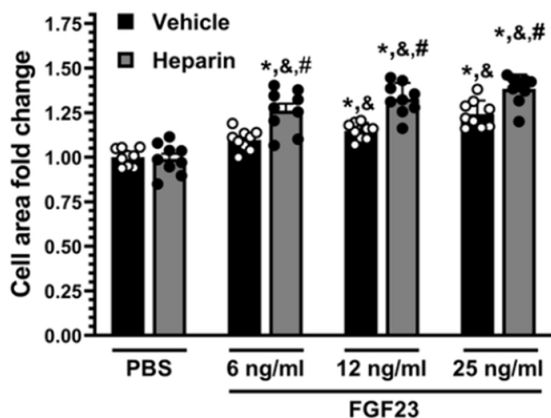


Figure 32. Heparin Increases the Effects of FGF23 on NRVMs

NRVMs were co-treated with FGF23 at indicated concentrations or vehicle (PBS), and with heparin (0.19 USP/mL) or vehicle. FGF23 treatments caused a stepwise elevation in cell area with increasing FGF23 concentrations. Heparin increased this effect at all FGF23 concentrations. (100 cells per slide, $n=3$ independent isolations, 300 total cells per condition; $*p \leq 0.05$ vs. PBS/PBS, $\&p \leq 0.05$ vs. PBS/heparin, $\#p \leq 0.05$ vs. FGF23 + vehicle at same concentrations).

myocytes, we wanted to determine whether heparin modulates the cardiac effects of FGF23. First, we co-treated NRVMs with increasing concentrations of FGF23 and with heparin for 48 hours. We found that the gradual FGF23-induced increase in cell area was further elevated in the presence of heparin in Fig. 32. Treatment with heparin by itself had no effect on NRVM area. Since FGF23 alters calcium handling and contractility in isolated ARVMs,²⁰² we studied the potential effects of heparin in this context. Perfusion of ARVMs with FGF23 for two minutes increased systolic $[Ca^{2+}]_i$ transients, but this change was not statistically significant in Fig. 33 a, c. However, when cardiac myocytes were co-perfused with FGF23 and heparin, further elevations in systolic $[Ca^{2+}]_i$ transients

we saw no binding with any FGF and FGFR, even in the presence of heparin. In Fig. 31c, we tested a 2-fold dilution effect with FGFR1 and FGFR4 to see how this affected binding. When no heparin was present, we detected binding to FGFR4 only at high concentrations of FGF23. With or without heparin we saw no binding to FGFR1, and with heparin present, we saw a dose-dependent decrease in FGF23 binding.

Since we found that heparin mainly facilitates FGF23 binding to FGFR4 in our previous work on these effects on cardiac

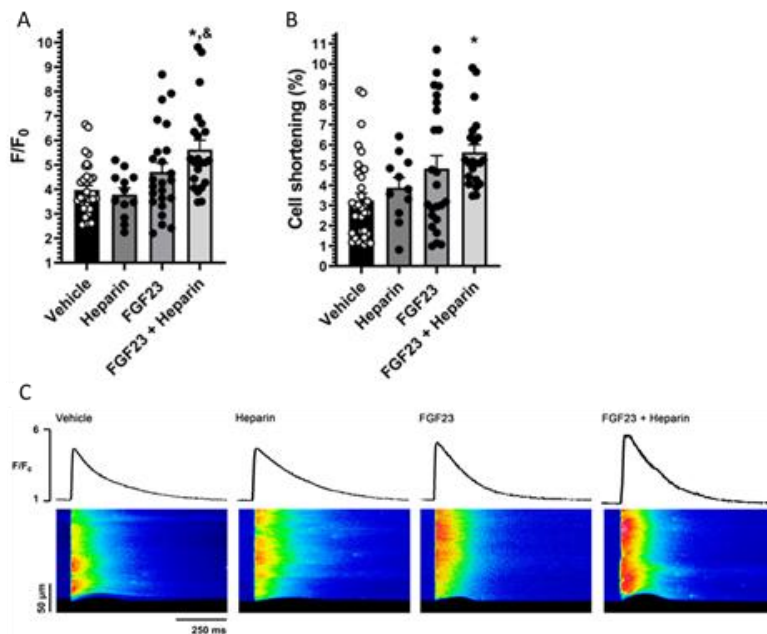


Figure 33. Heparin Increases the Effects of FGF23 Induced Calcium Handling

(a) ARVMs were treated with FGF23 (10 ng/mL), heparin (0.7 USP/mL) or a combination of both, and peak fluorescence $[Ca^{2+}]_i$ transients (F/F_0) were measured.

FGF23 increased $[Ca^{2+}]_i$, and this change significantly increased in the presence of heparin. (b) Representative line-scan images of ARVMs under 1 Hz field stimulation perfused with vehicle, heparin, FGF23, or FGF23 combined with heparin for the analysis shown in a. (c) ARVMs were treated with FGF23, heparin or a combination of both, and cell shortening after perfusion was measured. The addition of heparin significantly increased the effect of FGF23. (a, b) ($n = 5$, $n = 34$ (Vehicle), $n = 3$, $n = 12$ (Heparin), $n = 5$, $n = 24$ (FGF23), $n = 4$, $n = 22$ (FGF23 + Heparin); $*p \leq 0.05$ vs. Vehicle, & $p \leq 0.05$ vs. Heparin)

became significant. Furthermore, FGF23 increased cell contraction of ARVMs after two minutes of perfusion, which was significantly increased when cells were co-perfused with FGF23 and heparin in Fig. 33b. In

both ARVM studies, heparin by itself had no significant effects. We have previously shown that the treatment of isolated, adult mouse hearts with FGF23 for 30 minutes resulted in an increase in ventricular contraction as well as intracellular calcium.²⁰⁵ This

acute FGF23 effect occurs in a concentration-dependent manner and is mediated by

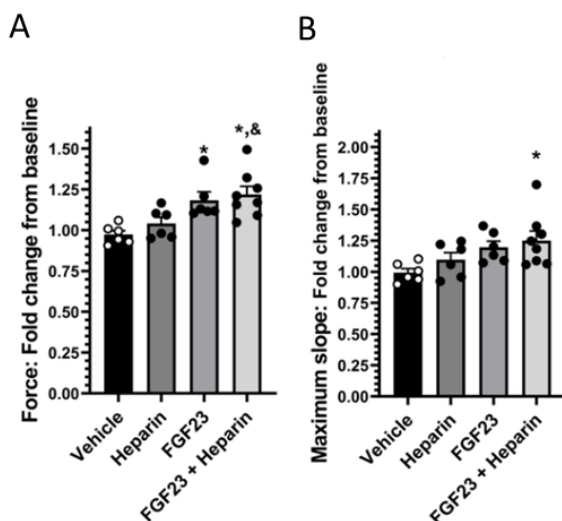


Figure 34. Heparin Increases the Effects of FGF23 on Cardiac Contraction

(a) Intact hearts were isolated from adult mice, attached to a force transducer, paced, and treated with either vehicle, heparin (0.06 USP/mL), FGF23 (9 ng/mL), or a combination of FGF23 and heparin while contractile output was monitored. Waveform changes were analyzed for peak contraction force. FGF23 increased force which was further elevated in the presence of heparin. (b) FGF23 with heparin also increased the maximum slope of force development of the contractile waveform. Comparison between groups was performed by one-way ANOVA followed by a post-hoc Tukey test (a,b). A significance level of $P < 0.05$ was accepted as statistically significant.); (a, b) $n = 6$ (Vehicle), $n = 6$ (Heparin), $n = 6$ (FGF23), $n = 8$ (FGF23 + Heparin); * $p \leq 0.05$ vs. Vehicle, & $p \leq 0.05$ vs. Heparin.

FGFR4.¹⁹⁰ To determine if heparin modulates FGF23's actions on cardiac contractility, we analyzed the contractile responses of isolated hearts from mice in the presence of FGF23 and heparin in Fig. 34 a-b. Treatment with FGF23 for 30 minutes increased cardiac contractile force compared to vehicle as previously reported.^{190, 205} When FGF23 was co-incubated with heparin prior to addition to the organ bath we detected a further increase in cardiac contractility force, when compared to treatment with FGF23 or heparin alone. While this additive effect of heparin on the acute FGF23 actions was significantly different from both vehicle and heparin treatment, it did not reach significance compared to FGF23 alone.

Discussion

While endocrine FGFs are known to have low affinity for heparin,^{14, 17} and

rely on klotho family members to act as a co-receptor, we have shown that this is not al-

ways the case. Previous literature has hinted that both FGF19 and FGF23 can bind heparin, just at a lower affinity than paracrine FGFs. This allows them to act as endocrine factors, but given that they still have affinity for heparin, it can still bind and act as a co-factor. Previous work has also shown that both FGF19 and FGF23 can have effects independent of klotho co-receptors,^{101, 213} and this is the likely mechanism behind that. Our initial screen in Fig. 30 identified that both FGF19 and FGF23 in fact could bind heparin, and this specifically influenced binding to FGFR4. Our later data showed minimal FGF19 binding compared to FGF23, and this was likely due to the lower amounts of FGF used in the later assays. This means FGF23 likely has a higher affinity for heparin and FGFR4 than FGF19. We further saw that while FGF23 bound FGFR4, this was a much lower affinity than when SKL is present. While this lower affinity means this may not be a major pathway of FGF23 signaling at physiological levels, the amounts used in these assays are seen in serum during CKD. This means that this is a likely a pathological FGF23-induced mechanism of signaling during CKD.

When we explored cellular models of FGF23 signaling, we found heparin could induce an increase in FGF23 based effects. We saw an increase in the area of NRVMs, as well as the calcium handling and contractility of myocytes. In ESRD, patients receive intravenous heparin during dialysis to avoid blood clotting in dialysis tubing. These patients have some of the highest elevations of FGF23,¹⁸⁵ and given the effects we see on cells, this may increase the effects of FGF23. This in turn means we may be increasing the potency of FGF23 in these patients by infusing heparin, and in turn contributing to FGF23's toxic effects and the high levels of CVD seen in these patients.

CHAPTER 5. HEPARIN INJECTIONS INCREASE THE EFFECTS OF FGF23 IN MOUSE MODELS OF FGF23 ELEVATION

Background

Once patients reach stage 5 of CKD, they have a GFR of under ml/min/1.73m^2 .²¹⁴ Their kidneys perform minimal filtration, and artificial means are required to prevent the accumulation of toxins in the bloodstream.¹⁶⁷ Hemodialysis the only available treatment option when patients have minimal kidney function, where an artificial system known as a dialyzer is utilized to filter a patient's blood. Vascular access is formed by an arteriovenous fistula or intravascular dialysis catheter, and blood is drawn through the machine through a semipermeable membrane. Blood is run counter-current to dialysate, which is a mixture of NaCHO_3 , NaCl , acid concentrate, and water.²¹⁵ Waste and particles that can fit through the membrane diffuse down the concentration gradient into the dialysate, providing some form of filtration that kidneys would normally perform. Sessions of dialysis last 3-4 hours, and these have to be repeated usually 3 times per week.²¹⁶

This process requires free flowing blood through small access points and tubing, so clotting can be a problem that interferes with this process. Unfractionated heparin is the most commonly used anticoagulant due to its low cost, history of use, and rapid dissipation of effects upon the end of the procedure.²¹⁷ The half-life seen for the clotting effect of heparin in patient serum is only 54 minutes.²¹⁸ In the case of over infusion, heparin is

relatively safe by infusing protamine sulfate, which can provide rapid blockade of heparin's blood thinning effects.²¹⁹ There is no standard heparin infusion method, as different combinations of bolus injections and intermittent over time injections can be used. Generally, patients receive 2,000-4000 IU of heparin at the start of treatment, and then can receive an hourly infusion from 500-2,000 IU.²²⁰ There is usually no clinical measurement of heparin during dialysis, visual monitoring is usually done by tracking low blood flow and coagulation in the machine, and more heparin is added as needed.²²⁰

Heparin is an interesting molecule, as it has been known as a blood thinner since the 1930s,²²¹ but its natural function is not an anticoagulant in cells. Heparin can be in size anywhere from 5-40 kDa, and it is composed of a carbohydrate backbone with numerous modifications and sulfations.²²² Heparin is found mainly on the cell surface and in the extracellular matrix, and has been found to bind to numerous proteins.²²² Given the diverse nature of heparin chains, it is believed that heparin may play a role in many diverse functions, but the limits to abilities and tools for analyzing carbohydrate chains have limited heparin research. As mentioned earlier, one of the major roles of heparin is the modulation of FGF signaling and excretion, and for the first time we aimed to explore its effects on FGF23-mediated changes in animal models.

Methods

FGF23 Serial Injections

FGF23 injections were conducted following a similar protocol established by us¹⁸³ and others.^{203, 223} Briefly, twelve-week old, male BALB/c mice (Jackson Laboratories) underwent tail vein injections. The day before the experiment, mice underwent

echocardiographic analysis, as described below. Mice were anesthetized in 2.5% isoflurane and placed on a heat pad. Each group consisted of 5 mice, and different groups were injected with isotonic saline, heparin, FGF23, or FGF23 and heparin combined. Per injection, we used 40 $\mu\text{g}/\text{kg}$ of FGF23 and 125 USP/kg of heparin dissolved in 200 μL of isotonic saline, with 8 hours between injections for a total of 5 consecutive days. All injections were performed via the lateral tail vein. On the morning of the sixth day, 16 hours after the final tail vein injection, animals underwent echocardiographic analysis and were sacrificed. Middle sections of hearts were cut along the short axis and stored overnight in 4% phosphate-buffered formaldehyde solution. Sections were sent to IDEXX Laboratories for embedding, hematoxylin and eosin (H&E) staining, and sectioning. Sections for wheat germ agglutinin (WGA) labeling were not stained by IDEXX.

Adenine Diet Mice

This diet-induced model of CKD, which develops kidney tubule-interstitial damage and cardiac hypertrophy, was done in accordance with previous studies.^{224, 225} We studied male and female mice in separate groups, based on the gender-specific effect of adenine, with females taking much longer (16-20 weeks) to develop kidney injury.²²⁶ Five-week old BALB/c mice (Jackson Laboratories) were put on the control diet for one week. After 1 week, male and female mice were each split into 4 groups, receiving control chow and saline injections, control chow and heparin injections, adenine chow and saline injections, or adenine chow and heparin injections. Mice were administered an adenine diet (0.2% adenine, Teklad) or control diet (same composition as adenine diet lacking adenine, Teklad) based on their group and injected via the lateral tail vein with 125 USP/kg heparin dissolved in isotonic saline or with isotonic saline as vehicle control. In-

jections were done 3x per week, every Monday, Wednesday, and Friday, to mimic a dialysis schedule. During injections, mice were briefly anesthetized with 2.5% isoflurane, and the injection was performed in the lateral tail vein. After 10 weeks, mice were sacrificed, and samples prepared as described above.

Morphology, Fluorescence Microscopy and Morphometry of Mouse and Rat Hearts

Short-axis heart sections were stained with H&E (IDEXX) and used for representative images. Pictures were taken on a Leica Dmi8 fluorescent microscope. We measured cross-sectional area of individual cardiac myocytes in paraffin-embedded short-axis sections. Paraffin sections underwent deparaffinization 2x for 5 minutes in Shandon Xylene Substitute and then rehydrated through a graded ethanol series (99%, 97%, 70%), 2x for 5 minutes each. Antigen retrieval was performed in a microwave for 15 minutes in 1x unmasking solution (H3300, Vector Labs). Slides were washed 3x for 5 minutes each in PBS, then incubated for 1 hour in blocking solution (1% BSA50 (Rockland), 0.1% coldwater fish skin gelatin (900033, Aurion), and 0.1% Tween 20)). Slides were washed 3x in PBS and then incubated in 10 $\mu\text{g}/\text{mL}$ of 594-conjugate WGA (W11262, Thermo Fisher) for 1 hour. Slides were washed 3x with PBS and then mounted in Prolong Diamond (P36961, Thermo Fisher). Immunofluorescence images were taken on a Leica Dmi8 fluorescent microscope with a 60x oil objective. ImageJ software (NIH) was used to quantify cross-sectional area of 25 cells per field in 4 fields along the mid-chamber free wall based on WGA-positive staining.

Echocardiography of Mouse Hearts

Echocardiographic analysis was performed on day 6 of the experiment for FGF23-injected mice, using a Vevo 770® High-Resolution Micro-Imaging System (FUJIFILM VisualSonics), equipped with an 707B-253 transducer. Animals were anesthetized with 1.5% isoflurane, and normal body temperature was monitored and maintained on a heating pad. For analysis, both B- and M-mode images were obtained in the short and long axis views. Correct positioning of the transducer was ensured using B-mode imaging in the long axis view, before switching to the short axis view. Image analysis was performed using the Vevo® 770 Workstation Software (FUJIFILM VisualSonics). Measurement and Calculation definitions (including formulas) for B-mode are presented in the Supplementary Information.

Serum Chemistry

At the end of the experiment, blood was collected from mice at sacrifice via cardiac puncture, transferred into microvette serum gel tubes (20.1344, Sarstedt) and centrifuged at 10,000 g for 5 minutes. Serum supernatants were collected and stored at -80°C. Analyses of standard serum chemistry parameters were performed at IDEXX BioAnalytics (60406, renal panel), serum blood urea nitrogen (BUN) was measured via Mass Spectrometry at the Bioanalytical Core of the UAB O'Brien Center for AKI.

Results

We investigated if the effects of heparin we see on a biochemical and cellular level could be observed in mouse models of FGF23 elevation. Given that heparin is used

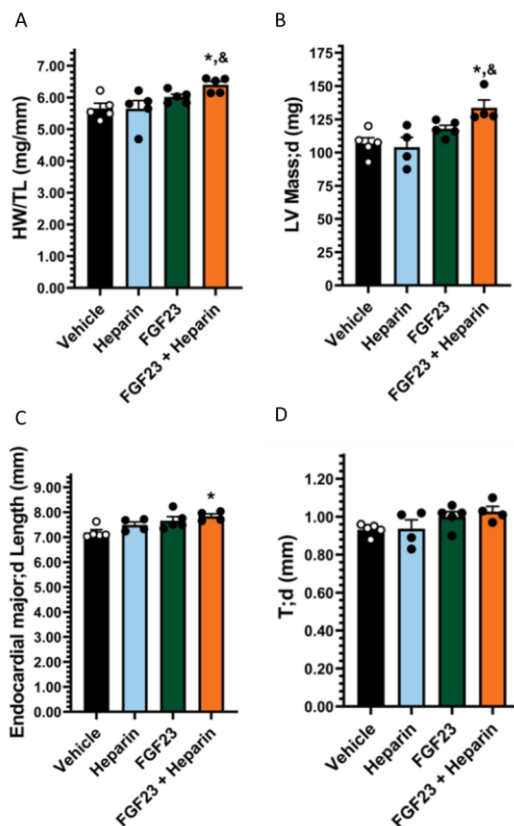


Figure 35. Heparin Increases the Effects of Recombinant FGF23 on Cardiac Hypertrophy

Twelve-week old, male BALB/c mice received i.v. injections, 2x daily, for 5 consecutive days, with either vehicle (saline), heparin (125 IU/kg), FGF23 (40 $\mu\text{g}/\text{kg}$), or FGF23 plus heparin, after which the mice underwent echocardiographic analysis and were sacrificed. In mice receiving FGF23 and heparin combined, (a) the ratio of heart weight to tibia length (b) left ventricular (LV) mass in diastole (c) endocardial major axis in diastole (d) T;d, Comparison between groups was performed in form of a one-way ANOVA followed by a post-hoc Tukey test (a-d) (a-d) $n = 4-5$; * $p \leq 0.05$ vs. Vehicle, & $p \leq 0.05$ vs. Heparin. All Values are expressed as mean \pm SEM.

during dialysis in ESRD, these effects could have real world implications for patients under these conditions. First, we co-injected FGF23 and heparin in mice. We have shown before that two tail vein injections of recombinant FGF23 protein at 40 $\mu\text{g}/\text{kg}$ per day for five consecutive days induces cardiac hypertrophy,¹⁸³ which has been confirmed by others.^{223, 227, 228} In Fig. 35, we injected male BALB/c mice with 40 $\mu\text{g}/\text{kg}$ of FGF23 and 125 USP/kg of heparin separately and to-

gether. Mice co-injected with FGF23 and heparin with the only group that showed statistical significance in HW/TL, a common readout for increases in cardiac size as seen in Fig. 35a. When analyzed via echocardiography in Fig. 35b-d, the FGF23 and heparin injected mice developed a significant lengthening of the heart, eccentric cardiac hypertrophy and increased left ventricular (LV) mass. As seen in Table 3, the increase in cardiac mass was not accompanied by changes in cardiac function, such as ejection

fraction or fractional shortening similar to what we previously found in a genetic mouse model with systemic FGF23 elevations.²¹¹ Representative pictures of cross sectional area by H/E stains can be seen in Fig. 36a, and B-mode images in Fig. 36b.

Table 3: FGF23 echocardiography

	Vehicle	Heparin	FGF23	FGF23 + Heparin
Endocardial Area;d (mm ²)	8.916 ± 0.978	7.893 ± 0.260	8.420 ± 0.365	9.573 ± 0.355
Endocardial Area;s (mm ²)	3.874 ± 0.428	3.415 ± 0.290	3.574 ± 0.340	4.398 ± 0.465
Epicardial Area;d (mm ²)	21.450 ± 1.321	19.940 ± 0.793	21.810 ± 0.595	24.180 ^{&} ± 0.608
Epicardial Area;s (mm ²)	17.860 ± 1.196	15.580 ± 0.405	18.480 ± 0.515	21.200 ^{&} ± 0.814
Endocardial %FAC (%)	56.040 ± 2.838	56.820 ± 3.164	57.750 ± 2.581	54.170 ± 4.196
Endocardial Volume;d (ul)	9.738 ± 1.938	7.083 ± 0.489	7.914 ± 0.697	9.960 ± 0.697
Endocardial Volume;s (ul)	2.020 ± 0.441	1.698 ± 0.235	1.790 ± 0.333	2.580 ± 0.469
Endocardial %EF (%)	78.540 ± 2.453	76.110 ± 2.820	77.910 ± 2.117	74.220 ± 4.307
Endocardial major;d Length (mm)	7.192 ± 0.111	7.493 ± 0.122	7.666 ± 0.156	7.843* ± 0.096
T;d (mm)	0.932 ± 0.014	0.938 ± 0.046	1.000 ± 0.027	1.028 ± 0.027
LV Mass;d (mg)	106.700 ± 4.366	104.100 ± 7.376	117.900 ± 2.606	133.600* ^{&} ± 5.959
Heart rate (BPM)	440.800 ± 7.896	433.300 ± 10.180	446.0 ± 9.524	449.500 ± 4.839

Values are expressed as mean ± SEM. Comparison between groups was performed in form of a one-way ANOVA followed by a post-hoc Tukey test. A level of P<0.05 was accepted as statistically significant, *p ≤ 0.05 vs. Vehicle, [&]p ≤ 0.05 vs. Heparin, [#]p ≤ 0.05 vs. FGF23, N=4-5.

It has been shown that the induction of kidney injury in wildtype mice by administration of an adenine-containing diet significantly increases serum FGF23 levels²²⁴ and causes cardiac hypertrophy.²²⁵ Kidney and cardiac injury are more severe in males.²²⁶ We placed male and female BALB/c mice on an 0.2% adenine diet for ten weeks starting at six weeks of age. Throughout the feeding study, mice were injected via the tail vein with heparin at 125 USP/kg or saline three times per week, similar to a dialysis style schedule. After ten weeks, serum levels of FGF23 and creatinine were significantly elevated in male adenine mice when compared to mice on control chow as seen in Table 4, and the heparin injections had no statistical effect on these levels. Unlike in males, in females we

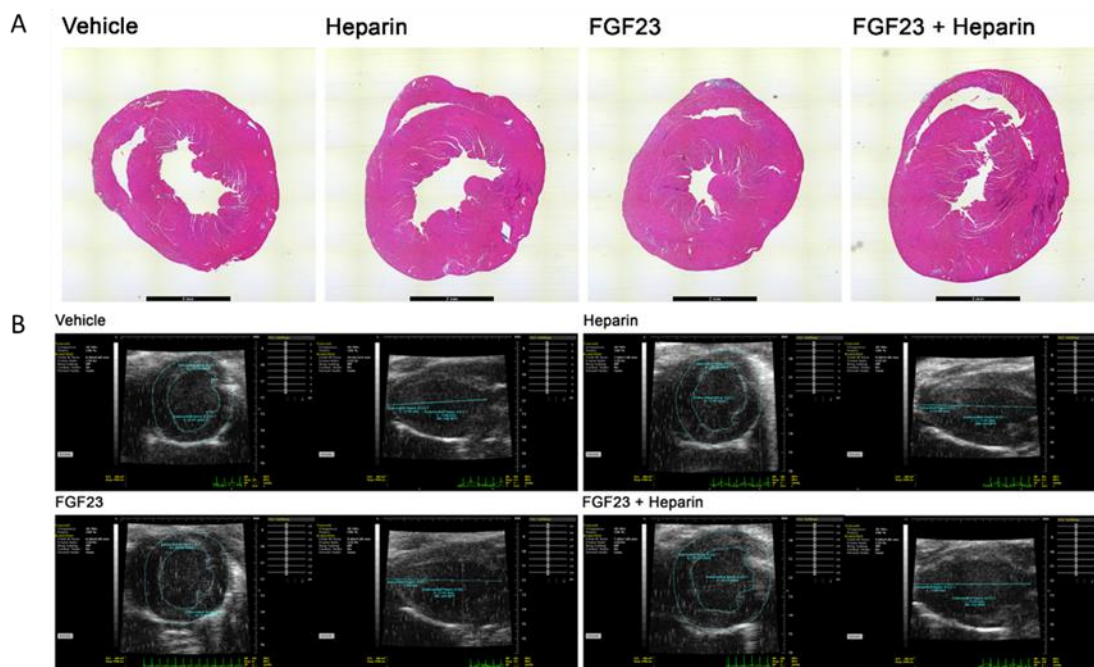


Figure 36 Representative Pictures of Cardiac Effects of FGF23 Injections
 (a) Representative H&E stainings of cardiac cross-sections from all groups are shown (scale bar = 2 mm) (b) Representative B-mode ultrasound images (short axis and long axis view)

saw no elevations in creatinine, and FGF23 elevations but at lower levels than males. In Fig. 37, we analyzed the cardiac effects of this diet and injections. Compared to male mice receiving control chow, adenine mice showed increases in the ratio of heart weight to body weight as well as cross sectional area of individual myocytes, which both were exasperated by heparin injections (Fig. 37a-b). Heparin injections in mice on a control diet had no effect on the heart. While female mice did not have an increase in HW/BW, heparin injections in female adenine mice induced a significant increase in the area of individual cardiac myocytes as seen in Fig. 37c-d. Representative H/E images and WGA are shown in Fig. 37 e-f. Combined our two animal models indicate that while frequent heparin injections by themselves do not affect the heart, they promote cardiac hypertrophy in the presence of systemic FGF23 elevations, as the case in CKD.

Table 4: Adenine model serum chemistry

Males				
	Vehicle	Heparin	Adenine	Adenine + Heparin
Albumin (g/dL)	2.90 ± 0.05	2.73 ± 0.05	2.92 ± 0.10	2.86 ± 0.05
Total Protein (g/dL)	4.82 ± 0.09	4.55 ± 0.10	5.06 ^{&} ± 0.16	4.80 ± 0.07
BUN (mg/dL)	22.60 ± 2.11	20.25 ± 0.48	31.20 ± 3.97	33.20 ^{*&} ± 2.18
Creatinine (mg/dL)	0.74 ± 0.03	0.65 ± 0.05	1.40 ^{*&} ± 0.21	1.58 ^{*&} ± 0.08
Calcium (mg/dL)	8.58 ± 0.07	8.48 ± 0.11	8.88 ± 0.23	8.54 ± 0.20
Phosphorus (mg/dL)	9.68 ± 0.23	7.05 [*] ± 0.37	13.64 ^{*&} ± 0.84	11.12 ^{&#} ± 0.65
Intact FGF23 (pg/ml)	496.50 ± 27.10	406.00 ± 22.32	6053 ^{*&} ± 1024	7080 ^{*&} ± 586.30
Chloride (mmol/L)	110.00 ± 0.45	111.30 ± 0.48	108.40 ± 2.34	113.40 ± 1.29
Potassium (mmol/L)	5.30 ± 0.09	5.05 ± 0.13	5.76 ± 0.23	5.00 [#] ± 0.17
Sodium (mmol/L)	155.60 ± 0.51	153.00 ± 1.08	156.40 ± 1.72	156.40 ± 0.75
Females				
	Vehicle	Heparin	Adenine	Adenine + Heparin
Albumin (g/dL)	3.06 ± 0.02	3.06 ± 0.05	3.08 ± 0.04	2.90 ± 0.06
Total Protein (g/dL)	4.68 ± 0.04	4.72 ± 0.06	4.74 ± 0.08	4.63 ± 0.08
BUN (mg/dL)	29.00 ± 4.49	24.40 ± 4.01	24.80 ± 1.39	28.25 ± 2.02
Creatinine (mg/dL)	0.81 ± 0.04	0.64 ± 0.07	0.95 ^{&} ± 0.03	1.05 ^{*&} ± 0.02
Calcium (mg/dL)	8.68 ± 0.07	8.94 ± 0.09	9.00 ± 0.14	9.23 [*] ± 0.18
Phosphorus (mg/dL)	9.18 ± 0.35	8.00 ± 0.37	10.42 ^{&} ± 0.52	10.60 ^{&} ± 0.47
Intact FGF23 (pg/ml)	612.00 ± 48.38	890.80 ± 247.20	4083 ^{*&} ± 240.60	4638 ^{*&} ± 403.80
Chloride (mmol/L)	110.40 ± 0.60	111.40 ± 0.51	107.00 ^{*&} ± 0.71	110.80 [#] ± 0.48
Potassium (mmol/L)	4.60 ± 0.05	4.34 ± 0.10	4.82 ± 0.20	4.75 ± 0.06
Sodium (mmol/L)	152.60 ± 0.24	151.60 ± 0.81	151.80 ± 1.69	152.80 ± 0.75

Values are expressed as mean ± SEM. Comparison between groups was performed in form of a one-way ANOVA followed by a post-hoc Tukey test. A level of $P < 0.05$ was accepted as statistically significant, * $p \leq 0.05$ vs. Vehicle, & $p \leq 0.05$ vs. Heparin, # $p \leq 0.05$ vs. Adenine, N=4-5.

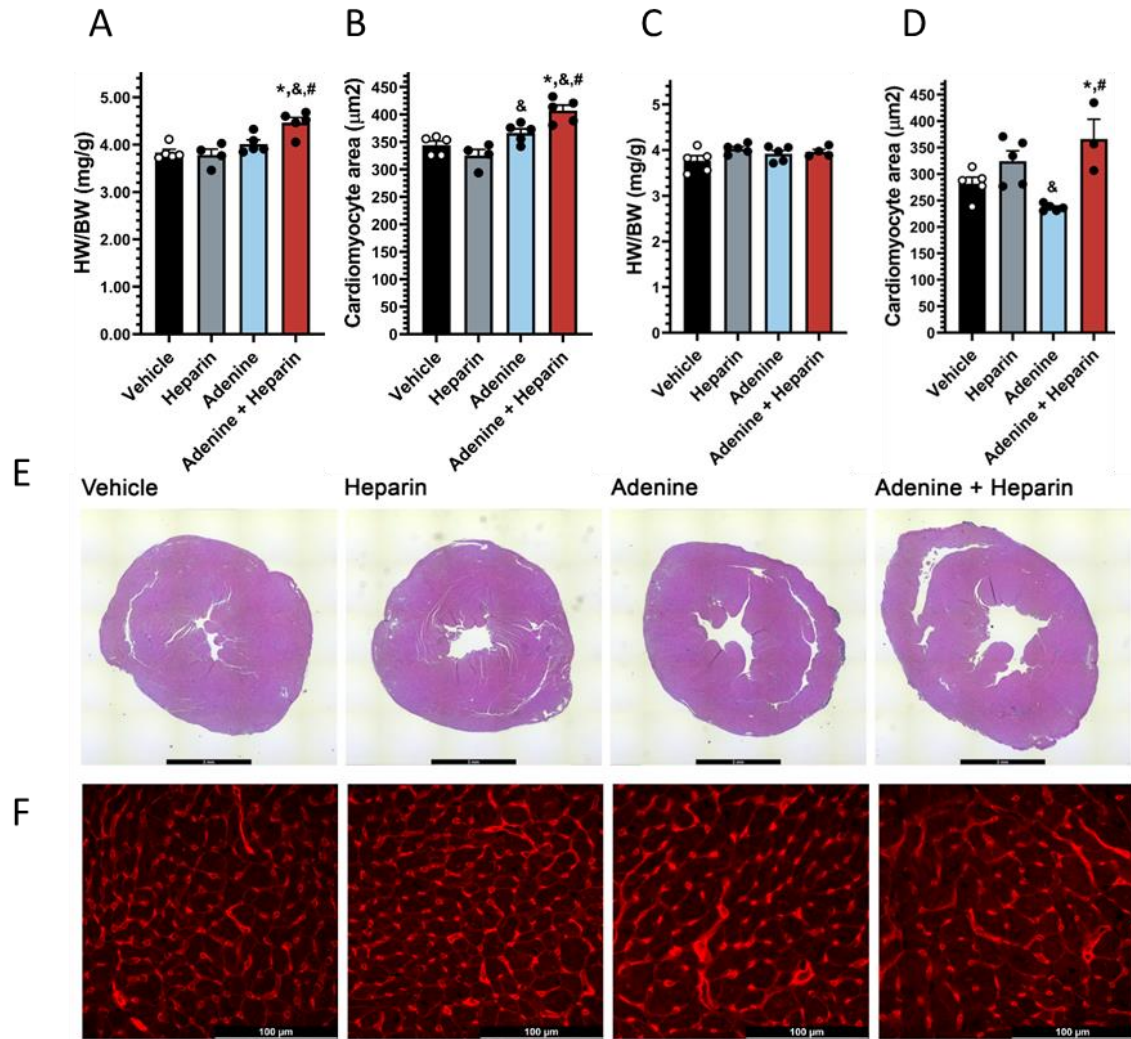


Figure 37. Heparin Increases the Effects of FGF23 in a Diet Induced Model of CKD (a-f) Five-week old, male BALB/c were administered a 0.2% adenine diet or control chow. After 1 week, mice were i.v. injected 3x per week with heparin (125 IU/kg) or saline. (a) The ratio of heart weight to body weight, and (b) area of individual cardiac myocytes in male adenine mice injected with heparin. (c) The ratio of heart weight to body weight, and (d) area of individual cardiac in female adenine mice injected with heparin. (e) Representative H&E stainings of cardiac cross-sections from all groups are shown (scale bar = 2 mm), and (f) representative images of cardiac WGA stainings for the quantification shown in g (scale bar = 100 μm). Comparison between groups was performed in form of a one-way ANOVA followed by a post-hoc Tukey test; $n = 4-5$; $*p \leq 0.05$ vs. Vehicle, $\&p \leq 0.05$ vs. Heparin, $\#p \leq 0.05$ vs. Adenine. All Values are expressed as mean \pm SEM.

Discussion

Similar to its cellular effects, we found heparin was able to exasperate FGF23 effects on cardiac tissue in models of FGF23 elevation. Our first model, the FGF23 injection mouse, is a model we previously utilized to show FGF23 can induce effects on the heart. CKD is a multifactorial disease where other elevations such as uremic toxins, phosphate, and blood pressure can play roles in cardiac hypertrophy. This model of elevation allows us to exclude all of that, and isolate FGF23 as the only inducer of hypertrophy. We saw this effect by both heart size through gravimetric and ultrasound, proving in both ways that heart size was increased. Interestingly, it was specifically a lengthening of the heart that we saw, and FGF23 did not affect any functional readouts. While this was the case for our short-term readout over five days, this does not rule out any long-term effects. If the FGF23 injections were extended out long-term, there very likely could be cumulative effects if heart mass continues to grow and long-term signaling is changed. In our model of kidney damage, we also saw heparin show an increase in cardiac hypertrophy. We saw heparin have no effect on other CKD based parameters, such as phosphate, kidney damage, or FGF23 levels, pointing to this is based on increasing FGF23's affinity for FGFR4. Other effects still cannot be ruled out, and this study leaves open the case for further work utilizing the FGFR4 knockout mouse to further prove this is truly FGF23-dependent.

CHAPETER 6: CONCLUSION

Discussion of Current Results

SKL as a Co-Factor for FGF23 Signaling

Overall, our results detail that there are multiple co-factors that can modulate FGF23 signaling. While KL was a known factor to increase the affinity of FGF23 to FGFR1, SKL was hypothesized to have multiple different functions independent of FGF23.^{67, 86} We show that SKL does in fact bind FGF23 independent of FGFRs, as well as bind FGFRs independent of FGF23. As published recently, it does in fact act as a scaffold for an increase in FGF signaling.⁴³ Surprisingly, SKL does not just act as a scaffold for FGFR1, but can make FGF23 promiscuous and bind to FGFR1c, FGFR3c, and FGFR4. By binding directly to FGFRs, SKL does not only increase the affinity for FGF23, but also inhibits paracrine FGF signaling. In addition, we also show heparin can act as a novel co-factor for FGF23 binding to FGFR4. Given the role FGF23 plays in CKD, heparin has the potential to push FGF23 towards FGFR4 signaling, which affects cardiac signaling and long-term dysfunction.

Our identification of SKL's function and binding explains the role that SKL can modulate FGF23 signaling. The fact that SKL has such a high affinity for FGF23 means that SKL secreted from the kidney, or external administration of SKL would result in

binding of FGF23 in serum. This in turn would mean that this complex can circulate and exert its effects in cell types that express FGFR1c. Given that FGFR1c is expressed in numerous tissue types, SKL and FGF23 could have far reaching effects across many tissue types. One of the interesting effects that could be explained by this is in the SKL AAV mouse. Surprisingly, multiple papers have reported this mouse has highly elevated levels of FGF23.^{200, 229} Given that FGF23 producing tumors have been shown to have mutations in FGFR1 which lead to auto-activation,¹¹⁶ this could be the mechanism behind these FGF23 elevations in this mouse. If the massive levels of SKL bind to FGF23 in serum, this complex would be able to bind FGFR1 in osteocytes and promote more FGF23 production, leading to a cycle of concurrent FGF23 elevations. This mechanism of increasing FGF23 affinity for FGFR1 may also explain SKLs therapeutic potential in two ways. One may be by increasing the availability of binding in the kidney for FGF23. Recent work has shown that SKL administration increases phosphate excretion into urine and a lowering of serum phosphate levels.⁴³ If KL expression is the limiting potential for FGF23 signaling in the kidney or if KL expression is lowered due to disease, this outside source of SKL bound to FGF23 can overcome this and allow for a return in signaling ability. A secondary mechanism could be the ability of SKL to mediate FGF23 signal in many other cell types. FGFR1 activation in tissues under insult during disease states like cardiac tissue during CKD may in fact be protected by this receptor activation.

Surprisingly, we found not only that SKL can increase FGF23 binding to FGFR1, but also for FGFR3 and FGFR4. This makes FGF23 promiscuous for multiple receptors, which is interesting due to the fact the FGF23 is published to be responsible for phosphate excretion and PTH regulation, and studies have pointed to FGFR1 in this. Groups

have looked into FGF23 effects and tried to find if they were dependent on any FGFR isoform other than FGFR1. In the kidney, FGFR3 or FGFR4 knockout models have not shown to play any role in the renal effects of FGF23, while the kidney does express both of these receptors.⁵⁵ Given that FGFR3 and FGFR4 are poor mitogenic receptors and have weaker activation of MAPK signaling,^{9, 33} there may be effects that are missed by the common screens for FGFR activation and FGF23 sensitivity.²⁶ More detailed techniques that look at other FGFR activation pathways and effects may elucidate that SKL and KL can have other FGFR dependent functions outside of classically thought of effects.

While SKL has a strong affinity for FGF23, it shows even higher affinity for FGFR1 independent of FGF23. This is in fact the strongest binding for SKL that we observed. This surprisingly strong binding can have multiple effects on SKL's properties. First, this may have implications for SKL cleavage and excretion. The endocrine FGFs are able to act as hormones, unlike their paracrine family members, due to the fact that they have a lower affinity for heparin¹⁶ and are able to escape the cellular glycocalyx. If SKL has such a strong affinity for FGFR1, this may interfere with cleavage and excretion of SKL. Given the challenges around SKL detection, better assays will need to be devised to further analyze how SKL circulates in respect to this binding. This may also explain our struggles in purifying SKL from cellular media. In our HEK293 cell system with SKL under stable overexpression, we were unable to detect any SKL in media via our activity assay or purify and protein out of the media during testing (data not shown). This may not be due to SKL not being secreted, but due to SKL binding FGFR1 so strongly and being bound to cells. Due to this, we purified SKL from cellular lysates, and this

would have also in turn purified SKL from the extracellular membrane. To further elucidate this, we would need to either knockout FGFR1 expression in our cell system or cleave it off the cell surface via proteases. Furthermore, this binding to FGFR1 was shown by our data to interfere with paracrine FGF signaling. Given the multitude of effects paracrine FGFs can have, and FGFR1's expression across many tissue types, this could have profound effects. The KL overexpression mouse has a 30% increased lifespan, with major changes in multiple parameters not related to classical FGF23 signaling⁵¹, so this could very well likely be from modulating other FGF signaling.⁵¹

Our SKL activity assay not only helped identify receptor binding for SKL but is a novel method to measure SKL activity, as well as levels seen in animal models of SKL. By measuring SKL activity, we were able to perfect our purification method, and produce a SKL protein that is stable and has high activity. When trying to work with SKL from other sources, we struggled with lot variability and a lack of activity related to FGF23. Given the recent data regarding the novel zinc ion in SKL,¹⁰⁵ we believe this is the source of many of the issues related to SKL stability. Our early procedures that utilized buffers with chelators resulted in a SKL protein with poor activity, similar to what we see in some of the commercially related products. This has profound effect in the literature, as multiple groups have used these preparations of SKL to test its therapeutic potential. The true effects of SKL may be missed due to the fact that current sources of SKL are not taking this into account. Our assay also identified a very short half-life for SKL, which was under 15 minutes. This corroborates recent work by Pfizer, which shows their SKL also has a very short half-life.⁵⁴ While they saw protection from kidney damage in a mouse model of AKI when injected with their SKL, this would likely not be the case in a chron-

ic damage model where effects happen over time.⁵⁴ This shows that SKL would likely have to undergo modifications to unlock its therapeutic potential similar to other protein based drugs.^{143, 152}

While our SKL activity assay was able to measure SKL levels in serum, its limit of detection was not low enough to elucidate the existence of SKL and measure how disease states can affect its levels. While this is disheartening, there are multiple ways to improve our assay in future iterations to achieve this goal. We have yet to optimize buffers and additives that could play a role in increasing binding in serum and detection in our assay. The other method would be to increase the potential binding of FGFR1 and FGF23 to SKL. We utilize these two proteins as pseudo antibodies in a sandwich ELISA, and mutation analysis could create mutants that have a stronger binding affinity for SKL. The rate-limiting step in ELISAs is usually the quality of the coated antibody, so our early stage focus would be on creating an FGF23 variant that has a stronger affinity for SKL. Recent work on alanine substitution in FGF19 revealed the replacement of an alanine in a.a. 194 led to a variant that bound BKL ten times stronger than the wildtype protein.¹⁵⁷ FGF23 surprisingly shares this residue with FGF19, and it could be interesting if a similar substitution would have a similar effect on FGF23 binding to SKL.

Heparin as a Co-Factor for FGF23 Signaling

Our study shows that in the absence of KL, heparin can mediate the interaction between FGF23 and FGFR4. This lines up with previous studies in BaF3 cells expressing FGFR1c, FGFR2c, FGFR3c, or FGFR4, where in the absence of klotho, heparin significantly increased the mitogenic response to FGF23 treatments.^{3, 22} Based on our binding assay, FGF23 and heparin must have pre-formed before binding to FGFR ectodomains,

which is further supported by binding studies showing that FGF23 can directly bind heparin columns with low affinity.¹⁴ Our study suggests that heparin acts as a KL-independent FGF23 co-receptor that mediates low affinity binding of FGF23 to FGFRs, with the potential to contribute to signaling during setting of FGF23 elevation.¹⁸³ While we found SKL acts as a promiscuous co-receptor for FGF23, heparin seems to mainly facilitate the FGF23 interaction with only FGFR4. Our binding studies suggest that as known for paracrine FGFs, heparin also plays a dual role in the activation of FGFRs by FGF23. This binding of FGF23 to heparin is also plausible due to recent literature showing FGF23 binds heparin during the dimerization of the signaling unit leading to the formation of a symmetric 2:2:2:2 FGF23-FGFR1c-SKL-HS quaternary complex and subsequent activation of Ras/MAPK signaling.⁴³ While we show in our plate based assay that the interaction between FGF23 and SKL is heparin-independent, we do not measure the formation of dimerization complex formations.

Similar to how SKL may encourage FGF23 to bind to FGFR1, heparin might force FGF23 into FGFR4 signaling and away from FGFR1c. This has been shown by the finding that heparin blocks the inhibitory actions of FGF23 on phosphate uptake in cultured proximal tubular cells that are mediated by FGFR1c.²³⁰ Furthermore, by promoting FGF23 binding to FGFR4, heparin might compete with the binding of paracrine FGFs to FGFR4, such as FGF1, and thereby block FGF1/FGFR4-mediated effects. This has been shown for FGF19, where FGF19/heparin competes with FGF1 for FGFR4 binding.⁹³ Just like SKL acting as a dual modulator of signaling and blockade, heparin could have other pleiotropic effects during times of elevation of FGF23 and heparin.

It has previously been reported that in the absence of BKL, heparin sulfate can increase the binding of FGF19 specifically to FGFR4 but to none of the other FGFR isoforms and promote FGF19/FGFR4-mediated activation of Ras/MAPK signaling in HEK293 cells and proliferation in BaF3 cells.^{23, 93, 231-234} Furthermore, an FGF19 mutant form that lacks the BKL-binding site can still bind FGFR4 in the presence of heparin sulfate.²³² At high concentrations, our binding assay also identified this could happen, similar to FGF23. While this was the case for FGF19, we did not see this effect with FGF21. This in turn matches published literature, as FGF21 was the only FGF isoform in previous studies found to have no affinity for heparin.¹⁴

Furthermore, we noticed this effect not just biochemically, but also in both cells and in mouse models of FGF23 elevations. We have previously shown that cardiac myocytes do not express KL, and their response to FGF23 is KL-independent, by signaling through FGFR4.¹⁹³ Given our data, this effect is not likely co-factor-independent, but heparin on the cell surface is acting as a co-factor for signaling. While there may be some heparin on the myocytes that can aide in signaling, we were curious if the addition of excess heparin could illicit an increase in FGFR4-dependent signaling. We saw heparin addition increase cellular effects on increases in cell area, calcium handling, and contraction that are all FGF23-mediated through FGFR4. This shows that when heparin levels are increased externally, they can provide an increase in FGF23 affinity for FGFR4 and increased signaling. On top of this, we found heparin administration in models of FGF23 elevations in mice was also able to increase the cardiac effects of FGF23. Given this, heparin can act as a soluble co-receptor for FGF23, similarly to SKL. Based on this, these

co-factors could act as competing interests during administrations, pushing FGF23 towards different receptors and effects.

Therapeutic Implications

SKL has been proposed as a therapeutic agent, showing promises in multiple models of disease.^{62, 71, 87} Our studies identify a way to measure SKL activity and how to purify a more bioactive protein, which are essential to unlocking the potential of SKL. Given the lack of activity we see in currently commercially available SKL, this means studies could be lacking some of the true effects of SKL. Our studies identify two lacking areas that SKL must be improved upon to become a better therapeutic agent. The first would be the activity currently seen by SKL. We show SKL can bind both FGF23 and FGFR1, with FGFR1 being the strongest binder of SKL. Previous work shows KL has a binding affinity for FGFR1c of $K_D = 72$ nM.⁹² While this is strong for the physiological levels of a wildtype protein, for a drug candidate this is not currently acceptable. The amount of SKL required to achieve results in a long-term chronic disease would be uneconomical. Given the ability of our assay to measure SKL activity, this could be a necessary tool to develop a SKL-based mimetic that shows this increased potency required for a drug. Many antibody-based drugs show a binding affinity greater than 1 nM, which would be a similar requirement for SKL. Given the size of the RBA in SKL that binds FGFR1 is under 50 a.a.,⁴³ this should be a screenable approach to creating a mimetic with stronger affinities. The secondary issue is the short half-life of under 15 minutes for bioactive SKL in serum. Recent work by Pfizer found a similar result in their HEK293 cell-made SKL, but when they created SKL in CHO cells, they found a half-life over 12 hours.⁵⁴ Upon further analysis, they found this version of SKL had a modified glycosyla-

tion pattern that played a role in the half-life. When analyzing FGF23 signaling, they found this SKL had much poorer signaling potential. Given this glycosylation may play an outsized role in both half-life and binding for SKL. While they do not modify the glycosylation sites of SKL, they hypothesize this may be a novel pathway to increase SKL's activity and half-life, leading to a better drug candidate. We also provide interesting therapeutic findings in relation to the actions of SKL on cardiac myocytes. We found surprisingly that SKL can bind FGFR1 and FGFR4 and directly inhibit the pathologic actions of FGF23 on cardiac myocytes. While this finding might explain previous *in vivo* studies showing that elevating SKL levels in animal models of CKD has cardio-protective effects,²³⁵⁻²³⁹ the precise mechanism remains unknown. Since we found that SKL increases the affinity of FGF23 for both FGFRs, SKL does not simply block FGF23 access to the heart but rather promotes FGF23 binding to its cardiac target cells. As hypothesized before,²³⁹⁻²⁴¹ SKL might induce a switch from FGF23-induced KL-independent PLC γ to KL-dependent MAPK signaling,²⁰³ and thereby from FGF23-induced pathologic to protective cardiac events. Alternatively, since SKL has higher affinity for FGFR1 than for FGFR4, SKL might force FGF23 into FGFR1/SKL binding and cardio-protective signaling and away from KL-independent, pro-hypertrophic signaling that is mediated by FGFR4.^{193, 203} Our findings set the stage for pre-clinical CKD studies with the goal to test potential cardio-protective effects of SKL.

We propose that the novel heparin mechanistic findings have several important implications for pathologies that are associated with elevated FGF23 levels such as CKD. We believe that our study has a major impact for ESRD patients on hemodialysis, who frequently receive heparin infusions to prevent blood clotting during the dialysis process.

Since hemodialysis does not reduce serum FGF23 levels, these patients are exposed to both, constant systemic elevations of FGF23 and heparin. We found that heparin specifically increases FGF23 binding to FGFR4, the FGFR isoform that mediates the pathologic actions of FGF23 on cardiac myocytes, and thereby promotes the acute effects of FGF23 on increasing contractility, dysregulating intracellular calcium and enhancing arrhythmogenicity as well as the prolonged FGF23 effects of inducing hypertrophic cell growth. Combined, these cellular alterations might result in accelerated pathologic cardiac remodeling, as supported by our two mouse models with systemic FGF23 elevations, where frequent heparin injections worsened the cardiac phenotype, while heparin injections by themselves in healthy control animals had no cardiac effects. Overall, our study suggests that heparin aggravates the cardiac actions of FGF23, and that individuals with elevated serum FGF23 levels should not receive heparin-based therapies. We believe this points to the idea that heparin infusions contribute to the extremely high mortality rates of hemodialysis patients, and that removal of heparin from the dialysis process can improve cardiac outcomes and survival in hemodialysis patients, which based on our experimental work should be tested in clinical studies.

REFERENCES

1. Gospodarowicz, D., *Purification of a fibroblast growth factor from bovine pituitary*. J Biol Chem, 1975. 250(7): p. 2515-20.
2. Gospodarowicz, D., H. Bialecki, and G. Greenburg, *Purification of the fibroblast growth factor activity from bovine brain*. J Biol Chem, 1978. 253(10): p. 3736-43.
3. Zhang, X., et al., *Receptor specificity of the fibroblast growth factor family. The complete mammalian FGF family*. J Biol Chem, 2006. 281(23): p. 15694-700.
4. Itoh, N. and D.M. Ornitz, *Evolution of the Fgf and Fgfr gene families*. Trends Genet, 2004. 20(11): p. 563-9.
5. Itoh, N. and D.M. Ornitz, *Fibroblast growth factors: from molecular evolution to roles in development, metabolism and disease*. The Journal of Biochemistry, 2010. 149(2): p. 121-130.
6. Goldfarb, M., *Voltage-gated sodium channel-associated proteins and alternative mechanisms of inactivation and block*. Cellular and molecular life sciences : CMLS, 2012. 69(7): p. 1067-1076.
7. Ornitz, D.M., *FGFs, heparan sulfate and FGFRs: complex interactions essential for development*. Bioessays, 2000. 22(2): p. 108-12.
8. Rapraeger, A.C., A. Krufka, and B.B. Olwin, *Requirement of heparan sulfate for bFGF-mediated fibroblast growth and myoblast differentiation*. Science, 1991. 252(5013): p. 1705-8.
9. Ornitz, D.M. and P. Leder, *Ligand specificity and heparin dependence of fibroblast growth factor receptors 1 and 3*. J Biol Chem, 1992. 267(23): p. 16305-11.
10. Häcker, U., K. Nybakken, and N. Perrimon, *Heparan sulphate proteoglycans: the sweet side of development*. Nat Rev Mol Cell Biol, 2005. 6(7): p. 530-41.
11. Iozzo, R.V., J.J. Zoeller, and A. Nyström, *Basement membrane proteoglycans: modulators Par Excellence of cancer growth and angiogenesis*. Mol Cells, 2009. 27(5): p. 503-13.
12. Esko, J.D. and U. Lindahl, *Molecular diversity of heparan sulfate*. J Clin Invest, 2001. 108(2): p. 169-73.
13. Makarenkova, H.P., et al., *Differential interactions of FGFs with heparan sulfate control gradient formation and branching morphogenesis*. Sci Signal, 2009. 2(88): p. ra55.
14. Asada, M., et al., *Glycosaminoglycan affinity of the complete fibroblast growth factor family*. Biochim Biophys Acta, 2009. 1790(1): p. 40-8.
15. Xu, R., et al., *Diversification of the structural determinants of fibroblast growth factor-heparin interactions: implications for binding specificity*. J Biol Chem, 2012. 287(47): p. 40061-73.
16. Belov, A.A. and M. Mohammadi, *Molecular mechanisms of fibroblast growth factor signaling in physiology and pathology*. Cold Spring Harb Perspect Biol, 2013. 5(6).
17. Goetz, R., et al., *Molecular insights into the klotho-dependent, endocrine mode of action of fibroblast growth factor 19 subfamily members*. Mol Cell Biol, 2007. 27(9): p. 3417-28.
18. Revest, J.M., L. DeMoerlooze, and C. Dickson, *Fibroblast growth factor 9 secretion is mediated by a non-cleaved amino-terminal signal sequence*. J Biol Chem, 2000. 275(11): p. 8083-90.
19. Steringer, J.P., H.M. Müller, and W. Nickel, *Unconventional secretion of fibroblast growth factor 2--a novel type of protein translocation across membranes?* J Mol Biol, 2015. 427(6 Pt A): p. 1202-10.
20. Degirolamo, C., C. Sabbà, and A. Moschetta, *Therapeutic potential of the endocrine fibroblast growth factors FGF19, FGF21 and FGF23*. Nat Rev Drug Discov, 2016. 15(1): p. 51-69.
21. Wu, X., et al., *Selective activation of FGFR4 by an FGF19 variant does not improve glucose metabolism in ob/ob mice*. Proceedings of the National Academy of Sciences of the United States of America, 2009. 106(34): p. 14379-14384.
22. Yu, X., et al., *Analysis of the biochemical mechanisms for the endocrine actions of fibroblast growth factor-23*. Endocrinology, 2005. 146(11): p. 4647-56.
23. Wu, X., et al., *Co-receptor requirements for fibroblast growth factor-19 signaling*. J Biol Chem, 2007. 282(40): p. 29069-72.

24. Kuro-o, M., et al., *Mutation of the mouse klotho gene leads to a syndrome resembling ageing*. Nature, 1997. 390(6655): p. 45-51.
25. Jimbo, R., et al., *Fibroblast growth factor 23 accelerates phosphate-induced vascular calcification in the absence of Klotho deficiency*. Kidney Int, 2014. 85(5): p. 1103-11.
26. Urakawa, I., et al., *Klotho converts canonical FGF receptor into a specific receptor for FGF23*. Nature, 2006. 444(7120): p. 770-4.
27. Goetz, R., et al., *Klotho coreceptors inhibit signaling by paracrine fibroblast growth factor 8 subfamily ligands*. Molecular and cellular biology, 2012. 32(10): p. 1944-1954.
28. Mason, I., *Initiation to end point: the multiple roles of fibroblast growth factors in neural development*. Nat Rev Neurosci, 2007. 8(8): p. 583-96.
29. Turner, N. and R. Grose, *Fibroblast growth factor signalling: from development to cancer*. Nat Rev Cancer, 2010. 10(2): p. 116-29.
30. Johnson, D.E., et al., *The human fibroblast growth factor receptor genes: a common structural arrangement underlies the mechanisms for generating receptor forms that differ in their third immunoglobulin domain*. Mol Cell Biol, 1991. 11(9): p. 4627-34.
31. Yeh, B.K., et al., *Structural basis by which alternative splicing confers specificity in fibroblast growth factor receptors*. Proc Natl Acad Sci U S A, 2003. 100(5): p. 2266-71.
32. Plotnikov, A.N., et al., *Structural basis for FGF receptor dimerization and activation*. Cell, 1999. 98(5): p. 641-50.
33. Ornitz, D.M., et al., *Receptor specificity of the fibroblast growth factor family*. J Biol Chem, 1996. 271(25): p. 15292-7.
34. Wang, J.K., G. Gao, and M. Goldfarb, *Fibroblast growth factor receptors have different signaling and mitogenic potentials*. Mol Cell Biol, 1994. 14(1): p. 181-8.
35. Duchesne, L., et al., *Transport of fibroblast growth factor 2 in the pericellular matrix is controlled by the spatial distribution of its binding sites in heparan sulfate*. PLoS Biol, 2012. 10(7): p. e1001361.
36. Bashkin, P., et al., *Basic fibroblast growth factor binds to subendothelial extracellular matrix and is released by heparitinase and heparin-like molecules*. Biochemistry, 1989. 28(4): p. 1737-43.
37. Vlodavsky, I., et al., *Endothelial cell-derived basic fibroblast growth factor: synthesis and deposition into subendothelial extracellular matrix*. Proc Natl Acad Sci U S A, 1987. 84(8): p. 2292-6.
38. Yayon, A., et al., *Cell surface, heparin-like molecules are required for binding of basic fibroblast growth factor to its high affinity receptor*. Cell, 1991. 64(4): p. 841-8.
39. Guimond, S.E. and J.E. Turnbull, *Fibroblast growth factor receptor signalling is dictated by specific heparan sulphate saccharides*. Curr Biol, 1999. 9(22): p. 1343-6.
40. Kreuger, J., et al., *Characterization of fibroblast growth factor 1 binding heparan sulfate domain*. Glycobiology, 1999. 9(7): p. 723-9.
41. Ling, L., et al., *Targeting the heparin-binding domain of fibroblast growth factor receptor 1 as a potential cancer therapy*. Molecular cancer, 2015. 14: p. 136-136.
42. Schlessinger, J., et al., *Crystal structure of a ternary FGF-FGFR-heparin complex reveals a dual role for heparin in FGFR binding and dimerization*. Mol Cell, 2000. 6(3): p. 743-50.
43. Chen, G., et al., *alpha-Klotho is a non-enzymatic molecular scaffold for FGF23 hormone signalling*. Nature, 2018. 553(7689): p. 461-466.
44. Kurosu, H., et al., *Regulation of fibroblast growth factor-23 signaling by klotho*. J Biol Chem, 2006. 281(10): p. 6120-3.
45. Kurosu, H., et al., *Tissue-specific expression of betaKlotho and fibroblast growth factor (FGF) receptor isoforms determines metabolic activity of FGF19 and FGF21*. J Biol Chem, 2007. 282(37): p. 26687-95.
46. Lemmon, M.A. and J. Schlessinger, *Cell signaling by receptor tyrosine kinases*. Cell, 2010. 141(7): p. 1117-1134.
47. Dailey, L., et al., *Mechanisms underlying differential responses to FGF signaling*. Cytokine Growth Factor Rev, 2005. 16(2): p. 233-47.
48. Mohammadi, M., et al., *A tyrosine-phosphorylated carboxy-terminal peptide of the fibroblast growth factor receptor (Flg) is a binding site for the SH2 domain of phospholipase C-gamma 1*. Mol Cell Biol, 1991. 11(10): p. 5068-78.

49. Hart, K.C., et al., *Transformation and Stat activation by derivatives of FGFR1, FGFR3, and FGFR4*. *Oncogene*, 2000. 19(29): p. 3309-20.
50. Dudka, A.A., S.M.M. Sweet, and J.K. Heath, *Signal transducers and activators of transcription-3 binding to the fibroblast growth factor receptor is activated by receptor amplification*. *Cancer research*, 2010. 70(8): p. 3391-3401.
51. Kurosu, H., et al., *Suppression of aging in mice by the hormone Klotho*. *Science*, 2005. 309(5742): p. 1829-33.
52. Zou, D., et al., *The role of klotho in chronic kidney disease*. *BMC Nephrol*, 2018. 19(1): p. 285.
53. Henrissat, B. and G. Davies, *Structural and sequence-based classification of glycoside hydrolases*. *Curr Opin Struct Biol*, 1997. 7(5): p. 637-44.
54. Zhong, X., et al., *Structure-function relationships of the soluble form of the antiaging protein Klotho have therapeutic implications for managing kidney disease*. *J Biol Chem*, 2020. 295(10): p. 3115-3133.
55. Liu, S., et al., *FGFR3 and FGFR4 do not mediate renal effects of FGF23*. *J Am Soc Nephrol*, 2008. 19(12): p. 2342-50.
56. Razzaque, M.S., *The FGF23-Klotho axis: endocrine regulation of phosphate homeostasis*. *Nat Rev Endocrinol*, 2009. 5(11): p. 611-9.
57. Razzaque, M.S., et al., *Premature aging-like phenotype in fibroblast growth factor 23 null mice is a vitamin D-mediated process*. *Faseb j*, 2006. 20(6): p. 720-2.
58. Liu, S. and L.D. Quarles, *How fibroblast growth factor 23 works*. *J Am Soc Nephrol*, 2007. 18(6): p. 1637-47.
59. Nakatani, T., M. Ohnishi, and M.S. Razzaque, *Inactivation of klotho function induces hyperphosphatemia even in presence of high serum fibroblast growth factor 23 levels in a genetically engineered hypophosphatemic (Hyp) mouse model*. *Faseb j*, 2009. 23(11): p. 3702-11.
60. Olauson, H., et al., *Parathyroid-specific deletion of Klotho unravels a novel calcineurin-dependent FGF23 signaling pathway that regulates PTH secretion*. *PLoS Genet*, 2013. 9(12): p. e1003975.
61. Krajisnik, T., et al., *Fibroblast growth factor-23 regulates parathyroid hormone and 1 α -hydroxylase expression in cultured bovine parathyroid cells*. *J Endocrinol*, 2007. 195(1): p. 125-31.
62. Dubal, D.B., et al., *Life extension factor klotho enhances cognition*. *Cell Rep*, 2014. 7(4): p. 1065-76.
63. Dubal, D.B., et al., *Life extension factor klotho prevents mortality and enhances cognition in hAPP transgenic mice*. *J Neurosci*, 2015. 35(6): p. 2358-71.
64. Zimmer, C., *One Day There May Be a Drug to Turbocharge the Brain. Who Should Get It?*, in *New York Times*. 2019. p. Section D Pg 1.
65. Matsumura, Y., et al., *Identification of the human klotho gene and its two transcripts encoding membrane and secreted klotho protein*. *Biochem Biophys Res Commun*, 1998. 242(3): p. 626-30.
66. Shiraki-Hida, T., et al., *Structure of the mouse klotho gene and its two transcripts encoding membrane and secreted protein*. *FEBS Lett*, 1998. 424(1-2): p. 6-10.
67. Tohyama, O., et al., *Klotho is a novel beta-glucuronidase capable of hydrolyzing steroid beta-glucuronides*. *J Biol Chem*, 2004. 279(11): p. 9777-84.
68. Hu, M.C., et al., *Renal Production, Uptake, and Handling of Circulating α Klotho*. *J Am Soc Nephrol*, 2016. 27(1): p. 79-90.
69. Chen, C.D., et al., *Identification of cleavage sites leading to the shed form of the anti-aging protein klotho*. *Biochemistry*, 2014. 53(34): p. 5579-87.
70. Bloch, L., et al., *Klotho is a substrate for alpha-, beta- and gamma-secretase*. *FEBS Lett*, 2009. 583(19): p. 3221-4.
71. Neyra, J.A. and M.C. Hu, *Potential application of klotho in human chronic kidney disease*. *Bone*, 2017. 100: p. 41-49.
72. Mencke, R., et al., *Human alternative Klotho mRNA is a nonsense-mediated mRNA decay target inefficiently spliced in renal disease*. *JCI Insight*, 2017. 2(20).
73. Hu, M.C., et al., *Klotho deficiency causes vascular calcification in chronic kidney disease*. *J Am Soc Nephrol*, 2011. 22(1): p. 124-36.
74. Manya, H., K. Akasaka-Manya, and T. Endo, *Klotho protein deficiency and aging*. *Geriatr Gerontol Int*, 2010. 10 Suppl 1: p. S80-7.

75. Zhao, Y., et al., *Klotho depletion contributes to increased inflammation in kidney of the db/db mouse model of diabetes via RelA (serine)536 phosphorylation*. *Diabetes*, 2011. 60(7): p. 1907-16.
76. Hu, M.C., M. Kuro-o, and O.W. Moe, *Klotho and chronic kidney disease*. *Contrib Nephrol*, 2013. 180: p. 47-63.
77. Devaraj, S., et al., *Validation of an immunoassay for soluble Klotho protein: decreased levels in diabetes and increased levels in chronic kidney disease*. *Am J Clin Pathol*, 2012. 137(3): p. 479-85.
78. Semba, R.D., et al., *Plasma klotho and cardiovascular disease in adults*. *J Am Geriatr Soc*, 2011. 59(9): p. 1596-601.
79. Adema, A.Y., et al., *α -Klotho is unstable in human urine*. *Kidney Int*, 2015. 88(6): p. 1442-1444.
80. Heijboer, A.C., et al., *Laboratory aspects of circulating α -Klotho*. *Nephrol Dial Transplant*, 2013. 28(9): p. 2283-7.
81. Neyra, J.A., et al., *Performance of soluble Klotho assays in clinical samples of kidney disease*. *Clin Kidney J*, 2020. 13(2): p. 235-244.
82. Liu, H., et al., *Augmented Wnt signaling in a mammalian model of accelerated aging*. *Science*, 2007. 317(5839): p. 803-6.
83. Wang, Y., M. Kuro-o, and Z. Sun, *Klotho gene delivery suppresses Nox2 expression and attenuates oxidative stress in rat aortic smooth muscle cells via the cAMP-PKA pathway*. *Aging Cell*, 2012. 11(3): p. 410-7.
84. Chang, Q., et al., *The beta-glucuronidase klotho hydrolyzes and activates the TRPV5 channel*. *Science*, 2005. 310(5747): p. 490-3.
85. Rakugi, H., et al., *Anti-oxidative effect of Klotho on endothelial cells through cAMP activation*. *Endocrine*, 2007. 31(1): p. 82-7.
86. Dalton, G., et al., *Soluble klotho binds monosialoganglioside to regulate membrane microdomains and growth factor signaling*. *Proc Natl Acad Sci U S A*, 2017. 114(4): p. 752-757.
87. Wolf, I., et al., *Klotho: a tumor suppressor and a modulator of the IGF-1 and FGF pathways in human breast cancer*. *Oncogene*, 2008. 27(56): p. 7094-105.
88. Abramovitz, L., et al., *KL1 internal repeat mediates klotho tumor suppressor activities and inhibits bFGF and IGF-1 signaling in pancreatic cancer*. *Clin Cancer Res*, 2011. 17(13): p. 4254-66.
89. Ding, X., et al., *β Klotho is required for fibroblast growth factor 21 effects on growth and metabolism*. *Cell Metab*, 2012. 16(3): p. 387-93.
90. Ito, S., et al., *Molecular cloning and expression analyses of mouse betaklotho, which encodes a novel Klotho family protein*. *Mech Dev*, 2000. 98(1-2): p. 115-9.
91. Ito, S., et al., *Impaired negative feedback suppression of bile acid synthesis in mice lacking betaKlotho*. *J Clin Invest*, 2005. 115(8): p. 2202-8.
92. Goetz, R., et al., *Klotho coreceptors inhibit signaling by paracrine fibroblast growth factor 8 subfamily ligands*. *Mol Cell Biol*, 2012. 32(10): p. 1944-54.
93. Xie, M.H., et al., *FGF-19, a novel fibroblast growth factor with unique specificity for FGFR4*. *Cytokine*, 1999. 11(10): p. 729-35.
94. Kim, I., et al., *Differential regulation of bile acid homeostasis by the farnesoid X receptor in liver and intestine*. *J Lipid Res*, 2007. 48(12): p. 2664-72.
95. Inagaki, T., et al., *Fibroblast growth factor 15 functions as an enterohepatic signal to regulate bile acid homeostasis*. *Cell Metab*, 2005. 2(4): p. 217-25.
96. Holt, J.A., et al., *Definition of a novel growth factor-dependent signal cascade for the suppression of bile acid biosynthesis*. *Genes Dev*, 2003. 17(13): p. 1581-91.
97. Yang, C., et al., *Control of lipid metabolism by adipocyte FGFR1-mediated adipohepatic communication during hepatic stress*. *Nutr Metab (Lond)*, 2012. 9(1): p. 94.
98. Yang, C., et al., *Differential specificity of endocrine FGF19 and FGF21 to FGFR1 and FGFR4 in complex with KLB*. *PLoS One*, 2012. 7(3): p. e33870.
99. Tomlinson, E., et al., *Transgenic mice expressing human fibroblast growth factor-19 display increased metabolic rate and decreased adiposity*. *Endocrinology*, 2002. 143(5): p. 1741-7.
100. Benoit, B., et al., *Fibroblast growth factor 19 regulates skeletal muscle mass and ameliorates muscle wasting in mice*. *Nat Med*, 2017. 23(8): p. 990-996.
101. Wu, X., et al., *Separating mitogenic and metabolic activities of fibroblast growth factor 19 (FGF19)*. *Proc Natl Acad Sci U S A*, 2010. 107(32): p. 14158-63.

102. Kharitononkov, A., et al., *FGF-21 as a novel metabolic regulator*. J Clin Invest, 2005. 115(6): p. 1627-35.
103. Nishimura, T., et al., *Identification of a novel FGF, FGF-21, preferentially expressed in the liver*. Biochim Biophys Acta, 2000. 1492(1): p. 203-6.
104. Muise, E.S., et al., *Adipose fibroblast growth factor 21 is up-regulated by peroxisome proliferator-activated receptor gamma and altered metabolic states*. Mol Pharmacol, 2008. 74(2): p. 403-12.
105. Adams, A.C., et al., *FGF21 requires β klotho to act in vivo*. PLoS One, 2012. 7(11): p. e49977.
106. Fisher, F.M., et al., *FGF21 regulates PGC-1 α and browning of white adipose tissues in adaptive thermogenesis*. Genes Dev, 2012. 26(3): p. 271-81.
107. BonDurant, L.D., et al., *FGF21 Regulates Metabolism Through Adipose-Dependent and -Independent Mechanisms*. Cell Metab, 2017. 25(4): p. 935-944.e4.
108. Zhang, Y., et al., *The starvation hormone, fibroblast growth factor-21, extends lifespan in mice*. Elife, 2012. 1: p. e00065.
109. Wei, W., et al., *Fibroblast growth factor 21 promotes bone loss by potentiating the effects of peroxisome proliferator-activated receptor γ* . Proc Natl Acad Sci U S A, 2012. 109(8): p. 3143-8.
110. Owen, B.M., et al., *FGF21 contributes to neuroendocrine control of female reproduction*. Nat Med, 2013. 19(9): p. 1153-6.
111. Song, P., et al., *The Hormone FGF21 Stimulates Water Drinking in Response to Ketogenic Diet and Alcohol*. Cell Metab, 2018. 27(6): p. 1338-1347.e4.
112. Yamashita, T., M. Yoshioka, and N. Itoh, *Identification of a novel fibroblast growth factor, FGF-23, preferentially expressed in the ventrolateral thalamic nucleus of the brain*. Biochem Biophys Res Commun, 2000. 277(2): p. 494-8.
113. Hasegawa, H., et al., *Direct evidence for a causative role of FGF23 in the abnormal renal phosphate handling and vitamin D metabolism in rats with early-stage chronic kidney disease*. Kidney Int, 2010. 78(10): p. 975-80.
114. Isakova, T., et al., *Fibroblast growth factor 23 is elevated before parathyroid hormone and phosphate in chronic kidney disease*. Kidney Int, 2011. 79(12): p. 1370-8.
115. Kolek, O.I., et al., *1 α ,25-Dihydroxyvitamin D3 upregulates FGF23 gene expression in bone: the final link in a renal-gastrointestinal-skeletal axis that controls phosphate transport*. Am J Physiol Gastrointest Liver Physiol, 2005. 289(6): p. G1036-42.
116. Kinoshita, Y., et al., *Ectopic expression of Klotho in fibroblast growth factor 23 (FGF23)-producing tumors that cause tumor-induced rickets/osteomalacia (TIO)*. Bone Rep, 2019. 10: p. 100192.
117. Yoshiko, Y., et al., *Mineralized tissue cells are a principal source of FGF23*. Bone, 2007. 40(6): p. 1565-73.
118. Tagliabracci, V.S., et al., *Dynamic regulation of FGF23 by Fam20C phosphorylation, GalNAc-T3 glycosylation, and furin proteolysis*. Proc Natl Acad Sci U S A, 2014. 111(15): p. 5520-5.
119. Benet-Pages, A., et al., *FGF23 is processed by proprotein convertases but not by PHEX*. Bone, 2004. 35(2): p. 455-62.
120. Goetz, R., et al., *Isolated C-terminal tail of FGF23 alleviates hypophosphatemia by inhibiting FGF23-FGFR-Klotho complex formation*. Proc Natl Acad Sci U S A, 2010. 107(1): p. 407-12.
121. Kato, K., et al., *Polypeptide GalNAc-transferase T3 and familial tumoral calcinosis. Secretion of fibroblast growth factor 23 requires O-glycosylation*. J Biol Chem, 2006. 281(27): p. 18370-7.
122. Takeuchi, Y., et al., *Venous sampling for fibroblast growth factor-23 confirms preoperative diagnosis of tumor-induced osteomalacia*. J Clin Endocrinol Metab, 2004. 89(8): p. 3979-82.
123. Khosravi, A., et al., *Determination of the elimination half-life of fibroblast growth factor-23*. J Clin Endocrinol Metab, 2007. 92(6): p. 2374-7.
124. Gattineni, J., et al., *FGF23 decreases renal NaPi-2a and NaPi-2c expression and induces hypophosphatemia in vivo predominantly via FGF receptor 1*. Am J Physiol Renal Physiol, 2009. 297(2): p. F282-91.
125. Bai, X., et al., *CYP24 inhibition as a therapeutic target in FGF23-mediated renal phosphate wasting disorders*. J Clin Invest, 2016. 126(2): p. 667-80.
126. Koizumi, M., H. Komaba, and M. Fukagawa, *Parathyroid function in chronic kidney disease: role of FGF23-Klotho axis*. Contrib Nephrol, 2013. 180: p. 110-23.

127. Ben-Dov, I.Z., et al., *The parathyroid is a target organ for FGF23 in rats*. J Clin Invest, 2007. 117(12): p. 4003-8.
128. Naugler, W.E., et al., *Fibroblast Growth Factor Signaling Controls Liver Size in Mice With Humanized Livers*. Gastroenterology, 2015. 149(3): p. 728-40.e15.
129. Wu, X., et al., *FGF19-induced hepatocyte proliferation is mediated through FGFR4 activation*. J Biol Chem, 2010. 285(8): p. 5165-70.
130. Nicholes, K., et al., *A mouse model of hepatocellular carcinoma: ectopic expression of fibroblast growth factor 19 in skeletal muscle of transgenic mice*. Am J Pathol, 2002. 160(6): p. 2295-307.
131. Li, Z., et al., *Circulating FGF19 closely correlates with bile acid synthesis and cholestasis in patients with primary biliary cirrhosis*. PLoS One, 2017. 12(6): p. e0178580.
132. Miura, S., et al., *Fibroblast growth factor 19 expression correlates with tumor progression and poorer prognosis of hepatocellular carcinoma*. BMC Cancer, 2012. 12: p. 56.
133. Tiong, K.H., et al., *Fibroblast growth factor receptor 4 (FGFR4) and fibroblast growth factor 19 (FGF19) autocrine enhance breast cancer cells survival*. Oncotarget, 2016. 7(36): p. 57633-57650.
134. Gao, L., et al., *FGF19/FGFR4 signaling contributes to the resistance of hepatocellular carcinoma to sorafenib*. J Exp Clin Cancer Res, 2017. 36(1): p. 8.
135. Pai, R., et al., *Inhibition of fibroblast growth factor 19 reduces tumor growth by modulating beta-catenin signaling*. Cancer Res, 2008. 68(13): p. 5086-95.
136. Pai, R., et al., *Antibody-mediated inhibition of fibroblast growth factor 19 results in increased bile acids synthesis and ileal malabsorption of bile acids in cynomolgus monkeys*. Toxicol Sci, 2012. 126(2): p. 446-56.
137. Li, F., et al., *Enhanced autocrine FGF19/FGFR4 signaling drives the progression of lung squamous cell carcinoma, which responds to mTOR inhibitor AZD2104*. Oncogene, 2020. 39(17): p. 3507-3521.
138. Rinella, M.E., *Nonalcoholic fatty liver disease: a systematic review*. Jama, 2015. 313(22): p. 2263-73.
139. Haas, J.T., S. Francque, and B. Staels, *Pathophysiology and Mechanisms of Nonalcoholic Fatty Liver Disease*. Annu Rev Physiol, 2016. 78: p. 181-205.
140. Lou, Y., et al., *Characterization of transcriptional modules related to fibrosing-NAFLD progression*. Sci Rep, 2017. 7(1): p. 4748.
141. Kaila, B. and M. Raman, *Obesity: a review of pathogenesis and management strategies*. Can J Gastroenterol, 2008. 22(1): p. 61-8.
142. Zhou, M., et al., *Separating Tumorigenicity from Bile Acid Regulatory Activity for Endocrine Hormone FGF19*. Cancer Res, 2014. 74(12): p. 3306-16.
143. DePaoli, A.M., et al., *FGF19 Analog as a Surgical Factor Mimetic That Contributes to Metabolic Effects Beyond Glucose Homeostasis*. Diabetes, 2019. 68(6): p. 1315-1328.
144. Harrison, S.A., et al., *NGM282 for treatment of non-alcoholic steatohepatitis: a multicentre, randomised, double-blind, placebo-controlled, phase 2 trial*. Lancet, 2018. 391(10126): p. 1174-1185.
145. Dushay, J., et al., *Increased fibroblast growth factor 21 in obesity and nonalcoholic fatty liver disease*. Gastroenterology, 2010. 139(2): p. 456-63.
146. Mraz, M., et al., *Serum concentrations and tissue expression of a novel endocrine regulator fibroblast growth factor-21 in patients with type 2 diabetes and obesity*. Clin Endocrinol (Oxf), 2009. 71(3): p. 369-75.
147. Fisher, F.M., et al., *Obesity is a fibroblast growth factor 21 (FGF21)-resistant state*. Diabetes, 2010. 59(11): p. 2781-9.
148. Badman, M.K., et al., *Fibroblast growth factor 21-deficient mice demonstrate impaired adaptation to ketosis*. Endocrinology, 2009. 150(11): p. 4931-40.
149. Maratos-Flier, E., *Fatty liver and FGF21 physiology*. Exp Cell Res, 2017. 360(1): p. 2-5.
150. Wenthe, W., et al., *Fibroblast growth factor-21 improves pancreatic beta-cell function and survival by activation of extracellular signal-regulated kinase 1/2 and Akt signaling pathways*. Diabetes, 2006. 55(9): p. 2470-8.
151. Holland, W.L., et al., *An FGF21-adiponectin-ceramide axis controls energy expenditure and insulin action in mice*. Cell Metab, 2013. 17(5): p. 790-7.

152. Kharitononkov, A., et al., *Rational design of a fibroblast growth factor 21-based clinical candidate, LY2405319*. PLoS One, 2013. 8(3): p. e58575.
153. Adams, A.C., et al., *LY2405319, an Engineered FGF21 Variant, Improves the Metabolic Status of Diabetic Monkeys*. PLoS One, 2013. 8(6): p. e65763.
154. Gaich, G., et al., *The effects of LY2405319, an FGF21 analog, in obese human subjects with type 2 diabetes*. Cell Metab, 2013. 18(3): p. 333-40.
155. Charles, E.D., et al., *Pegbelfermin (BMS-986036), PEGylated FGF21, in Patients with Obesity and Type 2 Diabetes: Results from a Randomized Phase 2 Study*. Obesity (Silver Spring), 2019. 27(1): p. 41-49.
156. Talukdar, S., et al., *A Long-Acting FGF21 Molecule, PF-05231023, Decreases Body Weight and Improves Lipid Profile in Non-human Primates and Type 2 Diabetic Subjects*. Cell Metab, 2016. 23(3): p. 427-40.
157. Agrawal, A., et al., *Molecular elements in FGF19 and FGF21 defining KLB/FGFR activity and specificity*. Mol Metab, 2018. 13: p. 45-55.
158. Athonvarangkul, D. and K.L. Insogna, *New Therapies for Hypophosphatemia-Related to FGF23 Excess*. Calcif Tissue Int, 2020.
159. Bai, X.Y., et al., *The autosomal dominant hypophosphatemic rickets R176Q mutation in fibroblast growth factor 23 resists proteolytic cleavage and enhances in vivo biological potency*. J Biol Chem, 2003. 278(11): p. 9843-9.
160. Rafaelsen, S.H., et al., *Exome sequencing reveals FAM20c mutations associated with fibroblast growth factor 23-related hypophosphatemia, dental anomalies, and ectopic calcification*. J Bone Miner Res, 2013. 28(6): p. 1378-85.
161. Onishi, T., et al., *Phex mutation causes overexpression of FGF23 in teeth*. Arch Oral Biol, 2008. 53(2): p. 99-104.
162. Lorenz-Depiereux, B., et al., *DMP1 mutations in autosomal recessive hypophosphatemia implicate a bone matrix protein in the regulation of phosphate homeostasis*. Nat Genet, 2006. 38(11): p. 1248-50.
163. Aono, Y., et al., *Therapeutic effects of anti-FGF23 antibodies in hypophosphatemic rickets/osteomalacia*. J Bone Miner Res, 2009. 24(11): p. 1879-88.
164. Folpe, A.L., et al., *Most osteomalacia-associated mesenchymal tumors are a single histopathologic entity: an analysis of 32 cases and a comprehensive review of the literature*. Am J Surg Pathol, 2004. 28(1): p. 1-30.
165. Fukumoto, S., *Diagnostic Modalities for FGF23-Producing Tumors in Patients with Tumor-Induced Osteomalacia*. Endocrinol Metab (Seoul), 2014. 29(2): p. 136-43.
166. Levey, A.S., et al., *Definition and classification of chronic kidney disease: a position statement from Kidney Disease: Improving Global Outcomes (KDIGO)*. Kidney Int, 2005. 67(6): p. 2089-100.
167. Thomas, R., A. Kalso, and J.R. Sedor, *Chronic kidney disease and its complications*. Prim Care, 2008. 35(2): p. 329-44, vii.
168. Coresh, J., et al., *Prevalence of chronic kidney disease and decreased kidney function in the adult US population: Third National Health and Nutrition Examination Survey*. Am J Kidney Dis, 2003. 41(1): p. 1-12.
169. Coresh, J., et al., *Prevalence of chronic kidney disease in the United States*. Jama, 2007. 298(17): p. 2038-47.
170. Collins, A.J., et al., *Excerpts from the United States Renal Data System 2004 annual data report: atlas of end-stage renal disease in the United States*. Am J Kidney Dis, 2005. 45(1 Suppl 1): p. A5-7, s1-280.
171. Honeycutt, A.A., et al., *Medical costs of CKD in the Medicare population*. J Am Soc Nephrol, 2013. 24(9): p. 1478-83.
172. Iglehart, J.K., *Bundled payment for ESRD--including ESAs in Medicare's dialysis package*. N Engl J Med, 2011. 364(7): p. 593-5.
173. Saran, R., et al., *US Renal Data System 2017 Annual Data Report: Epidemiology of Kidney Disease in the United States*. Am J Kidney Dis, 2018. 71(3 Suppl 1): p. A7.
174. Go, A.S., et al., *Chronic kidney disease and the risks of death, cardiovascular events, and hospitalization*. N Engl J Med, 2004. 351(13): p. 1296-305.

175. Baigent, C., K. Burbury, and D. Wheeler, *Premature cardiovascular disease in chronic renal failure*. *Lancet*, 2000. 356(9224): p. 147-52.
176. Di Lullo, L., et al., *Left Ventricular Hypertrophy in Chronic Kidney Disease Patients: From Pathophysiology to Treatment*. *Cardiorenal Med*, 2015. 5(4): p. 254-66.
177. Zoccali, C., et al., *Prognostic value of echocardiographic indicators of left ventricular systolic function in asymptomatic dialysis patients*. *J Am Soc Nephrol*, 2004. 15(4): p. 1029-37.
178. Zager, P.G., et al., *"U" curve association of blood pressure and mortality in hemodialysis patients*. *Medical Directors of Dialysis Clinic, Inc. Kidney Int*, 1998. 54(2): p. 561-9.
179. Appel, L.J., et al., *Intensive blood-pressure control in hypertensive chronic kidney disease*. *N Engl J Med*, 2010. 363(10): p. 918-29.
180. de Boer, I.H., et al., *Temporal trends in the prevalence of diabetic kidney disease in the United States*. *JAMA*, 2011. 305(24): p. 2532-9.
181. Levi, M., et al., *Mechanisms of phosphate transport*. *Nat Rev Nephrol*, 2019. 15(8): p. 482-500.
182. Moe, S.M., G.A. Block, and C.B. Langman, *Oral phosphate binders in patients with kidney failure*. *N Engl J Med*, 2010. 363(10): p. 990; author reply 990.
183. Faul, C., et al., *FGF23 induces left ventricular hypertrophy*. *J Clin Invest*, 2011. 121(11): p. 4393-408.
184. Isakova, T., et al., *Fibroblast growth factor 23 and risks of mortality and end-stage renal disease in patients with chronic kidney disease*. *JAMA*. 305(23): p. 2432-9.
185. Wolf, M., *Update on fibroblast growth factor 23 in chronic kidney disease*. *Kidney Int*, 2012. 82(7): p. 737-47.
186. Gutierrez, O.M., et al., *Fibroblast growth factor 23 and mortality among patients undergoing hemodialysis*. *N Engl J Med*, 2008. 359(6): p. 584-92.
187. Jean, G., et al., *High levels of serum fibroblast growth factor (FGF)-23 are associated with increased mortality in long haemodialysis patients*. *Nephrol Dial Transplant*, 2009. 24(9): p. 2792-6.
188. Gutierrez, O.M., et al., *Fibroblast growth factor 23 and left ventricular hypertrophy in chronic kidney disease*. *Circulation*, 2009. 119(19): p. 2545-52.
189. Mirza, M.A., et al., *Serum intact FGF23 associate with left ventricular mass, hypertrophy and geometry in an elderly population*. *Atherosclerosis*, 2009. 207(2): p. 546-51.
190. Grabner, A., et al., *FGF23/FGFR4-mediated left ventricular hypertrophy is reversible*. *Sci Rep*, 2017. 7(1): p. 1993.
191. Leifheit-Nestler, M., et al., *Induction of cardiac FGF23/FGFR4 expression is associated with left ventricular hypertrophy in patients with chronic kidney disease*. *Nephrol Dial Transplant*, 2016. 31(7): p. 1088-99.
192. Han, X., et al., *FGF23 induced left ventricular hypertrophy mediated by FGFR4 signaling in the myocardium is attenuated by soluble Klotho in mice*. *J Mol Cell Cardiol*, 2020. 138: p. 66-74.
193. Grabner, A., et al., *Activation of Cardiac Fibroblast Growth Factor Receptor 4 Causes Left Ventricular Hypertrophy*. *Cell Metab*, 2015. 22(6): p. 1020-32.
194. Chen, C.D., et al., *Insulin stimulates the cleavage and release of the extracellular domain of Klotho by ADAM10 and ADAM17*. *Proc Natl Acad Sci U S A*, 2007. 104(50): p. 19796-801.
195. Hu, M.C., et al., *Renal Production, Uptake, and Handling of Circulating alphaKlotho*. *J Am Soc Nephrol*, 2016. 27(1): p. 79-90.
196. Hu, M.C., M. Kuro-o, and O.W. Moe, *Secreted klotho and chronic kidney disease*. *Adv Exp Med Biol*, 2012. 728: p. 126-57.
197. Arbel Rubinstein, T., et al., *Klotho suppresses colorectal cancer through modulation of the unfolded protein response*. *Oncogene*, 2019. 38(6): p. 794-807.
198. Sachdeva, A., et al., *Klotho and the Treatment of Human Malignancies*. *Cancers (Basel)*, 2020. 12(6).
199. Moos, W.H., et al., *Klotho Pathways, Myelination Disorders, Neurodegenerative Diseases, and Epigenetic Drugs*. *Biores Open Access*, 2020. 9(1): p. 94-105.
200. Smith, R.C., et al., *Circulating alphaKlotho influences phosphate handling by controlling FGF23 production*. *J Clin Invest*, 2012. 122(12): p. 4710-5.
201. Hum, J.M., et al., *Sustained Klotho delivery reduces serum phosphate in a model of diabetic nephropathy*. *J Appl Physiol (1985)*, 2019. 126(4): p. 854-862.

202. Navarro-García, J.A., et al., *Fibroblast growth factor-23 promotes rhythm alterations and contractile dysfunction in adult ventricular cardiomyocytes*. *Nephrol Dial Transplant*, 2019. 34(11): p. 1864-1875.
203. Han, X., et al., *FGF23 induced left ventricular hypertrophy mediated by FGFR4 signaling in the myocardium is attenuated by soluble Klotho in mice*. *J Mol Cell Cardiol*, 2019. 138: p. 66-74.
204. Zhang, W., et al., *Role of mitogen-activated protein kinase in cardiac hypertrophy and heart failure*. *Exp Clin Cardiol*, 2003. 8(4): p. 173-83.
205. Touchberry, C.D., et al., *FGF23 is a novel regulator of intracellular calcium and cardiac contractility in addition to cardiac hypertrophy*. *Am J Physiol Endocrinol Metab*, 2013. 304(8): p. E863-73.
206. Xu, J., et al., *Acute glucose-lowering and insulin-sensitizing action of FGF21 in insulin-resistant mouse models--association with liver and adipose tissue effects*. *Am J Physiol Endocrinol Metab*, 2009. 297(5): p. E1105-14.
207. Zhang, F., et al., *Minireview: Roles of Fibroblast Growth Factors 19 and 21 in Metabolic Regulation and Chronic Diseases*. *Mol Endocrinol*, 2015. 29(10): p. 1400-13.
208. Reitman, M.L., *FGF21 mimetic shows therapeutic promise*. *Cell Metab*, 2013. 18(3): p. 307-9.
209. Struik, D., M.B. Dommerholt, and J.W. Jonker, *Fibroblast growth factors in control of lipid metabolism: from biological function to clinical application*. *Curr Opin Lipidol*, 2019. 30(3): p. 235-243.
210. Navarro-Garcia, J.A., et al., *Fibroblast growth factor-23 promotes rhythm alterations and contractile dysfunction in adult ventricular cardiomyocytes*. *Nephrol Dial Transplant*, 2019.
211. Wacker, M.J., et al., *Skeletal Muscle, but not Cardiovascular Function, Is Altered in a Mouse Model of Autosomal Recessive Hypophosphatemic Rickets*. *Front Physiol*, 2016. 7: p. 173.
212. Avin, K.G., et al., *Fibroblast Growth Factor 23 Does Not Directly Influence Skeletal Muscle Cell Proliferation and Differentiation or Ex Vivo Muscle Contractility*. *Am J Physiol Endocrinol Metab*, 2018.
213. Grabner, A., et al., *Activation of Cardiac Fibroblast Growth Factor Receptor 4 Causes Left Ventricular Hypertrophy*. *Cell Metab*, 2015. 22(6): p. 1020-32.
214. Inker, L.A., et al., *KDOQI US commentary on the 2012 KDIGO clinical practice guideline for the evaluation and management of CKD*. *Am J Kidney Dis*, 2014. 63(5): p. 713-35.
215. Vadakedath, S. and V. Kandi, *Dialysis: A Review of the Mechanisms Underlying Complications in the Management of Chronic Renal Failure*. *Cureus*, 2017. 9(8): p. e1603.
216. Murea, M., et al., *Narrative Review of Incremental Hemodialysis*. *Kidney Int Rep*, 2020. 5(2): p. 135-148.
217. Cronin, R.E. and R.F. Reilly, *Unfractionated heparin for hemodialysis: still the best option*. *Semin Dial*, 2010. 23(5): p. 510-5.
218. Brunet, P., et al., *Pharmacodynamics of unfractionated heparin during and after a hemodialysis session*. *Am J Kidney Dis*, 2008. 51(5): p. 789-95.
219. Boer, C., et al., *Anticoagulant and side-effects of protamine in cardiac surgery: a narrative review*. *Br J Anaesth*, 2018. 120(5): p. 914-927.
220. Shen, J.I. and W.C. Winkelmayr, *Use and safety of unfractionated heparin for anticoagulation during maintenance hemodialysis*. *Am J Kidney Dis*, 2012. 60(3): p. 473-86.
221. Oduah, E.I., R.J. Linhardt, and S.T. Sharfstein, *Heparin: Past, Present, and Future*. *Pharmaceuticals (Basel)*, 2016. 9(3).
222. Nugent, M.A., *Heparin sequencing brings structure to the function of complex oligosaccharides*. *Proc Natl Acad Sci U S A*, 2000. 97(19): p. 10301-3.
223. Andrukhova, O., et al., *FGF23 regulates renal sodium handling and blood pressure*. *EMBO Mol Med*, 2014. 6(6): p. 744-59.
224. Jia, T., et al., *A novel model of adenine-induced tubulointerstitial nephropathy in mice*. *BMC Nephrol*, 2013. 14: p. 116.
225. Clinkenbeard, E.L., et al., *Increased FGF23 protects against detrimental cardio-renal consequences during elevated blood phosphate in CKD*. *JCI Insight*, 2019. 4(4).
226. Diwan, V., et al., *Gender differences in adenine-induced chronic kidney disease and cardiovascular complications in rats*. *Am J Physiol Renal Physiol*, 2014. 307(11): p. F1169-78.
227. Slavic, S., et al., *Genetic Ablation of Fgf23 or Klotho Does not Modulate Experimental Heart Hypertrophy Induced by Pressure Overload*. *Sci Rep*, 2017. 7(1): p. 11298.

228. Han, X., et al., *Cardiovascular Effects of Renal Distal Tubule Deletion of the FGF Receptor 1 Gene*. J Am Soc Nephrol, 2018. 29(1): p. 69-80.
229. Smith, R.C., et al., *Circulating α Klotho influences phosphate handling by controlling FGF23 production*. J Clin Invest, 2012. 122(12): p. 4710-5.
230. Bowe, A.E., et al., *FGF-23 inhibits renal tubular phosphate transport and is a PHEX substrate*. Biochem Biophys Res Commun, 2001. 284(4): p. 977-81.
231. Wu, X., et al., *C-terminal tail of FGF19 determines its specificity toward Klotho co-receptors*. J Biol Chem, 2008. 283(48): p. 33304-9.
232. Wu, X., et al., *Selective activation of FGFR4 by an FGF19 variant does not improve glucose metabolism in ob/ob mice*. Proc Natl Acad Sci U S A, 2009. 106(34): p. 14379-84.
233. Nakamura, M., et al., *Sulfated glycosaminoglycans are required for specific and sensitive fibroblast growth factor (FGF) 19 signaling via FGF receptor 4 and betaKlotho*. J Biol Chem, 2011. 286(30): p. 26418-23.
234. Nakamura, M., et al., *Sulfated glycosaminoglycan-assisted receptor specificity of human fibroblast growth factor (FGF) 19 signaling in a mouse system is different from that in a human system*. J Biol Chem, 2013. 288(3): p. 321-30.
235. Hu, M.C., et al., *Klotho and phosphate are modulators of pathologic uremic cardiac remodeling*. J Am Soc Nephrol, 2015. 26(6): p. 1290-302.
236. Hu, M.C., et al., *Recombinant alpha-Klotho may be prophylactic and therapeutic for acute to chronic kidney disease progression and uremic cardiomyopathy*. Kidney Int, 2017. 91(5): p. 1104-1114.
237. Xie, J., et al., *Soluble Klotho Protects against Uremic Cardiomyopathy Independently of Fibroblast Growth Factor 23 and Phosphate*. J Am Soc Nephrol, 2015. 26(5): p. 1150-60.
238. Yang, K., et al., *Klotho Protects Against Indoxyl Sulphate-Induced Myocardial Hypertrophy*. J Am Soc Nephrol, 2015. 26(10): p. 2434-46.
239. Xiao, Z., et al., *FGF23 expression is stimulated in transgenic alpha-Klotho longevity mouse model*. JCI Insight, 2019. 4(23).
240. Grabner, A. and C. Faul, *The role of fibroblast growth factor 23 and Klotho in uremic cardiomyopathy*. Curr Opin Nephrol Hypertens, 2016. 25(4): p. 314-24.
241. Richter, B. and C. Faul, *FGF23 Actions on Target Tissues-With and Without Klotho*. Front Endocrinol (Lausanne), 2018. 9: p. 189.

APPENDIX:
INSTITUTIONAL ANIMAL CARE AND USE APPROVAL



MEMORANDUM

DATE: 08-Aug-2019
TO: Faul, Christian
FROM: 
 Robert A. Kesterson, Ph.D., Chair
 Institutional Animal Care and Use Committee (IACUC)
SUBJECT: NOTICE OF APPROVAL

The following application was approved by the University of Alabama at Birmingham Institutional Animal Care and Use Committee (IACUC) on 08-Aug-2019.

Protocol PI: Faul, Christian
Title: Activation of Cardiac FGFR4 Causes Left Ventricular Hypertrophy
Sponsor: National Heart, Lung, and Blood Institute/NIH/DHHS
Animal Project Number (APN): IACUC-20860

This institution has an Animal Welfare Assurance on file with the Office of Laboratory Animal Welfare (OLAW), is registered as a Research Facility with the USDA, and is accredited by the Association for Assessment and Accreditation of Laboratory Animal Care International (AAALAC).

This protocol is due for full review by 23-Aug-2020.

Institutional Animal Care and Use Committee (IACUC)

403 Community Health on 19th | 933 19th Street South

Mailing Address:

CH19 403 | 1720 2nd Ave South | Birmingham AL 35294-2041

phone: 205.934.7692 | fax: 205.934.1188

www.uab.edu/iacuc | iacuc@uab.edu

**MEMORANDUM**

DATE: 16-Oct-2019
TO: Faul, Christian
FROM: 
Robert A. Kesterson, Ph.D., Chair
Institutional Animal Care and Use Committee (IACUC)
SUBJECT: NOTICE OF APPROVAL

The following application was approved by the University of Alabama at Birmingham Institutional Animal Care and Use Committee (IACUC) on 16-Oct-2019.

Protocol PI: Faul, Christian
Title: FGF21 causes left ventricular hypertrophy
Sponsor: American Diabetes Association, Inc.
Animal Project Number (APN): IACUC-21094

This institution has an Animal Welfare Assurance on file with the Office of Laboratory Animal Welfare (OLAW), is registered as a Research Facility with the USDA, and is accredited by the Association for Assessment and Accreditation of Laboratory Animal Care International (AAALAC).

This protocol is due for full review by 26-Nov-2020.

Institutional Animal Care and Use Committee (IACUC)

403 Community Health on 19th | 933 19th Street South

Mailing Address:

CH19 403 | 1720 2nd Ave South | Birmingham AL 35294-2041

phone: 205.934.7692 | fax: 205.934.1188

www.uab.edu/iacuc | iacuc@uab.edu

**MEMORANDUM**

DATE: 14-Oct-2019
TO: Faul, Christian
FROM: 
Robert A. Kesterson, Ph.D., Chair
Institutional Animal Care and Use Committee (IACUC)
SUBJECT: NOTICE OF APPROVAL

The following application was approved by the University of Alabama at Birmingham Institutional Animal Care and Use Committee (IACUC) on 14-Oct-2019.

Protocol PI: Faul, Christian
Title: Endocrine FGFs target the liver and contribute to inflammation and anemia
Sponsor: UAB DEPARTMENT
Animal Project Number (APN): IACUC-21109

This institution has an Animal Welfare Assurance on file with the Office of Laboratory Animal Welfare (OLAW), is registered as a Research Facility with the USDA, and is accredited by the Association for Assessment and Accreditation of Laboratory Animal Care International (AAALAC).

This protocol is due for full review by 13-Nov-2020.

Institutional Animal Care and Use Committee (IACUC)

403 Community Health on 19th | 933 19th Street South

Mailing Address:

CH19 403 | 1720 2nd Ave South | Birmingham AL 35294-2041

phone: 205.934.7692 | fax: 205.934.1188

www.uab.edu/iacuc | iacuc@uab.edu

**MEMORANDUM**

DATE: 10-Oct-2019
TO: Faul, Christian
FROM: 
Robert A. Kesterson, Ph.D., Chair
Institutional Animal Care and Use Committee (IACUC)
SUBJECT: NOTICE OF APPROVAL

The following application was approved by the University of Alabama at Birmingham Institutional Animal Care and Use Committee (IACUC) on 10-Oct-2019.

Protocol PI: Faul, Christian
Title: Effects of FGF21 and FGF23 on primary cell culture models
Sponsor: UAB DEPARTMENT
Animal Project Number (APN): IACUC-21490

This institution has an Animal Welfare Assurance on file with the Office of Laboratory Animal Welfare (OLAW), is registered as a Research Facility with the USDA, and is accredited by the Association for Assessment and Accreditation of Laboratory Animal Care International (AAALAC).

This protocol is due for full review by 03-Oct-2021.

Institutional Animal Care and Use Committee (IACUC)

403 Community Health on 19th | 933 19th Street South

Mailing Address:

CH19 403 | 1720 2nd Ave South | Birmingham AL 35294-2041

phone: 205.934.7692 | fax: 205.934.1188

www.uab.edu/iacuc | iacuc@uab.edu